Electromagnetic Fields in an H-plane Sectoral Waveguide Partially Loaded with Lossy Dielectric

by

Z. A. Delecki

A thesis

submitted for

the Degree of Master of Science

in the Faculty of Graduate Studies

University of Manitoba

Electrical Engineering Department

University of Manitoba

October, 1985

ELECTROMAGNETIC FIELDS IN AN H-PLANE SECTORAL WAVEGUIDE PARTIALLY LOADED WITH LOSSY DIELECTRIC

BY

Z.A. DELECKI

A thesis submitted to the Faculty of Graduate Studies of the University of Manitoba in partial fulfillment of the requirements of the degree of

MASTER OF SCIENCE

Abstract

This thesis presents an anlytical solution to the field in an H-plane sectoral waveguide partially loaded with a lossy substance. A survey of known methods of solution to the problem of parallel to sectoral waveguide is presented.

An application of Stokes's theorem to the parallel plate - sectoral waveguide junction allows us to find an analytical solution to join fields of parallel plate and sectoral waveguides. Inverse scattering of the electromagnetic wave on a discontinuity created by an imperfect dielectric placed inside such a sectoral waveguide is solved rigorously. A comparison between this method and others is outlined. The solution is examined with respect to computability of components involving series. Justification of the various assumptions and simplifications introduced is made. The solution is converted in the one port scattering parameters of a waveguide.

Possibility of recovering the information about the dielectric constant and loss tangent of the dielectric medium is discussed. A comparison between numerical results and experiment is shown, while conclusions and suggestions for future research are given.

Ackowledgement

The author wishes to thank Dr. M. Hamid of Electrical Engineering Department, who suggested the topic and guided the research. His interest, encouradegment and detailed discussions of many aspects are appreciated.

The author thanks Electrical Engineering Department for the use of computer typesetting facilities.

The author is very grateful to Mr. J. Stanier for reading of the manuscript of the thesis.

Table of Contents

Index of Symbols

$\vec{a}_x$, $\vec{a}_y$, $\vec{a}_z$ unit vectors in Cartesian coordinate system,

$\vec{a}_\rho$, $\vec{a}_\phi$, $\vec{a}_y$ unit vectors in the cylindrical coordinate system,

$A_0(\tau_0)$, $A_1(\tau_0)$, $A_2(\tau_0)$ ... coefficients of Debye's expansion of Hankel functions,

A_m coefficient of expansion of the straightforward point matching method,

$\vec{E}$ electric field vector,

$\vec{H}$ magnetic field vector,

$E^+(r)$, $H^+(r)$ amplitude functions of monochromatic far field, electric and magnetic, respectively,

F_n coefficient of expansion of the alternative point matching method,

$G(\tau)$ kernel of the Fourier transform,

$H_{m\nu}^{(1)}(k\rho)$, $H_{m\nu}^{(2)}(k\rho)$ Hankel functions of the first and second kinds, respectively,

$\vec{e}_{R_{1\varphi}}$, $\vec{h}_{R_{1\varphi}}$ electric and magnetic vector mode functions, respectively,

j imaginary unit of a complex number,

k free space propagation constant,

$\vec{n}$ normal unit vector,

R_1, R_2, R_3, R_4 regions of interest, details in text,

$\vec{s}$ vector along a closed path,

$\vec{S}$ surface normal vector,

$\vec{S}$ Poynting vector,

T_1^0 , Γ_1^0 zero order transmission and reflection coefficients of the parallel plate-sectoral waveguide junction, respectively,

T_1^1 , Γ_1^1 first order transmission and reflection coefficients, respectively, of the parallel plate-sectoral waveguide junction,

T_t , Γ_t total transmission and reflection coefficients of the parallel plate-sectoral waveguide junction,

V scalar potential field,

Y_0 free space admittance,

α flare angle of a horn antenna or differential parameter,

β parameter depending on the context,

γ_m waveguide propagation constant of the m-th mode,

δ_{r_m} relative error of return loss,

$\tan\delta$ loss tangent,

ϵ_0 free space permittivity,

ϵ_r, $\epsilon_{r\infty}$ low and high frequency relative dielectric constant, respectively,

$\zeta(r)$ free space phase function of the plane wave,

η index of refraction,

θ_1, θ_2, θ_3 angles of incidence, reflection and refraction, respectively,

λ_{cr} waveguide critical wavelength,

μ_0 free space permeability,

ν order of Hankel functions,

ρ_0 radius enclosing meniscus region R_2,

ρ, ϕ polar coordinates,

σ conductivity of a dielectric,

τ, ψ general coordinates of a point in complete point matching method,

τ_0, τ_1, τ_2, τ_3, τ_4 arguments of Debye's expansion of Hankel functions,

χ electric susceptibility,

ω angular frequency.

Note: all symbols are described in the text when they are used for the first time.

CHAPTER 1
Introduction

The use of horn antennas to ascertain dielectric properties of a great number of natural and industrial materials has found practical applications for a long period of time [1], although sufficiently rigorous theory of horn antennas with dielectric discontinuities, both in their internal space and in their near field, does not exist at present.

The ease in which horn antennas can be used is a motivation for building measuring equipment based upon different configurations involving one horn antenna reflection or two horn antenna transmission systems.

There is no doubt among researchers that horn antennas with dielectric insertions provide intriguing possibilities such as reduction of beam width and voltage standing wave ratio (VSWR). Additional factors include increase of peak power of the main lobe and, probably, decrease of unwanted crosspolarization [2], which plays a crucial role in the design of feeds for reflector anntenas.

The most significant difficulty to overcome in the mathematical aspects of analysis of a transversly loaded horn is the fact that the front of the internal wave is complex in general and does not always coincide with the dielectric discontinuity surface . This phenomenon results in the commonly called phase error considered in respect to the horn aperture. In order to solve rigorously the scattering of the wave of interest by any discontinuity, the field must be decomposed into E- and H- polarized waves with respect to a fixed point on a discontinuity surface [3]. Any arbitrary wave function can be represent by its plane integrals [4].

Another critical problem arises with respect to parallel plate and sectoral waveguides junctions. It is well known that such discontinuities have no exact solution due to the fact that regions associated with them cannot in most cases be

them cannot in most cases be described in a single cordinate system. Many researchers have contributed a great deal of work to determine analytically the scattering by such junctions. Among them the most significant contributors are Stevenson [5], Solymar [6], Fradin [7], Piefke [8], Hamid [9,13], Bahar [10], Lewin [11,12], Iskander [13]. In spite of the fact they have based their solutions on different concepts and theories, this question seems to be still open for an exhaustive treatment. All the above mentioned attempts discuss the case where in the internal space of the horn (or sectoral waveguide) only outward propagating modes exist.

In practice, methods based on the generalized scattering matrix concept [14] have been widely used by engineers for years. These methods improve significantly the performance of the design process, although at the expense of loss of the physical significance of many subtle occurences inside of the waveguide structure. The gap between practical and sophisticated scientific design appears to become larger and larger.

The purpose of this work is to establish the background necessary to determine dielectric properties of imperfect dielectrics and any related nonelectrical quantities (e.g. moisture content) from the back scattering coefficient in the feed parallel-plate waveguide. In this structure the feed waveguide is terminated by an H- plane sectoral waveguide, which is part of the sensor. The goal is to be obtained by solving the problem of scattering at the dielectric discontinuity as well as the scattering at the waveguide junction discontinuity resulting in the single reflection coefficient to be monitored in the feed waveguide.

CHAPTER 2

Survey of Methods Related to Waveguide Junctions

2.1. Point matching method

This method known also as the collocation method consists of choosing a linear combination of solutions of the Helmholtz equations in a waveguide such that the sum satisfies the boundary conditions at the discrete number of boundary points.

Since the parallel plate and sectoral waveguides (or waveguide-horn junction) have no common boundary (except for points **A** and **C** in fig.2.1) the matching procedure is carried for the meniscus region denoted in fig. 2.1 by **ABCDA.**

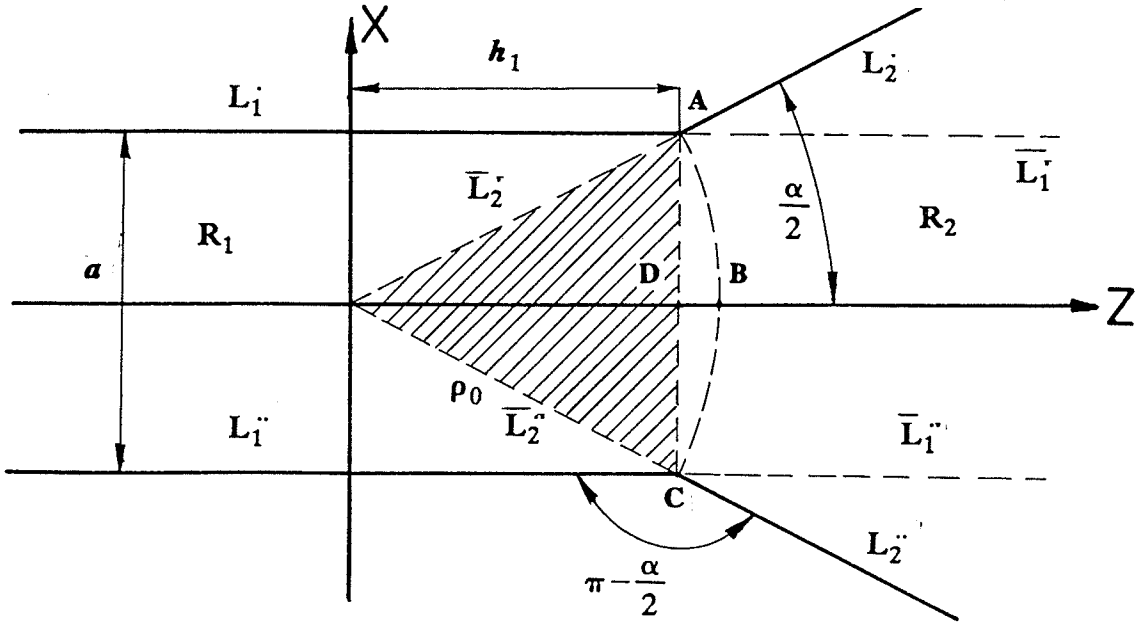

Fig. 2.1 Convex junction waveguide-horn

Lewin suggests the following representation of the waveguide field [11,12]

$$E_y = e^{-jk_1 z} + \sum_{m=1}^{\infty} \Gamma_m e^{jk_m z} \sin\left[\left(\frac{x}{a} + \frac{1}{2}\right)\right] \quad for\ z < h_1 \tag{2.1}$$

and the horn field

$$E_y = \sum_{m=1}^{\infty} T_m H^{(2)}_{\frac{m\pi}{\alpha}}(k\rho)\sin\left[m\pi\left(\frac{\phi}{\alpha}+\frac{1}{2}\right)\right] \quad for\ \rho \geq \rho_0 \tag{2.2}$$

In order to match both fields at the point **D** , the field given by (2.1) must be extended into the meniscus region. The problem becomes more difficult if we ask - to what extent the series (2.2) represents the field of the meniscus region ?

Expanding (2.2) for large values of the index m, the series becomes

$$E_y = \sum_{m=q}^{\infty} \Gamma\left(m\frac{\pi}{\alpha}\right) T_m e^{\left(jm\frac{\pi}{\alpha}+\frac{1}{2}\right)} \left(\frac{2}{k\rho}\right)^{\frac{m\pi}{\alpha}} \quad for\ \ q >> 1 \tag{2.3}$$

The wall current depends on the value $\frac{\partial E_y}{\partial \phi}$ at $\phi = \pm\frac{\alpha}{2}$. For ρ near ρ_0 it exhibits a singularity given by the sharp edge of the wedge of flare angle $\Pi - \frac{\alpha}{2}$.

Since T_m is asymptotic to $\left(\frac{k\rho_0}{2}\right)^{\frac{m\pi}{\alpha}} \frac{\Gamma\left(\frac{m\pi}{\alpha}\right)}{m^{\beta}}$, where β is some parameter, then $\frac{\partial E_y m}{\partial \phi}$ at $\phi = -\frac{\alpha}{2}$ varies as

$$E_{ym} = \left(\frac{\rho_0}{\rho}\right)^{\frac{m\pi}{\alpha}} m^{-\beta+1} \tag{2.4}$$

which is asymptotic to $\Gamma(2-\beta)\left(\frac{\rho-\rho_0}{\rho_0}\right)^{\beta-2}$ as ρ approaches ρ_0. In order to have the required form of singularity, the parameter β should be equal to

$$\beta = \frac{1+2\pi}{2\pi+\alpha} \tag{2.5}$$

which clearly says that series having m-th component given by (2.4) diverges for

$\rho < \rho_0$. This leads to the conclusion that extension of the series in the meniscus region is invalid, although the numerical results seem satisfactory [12].

A concise review of point matching methods is found in [15]. In general they can be subdivided into:

(a) straightforward point matching method (SPM);

(b) complete point matching method (CPM);

(c) alternative point matching (APM);

(d) extended point matching method (EPM).

The first three methods are based on an internal Rayleigh hypothesis, which assumes that an expansion of the form

$$V(\rho,\phi)=\sum_{m=-\infty}^{\infty} A_m J_m(k\rho)e^{jm\phi} \tag{2.6}$$

is valid everywhere in the region Ω_- (fig. 2.2), i. e.

$$\rho \leq \rho_0$$

where ρ_0 is the radius of convergence of the RHS of (2.6) and ρ is the radius of the observation point.

Equation (2.6) is a general solution of the equation

$$\nabla^2 V + k^2 V = 0 \tag{2.7}$$

with the following boundary condition on C:

$$V(\rho,\phi)=0 \quad \textit{for E-modes} \tag{2.8}$$

$$\frac{\partial V}{\partial n}(\rho,\phi)=0 \quad \textit{for H-modes} \tag{2.9}$$

where $P \in \Omega_-$ (see Fig. 2.2).

The straightforward point matching method assumes a numerically determined truncation order M and (2.6) is made to satisfy either boundary condition (2.8) or (2.9).

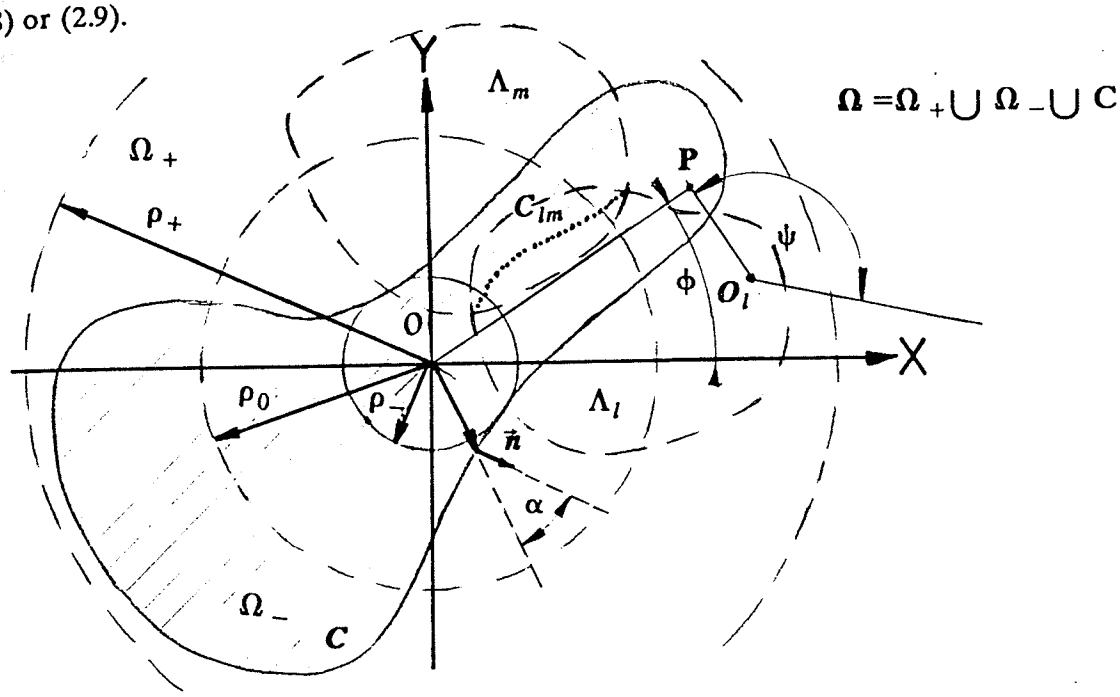

Fig. 2.2 Cross-section of a region surrounding an arbitrary shape waveguide

For Dirichlet boundary condition (2.8) SPM assumes

$$\sum_{m=-M}^{M} A_m (k\rho_n) e^{jm\theta_n} = 0 \tag{2.10}$$

where ρ^n, θ_n denote coordinates of points on C at which V is chosen to satisfy the boundary conditions. The truncation order M is estimated from the rate of convergence of either cutoff wave number or wave function.

Since in general SPM gives incorrect results for the wavefunction, the use of the trapezoidal integration rule to approximate certain exact integrals [16] points an extension of SPM to what is called the complete point matching method (CPM). In view of CPM, equation (2.10) has the form

$$\sum_{n=1}^{2M+1} F_n J_m \left\{k\rho_n\right\} e^{im\theta_n} = 0 \tag{2.11}$$

$$-M \leq m \leq M$$

where F_n is proportional to the density of certain equivalent surface sources at chosen points ρ_n, θ_n on C [16].

Using orthogonality, i.e. multiplying (2.11) by $e^{-jm\Psi_p}$ and then summing over m from $-\infty$ to ∞ one obtains the formula of the alternative point matching method (APM), i.e.

$$\sum_{n=1}^{2M+1} F_n e^{jk\rho_n \cos\left(\Psi_p - \theta_n\right)} = 0 \tag{2.12}$$

$$1 \leq p \leq (2M+1)$$

$$0 \leq \Psi_p \leq 2\pi$$

Because (2.10) - (2.12) differ in the index over which the summation is made, the wave functions computed by the SPM, CPM and APM are different in general. The least error sensitive method is CPM [15]. Since convergence of the point-matching technique has never been proven, mainly due to the assumed radius of convergence in the Rayleigh hypothesis not being always valid, Lewin and Bates proposed their modifications of the point matching formulation. Lewin [11] proposed the following representation of the field in the meniscus region **ABCDA** (fig. 2.1)

$$E_y = \int_o^\infty \sin\left[m\pi\left(\frac{x}{a}+\frac{1}{2}\right)\right]\left[f(m)e^{\Gamma_m z} + g(m)e^{-\Gamma_m z}\right]dm \tag{2.13}$$

where $f(m)$ and $g(m)$ are coefficient functions to be found.

This equation has to be matched to (2.1) on CDA (i.e. $z=h_1$)and to (2.2) on ABC (i.e. $\rho=\rho_0$). Similar matching is suggested for first derivatives of (2.1), (2.2) and (2.13). This concept is related to the idea of "Zwischenmedium" or

overlapping regions [17].

Bates [15] in his proposition of an extended point matching method (EPM) assumes that, in general, it is impossible to find a single series for V, which is valid throughout Ω_- (fig. 2.2). He takes a region $\Lambda_l \subset \Omega$ in which (2.6) may be written as

$$V\{\rho\phi\} = \sum_q D_{lq} Z_{lq}(\tau\psi) \quad for\ P \in \Lambda_1 \tag{2.14}$$

where the origin of the τ,ψ coordinates is a point O_l, which may or not lie in Λ_l.

The functional forms of the members of $[Z_{lq}]$ must accommodate any singularities which exist in Λ_l. There must be sufficient regions, say L of them, such that

$$\Omega_- \subset \Lambda_1 \cup \Lambda_2 \cup \ldots \cup \Lambda_L . \tag{2.15}$$

Denoting a continuous curve, which lies in $\Lambda_l \cap \Lambda_m \cap \Omega_-$ by C_{lm}, it is possible to match the RHS of (2.13) for $l = m$ and its derivative normal to C_{lm} to the RHS of (2.13) for $l = n$ and its derivative normal to C_{mn}. The matching is obtained for a finite number of points. Independently, for each L values of l, the RHS of (2.13) is made to satisfy the appropriate boundary conditions at a finite number of points on $C \cap \Lambda_l$. Similarily, for each M values of m, the RHS of (2.13) is made to satisfy the boundary conditions on $C \cap \Lambda_m$. This concept is similar to that of Lewin, but is formulated in a more sophisticated manner.

The common mark of point matching methods is that they are based on matching of a linear combination of Helmholtz equation solutions along certain boundaries. This results in the fundamental drawback of these methods - they fail whenever a jump in boundary conditions gives rise to a nonlinear partial differential equation.

2.2. Modal matching method

Let us consider an arbitrary waveguide junction as shown in fig. 2.3. An incident TE_{p0} mode with amplitude coefficient T_p strikes the junction as it travels in the positive z direction. The region on the generator side is denoted by R_1 while the region on the load side is denoted by R_2.

The field at the junction can be expanded in terms of normal waveguide modes in the region R_1, i.e.

$$\vec{E} = \left(1+\Gamma_p\right)\vec{e}_{R_1 p} + \sum_{i=1}^{\infty} \Gamma_i \vec{e}_{R_1 i} \tag{2.16}$$

and

$$\vec{H} = \left(1-\Gamma_p\right) T_p \vec{h}_{R_1 p} + \sum_{i=1}^{\infty} \Gamma_i \vec{h}_{R_1 i} \tag{2.17}$$

where in both equations $i \neq p$ and $\vec{e}_{R_1 i}$, $\vec{h}_{R_1 i}$ are called vector mode functions in region R_1.

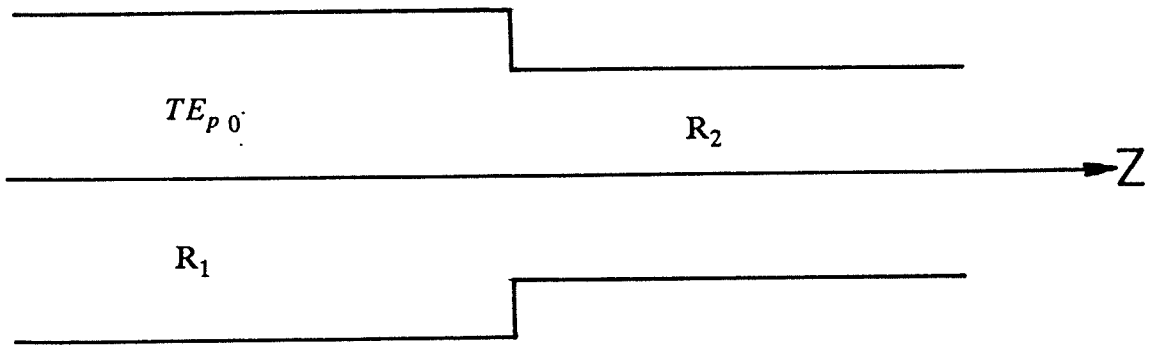

Fig. 2.3 An arbitrary waveguide discontinuity

The field in region R_2 may be expressed by a series of modes as follows

$$\vec{E} = \sum_{j=1}^{\infty} T_{nj} \left(\vec{e}_{R_2 j} + \sum_{k=1}^{\infty} s_{jk} \vec{e}_{R_2 k} \right) \tag{2.18}$$

$$\vec{H} = \sum_{j=1}^{\infty} T_{nj} \left(\vec{h}_{R_2 j} - \sum_{k=1}^{\infty} s_{jk} \vec{h}_{R_2 k} \right) \tag{2.19}$$

where $\vec{e}_{R_2 j}$ and $\vec{h}_{R_2 j}$ are transverse electric and magnetic vector mode functions in region R_2. s_{jk} is the scattering coefficient of the next $n+1$ junction in the direction of the load.

The scattering matrix contains information about propagation of the modes present between n and $n+1$ junctions and also scattering properties of junction $n+1$. This form of modal matching is found in [18]. In this method the solution of the junction nearest the load must be obtained first. This requires initial knowledge about termination of the waveguide. Often this knowledge is based upon assumptions of a perfectly matched or short line termination. This is one of the drawbacks of the method. This method is related to more general methods of point matching, i.e. instead of matching in a finite number of points, the latter method assumes the joining of the vector wave equation solutions in two regions on the abstract junction between them. In the form of (2.15) - (2.18) this method contains general knowledge about waveguide modes expressed in linear algebra terminology. Application of this method is confined to waveguides and transmission lines.

2.3 Schwartz - Neumann's method of overlapping regions

This method is an extension of Schwartz's original method, which allows solution of a harmonic differential equation in a region, which is the sum of two regions.

If it is known how to solve the problem separately in each of these regions, then the Schwartz - Neumann's method can be applied to the solution of the Dirichlet problem in a region, which is the common part (or intersection in terms of set theory terminology) of two other regions overlapping one another.

Let us consider fig. 2.1 and find the validity of the above methods according to [19] :

a. Schwartz's method is applicable for the boundary conditions on $L_1 \bigcup L_2$ enclosing the region $R_1 \bigcup R_2$ if solution in R_1 with the boundary conditions on $L_1 \bigcup \bar{L}_1$ and in R_2 with the boundary conditions on $L_2 \bigcup \bar{L}_2$ are known,

b. Schwartz - Neumann's method is applied to the boundary conditions on $\bar{L}_1 \bigcup \bar{L}_2$ surrounding the region $R_1 \bigcap R_2$ if solution in R_1 with the boundary conditions on $L_1 \bigcup \bar{L}_1$ and in R_2 with the boundary conditions on $L_2 \bigcup \bar{L}_2$ are known.

In view of the above interpretation, the meniscus region of interest (**ABCD** in fig.2.1) lies in the intersection of boundaries rather than regions. This can be formulated in terms of set theory

$$A = L_1^{\cdot} \bigcap L_2^{\cdot} \tag{2.20.1}$$

$$C = L_1^{\cdot\cdot} \bigcap L_2^{\cdot\cdot} \tag{2.20.2}$$

or alternatively

$$A = \bar{L}_1^{\cdot} \bigcap \bar{L}_2^{\cdot} \tag{2.21.1}$$

$$C = \bar{L}_1^{\cdot\cdot} \bigcap \bar{L}_2^{\cdot\cdot} \tag{2.21.2}$$

Since points **A** and **C** are associated with different coordinate systems in which known solutions exist, the region of meniscus is created by z = constant in the Cartesian coordinate system and ρ = constant, in the polar cordinate system.

Neumann's idea consists of representing the sought function, say $w(\rho,\phi)$, in the form of two functions

$$w(\rho,\phi)=u(\rho,\phi)+v(\rho,\phi) \tag{2.22}$$

The first of which satisfies Helmholtz equation in R_1 and the second satisfies the same equation in R_2.

The method of overlapping regions was succesfully employed by Iskander and Hamid [13] to solve for the scattering of electromagnetic waves at waveguide-horn junction. In their approach the junction is subdivided into two subregions; namely a semi-infinite parallel plate subregion R_1 of width a and the region R_2 in fig 2.1 described with respect to origin O by $r>0$ and $+\frac{\alpha}{2} < \phi < -\frac{\alpha}{2}$. These two regions overlap one another in the shaded isosceles triangular area (fig. 2.1)

$$R_1 \mathfrak{X} R_2=\sim\left[R_1 \subseteq R_2 \vee R_2 \subseteq R_1 \vee R_1 /\!/ R_2\right] \tag{2.23}$$

Iskander and Hamid expressed the total electric fields in regions R_1 and R_2 in terms of Green's functions and made those fields equal at every point within the triangular area of the overlapping region, or equivalently at every point on its boundary. Instead of the mathematically complicated Wiener-Hopf technique, they employed Schwartz's alternating method for the solution of the integral equation arising from comparing both electric fields on the nonelectric boundaries of overlapping region R_3. The iterative procedure starts by assuming the field on the nonmetalic boundary of region R_1 to have the value of $E_{yR_1}\Big|z=h_1$ (according to fig. 2.1) and then using the solution of the electric field equation in R_1 to compute the field on the nonmetalic boundary of region R_2 at $\phi=\pm\frac{\alpha}{2}$. Substituting these values in the field equation in the region R_2, the field on the boundary $z=h_1$ is calculated. Repeating this procedure several times the field on the

boundary is found with very small error.

Iskander and Hamid reported excellent convergence of the iteration procedure and high efficiency with regard to computer time needed.

The main drawback of the method seems to be that the transmission coefficient of the m −th mode T_m must be found from an additional power flow condition across the waveguide-horn junction. The first time the method of overlapping regions was applied to the problem of wave propagation around a corner was by Poritski and Blewett in [30].

2.4 **Ray theory methods**

2.4.1 **Geometrical optics as limiting case of physical optics**

Geometrical optics is ordinarily concerned with electromagnetic waves that are essentially plane (or cylindrical, spherical waves with $r \to \infty$) and that are propagated in uncharged medium. In order to show the above statement we assume that a formal solution of Maxwell's equations is

$$\vec{E}^{*}=\vec{E}^{+}(r)e^{-jk\zeta(r)} \tag{2.24.1}$$

$$\vec{H}^{*}=\vec{H}^{+}(r)e^{-jk\zeta(r)} \tag{2.24.2}$$

where $k=\frac{\omega}{c}=\frac{2\pi}{\lambda}$ as usual and $\zeta(r)$ is a function which depends on the medium and reduces to r for free space.

Let us substitute (2.24.1) and (2.24.2) into Maxwell's equations of the form

$$\nabla \times \vec{H}^{*}=j\omega\epsilon\vec{E}^{*} \tag{2.25.1}$$

$$\nabla \times \vec{E}^{*}=-j\omega\mu\vec{H}^{*} \tag{2.25.2}$$

$$\nabla\,(\mu\vec{H}^{*})=0 \tag{2.25.3}$$

$$\nabla\,(\epsilon\vec{E}^{*})=0 \tag{2.25.4}$$

Substituting (2.24.1) into the LHS of (2.25.2) and (2.24.2) into the LHS of (2.25.1) and using (2.25.4) and (2.25.3) respectively and several relevant vector identities [20], the following equivalent form of Maxwell's equations is obtained

$$\nabla\,\zeta\times\vec{H}^{+}+\epsilon c_0\vec{E}^{+}=\frac{1}{jk}\nabla\times\vec{H}^{+} \tag{2.26.1}$$

$$\nabla\,\zeta\times\vec{E}^{+}-\mu c_0\vec{H}^{+}=\frac{1}{jk}\nabla\times\vec{E}^{+} \tag{2.26.2}$$

$$\nabla\,\zeta\cdot\vec{H}^{+}=\frac{1}{jk\,\mu}\left(\nabla\,\mu\cdot\vec{H}^{+}+\mu\nabla\cdot\vec{H}^{+}\right) \tag{2.26.3}$$

$$\nabla\,\zeta\cdot\vec{E}^{+}=\frac{1}{jk\,\epsilon}\left(\nabla\,\epsilon\cdot\vec{E}^{+}+\epsilon\nabla\cdot\vec{E}^{+}\right) \tag{2.26.4}$$

If $k>>1$, then the right sides of (2.26.1 -2.26.4) becomes negligible. Neglecting the RHS of these equations and eliminating $\vec{H}^{+}$ from the first by using the second of these equations, we obtain

$$\nabla\,\zeta\times\left(\frac{1}{\mu c_0}\nabla\,\zeta\times\vec{E}^{+}\right)+\epsilon c_0\vec{E}^{+}=0 \tag{2.27}$$

Expanding the first term of the above equation, and using the well known triple product identity [20], we obtain

$$\nabla\,\zeta\left(\nabla\,\zeta\cdot\vec{E}_{+}\right)-\vec{E}^{+}\left(\nabla\,\zeta\cdot\nabla\,\zeta\right)+\epsilon\mu c_0^{2}\vec{E}^{+}=0 \tag{2.28}$$

Since the first term is zero from (2.26.4) we obtain from (2.28)

$$\nabla\,\zeta\cdot\nabla\,\zeta=\epsilon\mu c_0^{2}=\eta^{2} \tag{2.29}$$

which in the Cartesian coordinate system has the form

$$\left(\frac{\partial \zeta}{\partial x}\right)^2+\left(\frac{\partial \zeta}{\partial y}\right)^2+\left(\frac{\partial \zeta}{\partial z}\right)^2=\eta^2 \tag{2.30}$$

Equations (2.28) and (2.29) show how the direction of a fictitious ray is related to the index of refraction η at a given point. Both the above equations are the necessary and sufficient conditions that (2.23.1) - (2.23.2) be a solution of Maxwell's equations for geometrical optics approximation, i.e. $\lambda \to 0$.

2.4.2 Problem of parallel plate and sectoral waveguide junction in the scope of ray theory

Ray theory in the form known as geometrical theory of diffraction accounts for the abrupt discontinuity of a junction by edge diffracted rays emanating from the upper and lower edges of the junction under consideration (fig 2.1). Analysis of a junction of interest similar to this was initiated by Kinber [21]. He considered the interior problem of a horn fed by a parallel plate waveguide using the ray theory concept. The field in the wave region i.e. $kr > \nu >> 0$, is represented for each particular mode as the sum of two waves which satisfy condition (2.29) of geometrical optics. Kinber introduced a concept of the field as an effect of contribution from Brillouin's rays by using Debye's asymptotic expansion of the cylindrical Hankel functions for large arguments ($kr >> \nu$). In his concept each mode vector (in [21] -vector potential) rotates around a circle of radius $\frac{\nu_m}{k}$ with the centre at the horn apex (fig.2.4).

Debye's asymptotic form of $H_\nu^{(1),(2)}$ with accuracy confined to the first term is of the form

$$H_{\nu}^{(1,2)}(kr)=\frac{e^{\pm j\left[k\sqrt{r^2-\left(\frac{\nu}{k}\right)^2}-\frac{\nu}{k}\arccos\frac{\nu}{kr}+\frac{\pi}{4}\right]}}{k\sqrt{r^2-\left(\frac{\nu}{k}\right)^2}} \quad , \quad \nu=\frac{m\pi}{\alpha} \tag{2.31}$$

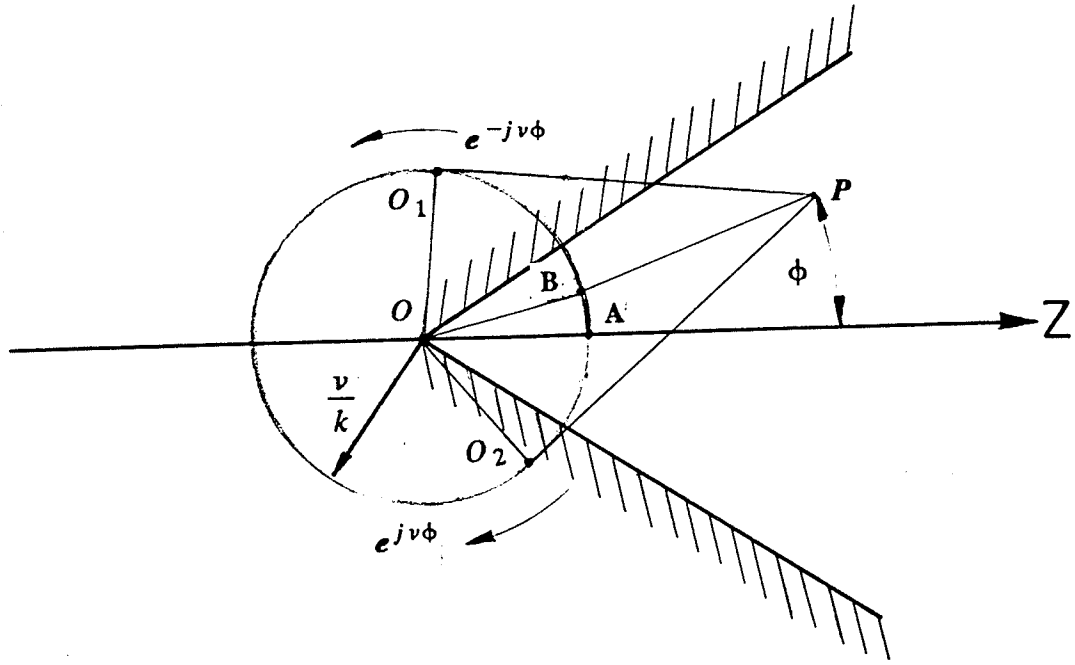

Fig. 2.4 The geometry of the interior problem of a sectoral horn antenna

By writing the phase factor of the form

$$f\left\{\phi\right\}=e^{\pm j\nu\phi} \tag{2.32}$$

it is found from fig. 2.4 that the phase is proportional to the length difference O_1P-O_1A-AB for $e^{+j\nu\phi}$, where

$$O_1P=\sqrt{r^2-\left(\frac{\nu}{k}\right)^2} \tag{2.33.1}$$

$$O_1A=\frac{\nu}{k}\omega=\frac{\nu}{k}\arccos\frac{\nu}{kr} \tag{2.33.2}$$

$$AB=\frac{\nu}{k}\phi \tag{2.33.3}$$

Similar expressions hold for the radiation point O_2. The points of radiation O_1 and O_2 are stationary with respect to an observation point P lying in the interior of the horn, thus the field of the point P is a sum of successively reflected rays, always two, the first from a clockwise and the second from a counterclockwise rotating vector having phase factor $e^{j\nu\phi}$ and $e^{-j\nu\phi}$, respectively. According to Fermat's principle the total length of each ray with respect to the radiation point O_1 or O_2 is a minimum subject to the condition that a ray undergoes a finite sequence of reflections at the horn walls.

The above concept of the electromagnetic field deals with the first order rays. The second order rays are associated with a formation of fringe waves at the rims of the horn; the third order with the incidence of the latter upon waveguide-horn junction. The total vector potential is finally expressed as

$$\vec{A} = j\omega \sum_{q=0}^{Q} \left(\sum_{m<M_q} \Phi_q^{(1,2)} e^{\pm k \Psi_{qm}} \right), \tag{2.34}$$

where Q is the number of groups of terms associated with the same order ν and M_q a number of terms in the q −th group.

The above method extended to eigenvalue analysis was used by Hamid [9] to find the reflection coefficient at a waveguide-horn junction.

Yee et al in [22] applied the ray theory method to reflection from the open end of a waveguide. They based their analysis on the previous work of Keller and Hamid. They considered a parallel plate waveguide propagating several modes. Similar to [21] the incident mode is decomposed into two plane waves, whose scattering by the edges at the termination produces the reflected field. The singly diffracted cylindrical wave, as known from the asymptotic theory of diffraction, originates at each edge and is represented by means of diffracted rays. Then the sum of the fields of the multiply reflected rays is converted into modal form. This

yields formulas for the reflection coefficients of the various modes due to single diffraction. In addition double and multiple diffraction terms are also taken into account yielding a number of improved formulas for reflection coefficient.

It is worthy to point out that Kinber and Popienchenko in [23] strongly disagree with the results in [22]. Their disagreement is based on the following reasoning :

- considering the diffraction at two successive wedges placed in such a way that the tip of the second wedge is in the neighborhood of the light shadow boundary of the first, it is necessary for the geometrical theory of diffraction method to apply that the "following" edge lies in the zone, in which the cylindrical fringe wave of diffraction at the preceding edge would be separated out from the half shadow region. Also in the open end of a waveguide the third and subsequent diffractions occur at the "following" edges lying on the light shadow line of the preceding diffraction, thus the edges cannot be considered as sources of a cylindrical wave.

The ray theory method gives accurate results everywhere it is applicable. Its applicability is confined to problems where $k >> 1$, which permits us to neglect the RHS of (2.25.1) - (2.25.4) and allows use of the first term of the complete Debye's expansion of the Hankel functions in the wave region, i.e. its asymptotic form for $\nu >> kr$ [24].

2.5 WKB method

Leonard and Yen [25] carried an exhaustive analysis of waveguide horn junctions. They based their work on previous work done by Rice [26] and Stevenson [5] and extended the WKB method to junctions having a large flare angle for the sectoral region.

The WKB method, also known as JWKB (Jeffreys, Wentzel, Kramers, Brillouin), is an approximate method of differential equation solution [33]. Let us have the ordinary differential equation

$$\frac{d^2E_y}{dz^2} - h^2 y = 0 \tag{2.35}$$

where $h = h(z)$ is a positive imaginary functions of z, twice differentiable and such that $h \to jc$, c being constant, as $v \to -\infty$. We desire the solution of (2.35) which, together with first derivative, is continuous everywhere and at $\pm\infty$ satisfies the conditions

$$E_y = e^{-jcz} + \Gamma e^{jcz} \tag{2.36}$$

with $z \to -\infty$ and

$$\frac{dE_y}{dz} + \left(h + \frac{1}{2h}\frac{dh}{dz}\right)E_y = 0 \tag{2.37}$$

The constant Γ is a reflection coefficient to be determined.

The exact expression for the reflection coefficient has the form

$$\Gamma = \frac{1}{2\sqrt{jc}} \int_{-\infty}^{\infty} e^{-\xi} E_y(z) \frac{d}{dz^2}\left(\frac{1}{\sqrt{h}}\right) dz \tag{2.38}$$

where $\xi = \xi\{z\} = jcz + \int_{-\infty}^{z} (h - jc)dz$

The integral (2.38) can be solved for small values of the reflection coefficient Γ and large values of the argument z by the substitution

$$E_y(z) = \sqrt{\frac{jc}{h}}\, e^{-\xi} \tag{2.39}$$

which is the WKB approximation.

Leonard and Yen [25] used the above method with their own extension of the vector transverse field components expansion and orthogonality properties and found that the electrical and magnetic eigenfunctions are identical for the two waveguides at the junction plane due to their identical cross-section. By matching the fields at the junction plane they obtained general expressions for zero-order and higher values of reflection - transmission coefficients. The Leonard and Yen's WKB method becomes extremely complicated for the third order coefficients, thus must be confined to waveguides having flare angles up to $15^{o}-20^{o}$, which is the main drawback of the method.

2.6 Other methods

It is necessary to mention briefly other methods which may be applied to the problem of interest. In the section 2.4.2 it was already shown that any wave propagating in the parallel plate waveguide can be represented by two plane waves. Then the problem can be solved by considering diffraction of each plane wave by a wedge. Describing the currents of walls and edges adequately to the character of the wave in waveguide, an integral equation for current distribution may be found which may be solved by either the Wiener-Hopf technique [34] or method of successive approximation and analytic continuation [19].

Other methods which might be employed for analyzing of waveguide discontinuities are:

- Schwartz-Christoffel transformation,

- perturbation method,

- the method of nets (finite difference method)[25],

- variational methods of Ritz and Galerkin,

- the method of moments.

CHAPTER 3

Properties of Parallel Plate and Sectoral Waveguide Modes

3.1 Mathematical properties of parallel plate waveguide modes

The well known derivations presented in this chapter serve as an introduction to study the fields in the case of a parallel plate and sectoral waveguide junction. There are two reasons for such a review:

- large variety of designations and symbols in a related problem which therefore requires some organization,
- the academic character of the thesis needs review of the basic information.

The TE_{m0} modes belong to the most commonly used class associated with parallel plate waveguides due to their simplicity in any mathematical treatment and the ease with which they are generated. For such modes, the electric field has a y −component only, i.e. $E_x = E_z = 0$.

For periodic fields with time factor $e^{j\omega t}$, Maxwell's equations (2.25.1) and (2.25.2) lead to

$$-\frac{\partial \vec{H}_x}{\partial z} + \frac{\partial \vec{H}_z}{\partial x} = j\omega\epsilon_0 \vec{E}_y \tag{3.1}$$

$$-\frac{\partial \vec{E}_y}{\partial z} = j\omega\mu_0 \vec{H}_x \tag{3.2}$$

$$\frac{\partial \vec{E}_y}{\partial x} = j\omega\mu_0 \vec{H}_z \tag{3.3}$$

By differentiating (3.2) and (3.3) and substituting the results into (3.1) we obtain the wave equation for $\vec{E}_y$

$$\frac{\partial^2 \vec{E}_y}{\partial x^2} + \frac{\partial^2 \vec{E}_y}{\partial z^2} + k^2 \vec{E}_y = 0 \tag{3.4}$$

where

$$k = \omega\sqrt{\epsilon_0 \mu_0} \tag{3.5}$$

subject to the following boundary conditions:

$$\vec{E}_y = 0 \quad at \quad x = -\frac{a}{2} \tag{3.6.1}$$

$$\vec{E}_y = 0 \quad at \quad x = \frac{a}{2} \tag{3.6.2}$$

Using the standard method of separation of variables, the formal solution of (3.4) is

$$\vec{E}_y = \vec{a}_y \sum_{m=1}^{\infty} \left(e^{-j\gamma_m z} + \Gamma_m e^{j\gamma_m z} \right) \sin\left[m\pi \left(\frac{x}{a} + \frac{1}{2} \right) \right] \tag{3.7}$$

with the amplitude of the z directed incident wave equal to unity. Also Γ_m is the reflection coefficient to be determined, while γ_m denotes the waveguide propagation constant, i.e.

$$\gamma_m = \sqrt{k^2 - \left(\frac{m\pi}{a} \right)^2} \tag{3.8}$$

Once we obtain the electric field component E_y, the remaining magnetic field components are found by using (3.2) and (3.3).

In most practical cases more than 90 % forward transferred energy corresponds to the fundamental TE_{10} mode. Hence (3.7) may rewritten in the form [27]

$$E_y = e^{-j\gamma_1 z} \sin\left[\pi \left(\frac{x}{a} + \frac{1}{2} \right) \right] + \sum_{m=1}^{\infty} \Gamma_m e^{j\gamma_m z} \sin\left[m\pi \left(\frac{x}{a} + \frac{1}{2} \right) \right] \tag{3.9}$$

where the reflection coefficient Γ_m must be determined from the boundary condition corresponding to the transverse termination of the waveguide.

3.2 Solution of internal fields in an H-plane sectoral waveguide (or horn)

The solution of the fields is found in the coordinate system associated with the same origin as for the waveguide, (see fig.2.1 or fig.4.1).

The vanishing field components are:

$$\vec{E}_\rho = \vec{E}_\phi = 0 \quad , \quad \vec{H}_y = 0 \tag{3.10}$$

The nonvanishing terms in of Maxwell's equations are:

$$j\omega\epsilon_0 \vec{E}_y = \frac{1}{\rho}\frac{\partial}{\partial\rho}(\rho\vec{H}_\phi) - \frac{1}{\rho}\frac{\partial \vec{h}_\rho}{\partial\phi} \tag{3.11}$$

$$\frac{1}{\rho}\frac{\partial \vec{E}_y}{\partial\phi} = -j\omega\mu_0 \vec{H}_\rho \tag{3.12}$$

$$\frac{\partial \vec{E}_y}{\partial\rho} = j\omega\mu_0 H_\phi \tag{3.13}$$

Repeating the procedure in section 2.1, the following partial differential equation is obtained:

$$\frac{1}{\rho}\frac{\partial}{\partial\rho}\left(\rho\frac{\partial \vec{E}_y}{\partial\rho}\right) + \frac{1}{\rho^2}\frac{\partial^2 \vec{E}_y}{\partial\phi} + k^2\vec{E}_y = 0 \tag{3.14}$$

which may be split into two ordinary differential equations after applying the method of separation of variables, i.e.

$$\frac{d^2R(\rho)}{d\rho_2} + \frac{1}{\rho}\frac{dR(\rho)}{d\rho} + \left(k^2 - \frac{p^2}{\rho^2}\right)R(\rho) = 0 \tag{3.15}$$

with the boundary conditions dependent on the manner of excitation and termination of a sectoral waveguide (horn) and

$$\frac{d^2\Phi(\phi)}{d\phi^2}+p^2\Phi(\phi)=0 \tag{3.16}$$

with the boundary condition

$$E_y=0 \quad for \quad \phi\pm\frac{\alpha}{2} \tag{3.17}$$

The separation constant p is found from the appropriate boundary condition.

The general solution for the sectoral waveguide fields is expressed in a form suitable for further considerations, i.e.

$$E_y=\sum_{m=1}^{\infty} T_m \sin\left[m\pi\left(\frac{\phi}{\alpha}+\frac{1}{2}\right)\right]\left[H_{m\nu}^{(2)}(k\rho)+\Gamma_{m2}H_{m\nu}^{(1)}(k\rho)\right] \tag{3.18}$$

where

$$\nu=\frac{\pi}{\alpha} \tag{3.19}$$

and T_m is the transmission coefficient from parallel plate to sectoral waveguide, Γ_{m2} is the reflection coefficient at the transverse dielectric interface between regions R_3 and R_4 in fig. 4.1. $H_{m\nu}^{(2)}$, $H_{m\nu}^{(1)}$ are cylindrical Hankel functions of the second and first kinds, respectively. The first one represents outgoing waves while the second represents incoming waves with respect to the apex of the sectoral waveguide. It should be noted that the magnetic field components are related to E_y by (3.12) and (3.13).

From a comparison of (3.9) and (3.18) it is evident that the transverse fields of the TE_{m0} mode are similar, except for a certain change in the complex amplitude of each mode due to conversion at the junction. The most important

similarities are:

- electric field E_y has only one component and is parallel to the y −axis,
- magnetic field components are perpendicular to the y −axis,
- E_y and H_x in the parallel plate waveguide vary with the coordinate x, since in the sectoral waveguide E_y and H_ϕ vary with the coordinate ϕ; in both cases the variation has a sinusoidal character,
- the index m either for parallel plate or sectoral waveguide characterizes the number of standing halfwaves between the walls, parallel to the electric field E_y,

The most significant difference is related to points of identical phase which lie in the plane z =constant with forward variation factor $e^{-j\gamma_1 z}$ and backward factor $e^{j\gamma_m z}$ for the parallel plate waveguide (3.9). For the sectoral waveguide they lie on a cylindrical surface (ρ=consant) with forward and backward phase coefficients $H_{m\nu}^{(2)}(k\rho)$ and $H_{m\nu}^{(1)}(k\rho)$, respectively, by analogy with the parallel plate waveguide (3.18). Another important difference is lack of existence in the sectoral waveguide of a critical wavelength λ_{cr}. This indicates that for any wave having an arbitrary index m, propagation may exist.

CHAPTER 4

Scattering Coefficients of the Parallel Plate-Sectoral Waveguide Junction

4.1 Formulation of the problem

The configuration of the dielectric loaded waveguide system under consideration is shown in fig. 4.1 . The parallel plate waveguide feeds the H -plane sectoral waveguide which is assumed to be long and to have an arbitrary flare angle α. The fields diffracted at the edges do not interact with those existing on the transversely oriented internal dielectric surface due to the fact that the dielectric is lossy and the sectoral waveguide is semi-infinite in length.

It is further assumed that the waveguide supports a single H_p (TE_{p0}) mode, where $p = 1, 2, 3, \ldots$, in the forward direction,(see fig.4.1). The effect of a discontinuous boundary at the junction causes a diffracted field with an infinite number of modes travelling in either direction of the junction.

4.2 Diffraction of a cylindrical wave at a transverse dielectric discontinuity in an H-plane sectoral waveguide.

Any TE-wave with arbitrary polarization can always be decomposed into a linear sum of perpendicular and parallel polarized waves [3] .

Let us consider an E-polarized wave having an arbitrary amplitude distribution described by the following field components:

$$E_y = f(\phi) H_{m\nu}^{(2)}(k\rho) \tag{4.1}$$

$$H_\phi = \frac{1}{j\omega\mu_0} \frac{\partial E_y}{\partial \rho} \tag{4.2}$$

$$H_\rho = -\frac{1}{j\omega\mu_0} \frac{1}{\rho} \frac{\partial E_y}{\partial \phi} \tag{4.3}$$

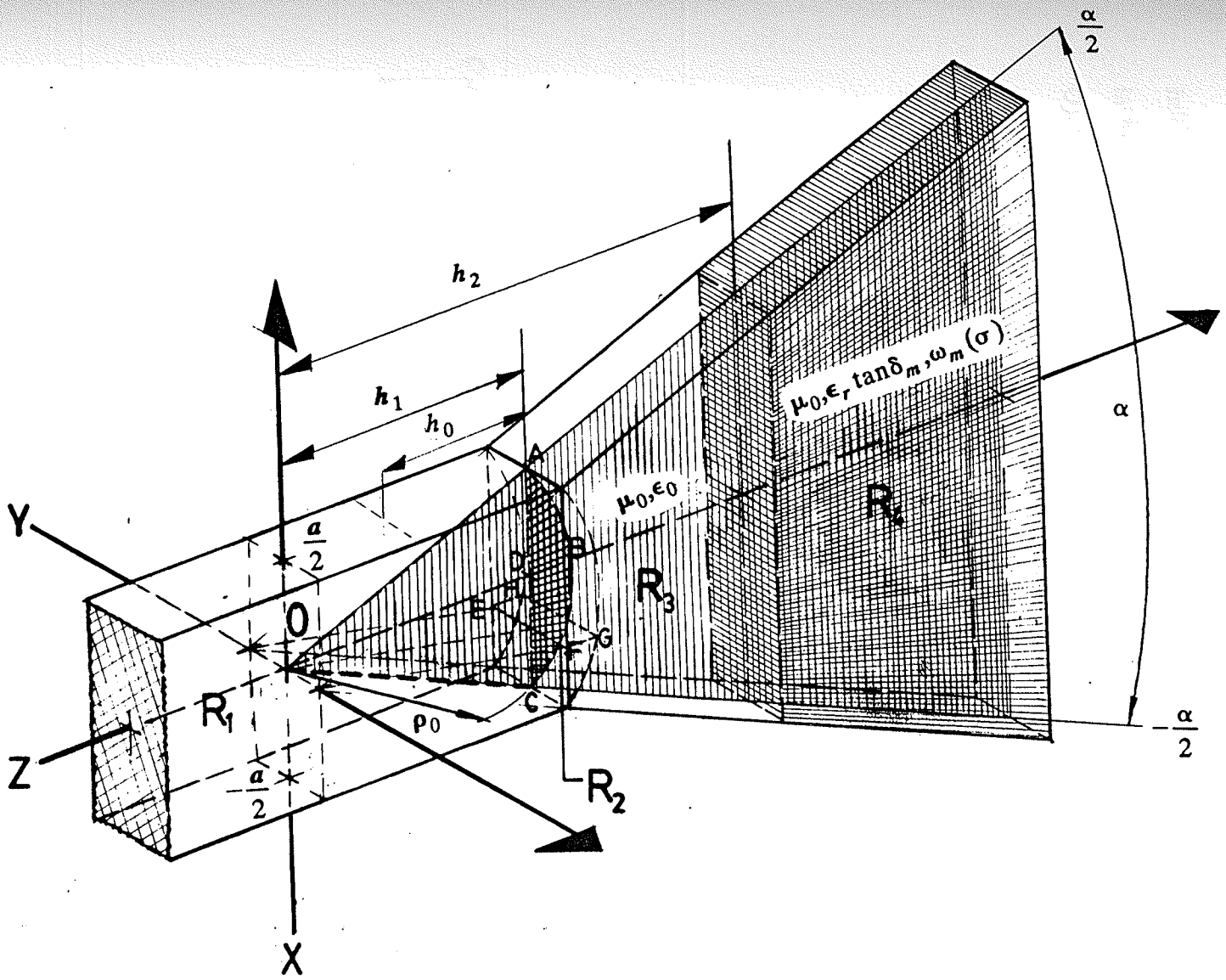

Fig.4.1. A LONGITUDINAL SEGMENT OF THE JUNCTION BETWEEN PARALLEL PLATE AND TRANSVERSELY LOADED SECTORAL WAVEGUIDES.

Initially, we let the dielectric discontinuity be over a half space oriented as shown in fig. 4.2 . The source of of the cylindrical wave is located at the origin (point O), which also denotes the apex of sectoral horn.

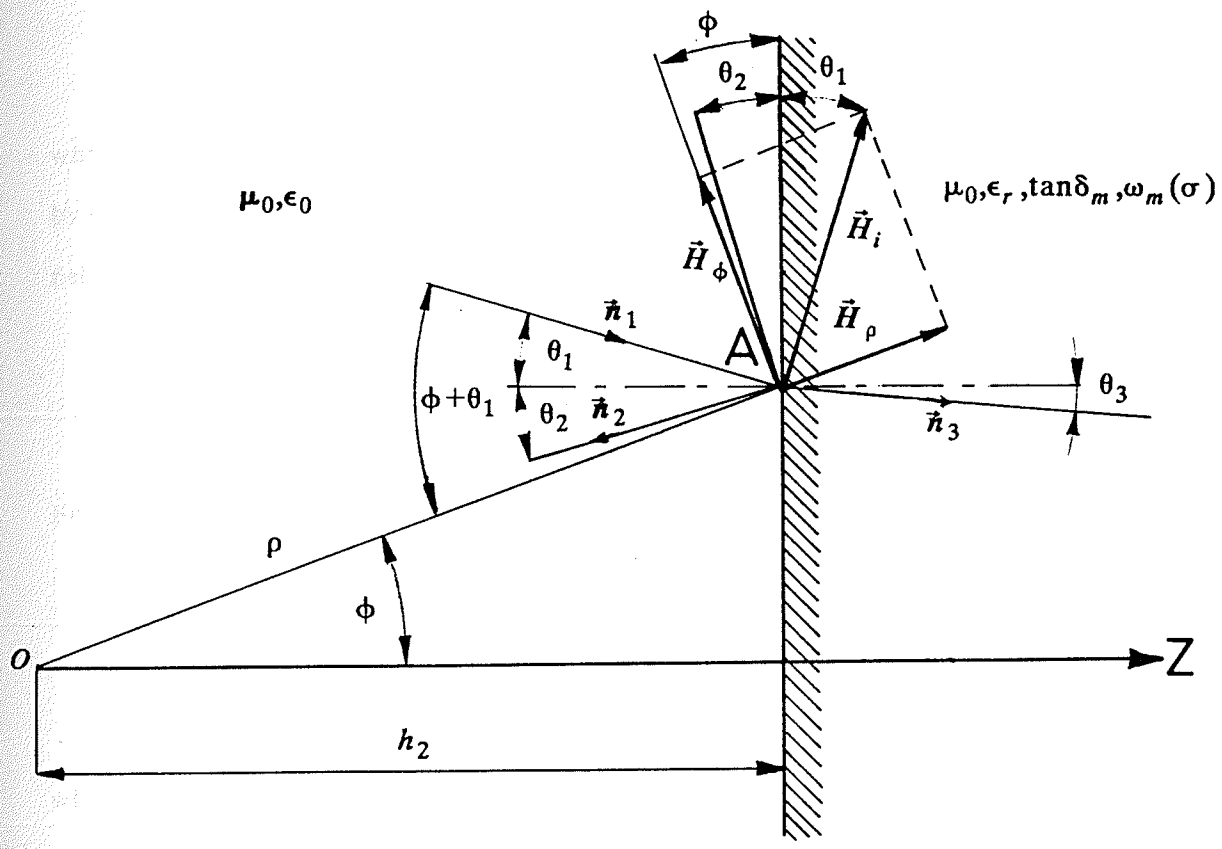

Fig. 4.2 A cylindrical electromagnetic wave incident upon half space.

The incident wave at the arbitrary point A is described by magnetic field components H_ρ and H_ϕ as shown in the figure. Since the electric field component E_y is perpendicular to the $\rho\phi$ plane, the incident electric field at the plane $z = h_2$ may be expressed in terms of the single coordinate ϕ, i.e.

$$E_y(z = h_2) = f(\phi) H_{m\nu}^{(2)}\left(\frac{kh_2}{\cos\phi}\right) \tag{4.4}$$

The wave at point A can be replaced by an equivalent plane wave in such a manner that the direction of propagation of the equivalent plane wave is given by

$$\hat{n}_1=\frac{\vec{E}_y\times\vec{H}_i}{\left[\vec{S}\right]} \tag{4.5}$$

where $\vec{S}$ denotes the Poynting vector at point A. The angle of incidence is found by considering either tangential ($\vec{H}_x$) or normal ($\vec{H}_z$) components of the magnetic field with respect to the air-dielectric interface at $z=h_2$ as shown in fig.4.2, i.e.

$$\sin\theta_1=\frac{H_\rho\cos\phi-H_\phi\sin\phi}{\sqrt{H_\rho^2+H_\phi^2}} \tag{4.6}$$

For point A the well known laws of reflection and refraction hold, i.e.

$$\theta_1=\theta_2 \tag{4.7}$$

$$\sin\theta_1=\eta\sin\theta_3 \tag{4.8}$$

where η denotes the complex index of refraction such that

$$\frac{1}{Z}=Y=Y_0\eta \tag{4.9}$$

while Z and Y denote the intrinsic impedance and admittance, respectively, for a propagating plane wave, and

$$Y_0=\sqrt{\frac{\epsilon_0}{\mu_0}}\,, \tag{4.10}$$

$$\eta=\sqrt{\epsilon_r(1-j\tan\delta)}\,, \tag{4.11}$$

$$\tan\delta=\frac{\sigma}{\omega\epsilon_0\epsilon_r} \tag{4.12}$$

for linear, homogeneous and isotropic dielectrics.

The index of refraction completely characterizes dielectric properties of the half space, $z > h_2$ (fig. 2.2). Continuity of the tangential electric field on the boundary requires that

$$E_1+E_2=E_3 \tag{4.13}$$

Continuity of the magnetic field tangential to the boundary gives

$$Y_0(E_1-E_2)\cos\theta_1=Y_0\eta E_3\cos\theta_3 \tag{4.14}$$

By using (4.8) the last equation takes the form

$$E_1-E_2=E_3\sqrt{\eta^2-\sin^2\theta} \tag{4.15}$$

which is the classical result [3, p.47].

Bearing in mind that along the surface $z=h_2$ the following identity holds

$$\frac{dE_y}{d\phi}=\frac{\partial E_y}{\partial\phi}+\frac{\partial E_y}{\partial\rho}\frac{d\rho}{d\phi} \tag{4.16}$$

and having found $\frac{\partial E_y}{\partial\phi}$ and $\frac{\partial E_y}{\partial\rho}$ from (4.2) - (4.3) and knowing that at $z=h_2$ the following holds

$$\frac{d\rho}{d\phi}=\frac{h_2\sin\phi}{\cos^2\phi} \tag{4.17}$$

we easily obtain

$$H_\rho\cos\phi-H_\phi\sin\phi=\frac{1}{j\omega\mu_0}\frac{\cos^2\phi}{h_2}\frac{dE_y}{d\phi} \tag{4.18}$$

By using (4.2), (4.3) and (4.16) the following identity is found

$$\vec{H}_\rho \cdot \vec{H}_\rho^{\,*} + \vec{H}_\phi \cdot \vec{H}_\phi^{\,*} =$$

$$= \frac{1}{(j\omega\mu_0)^2} \frac{1}{h_2^2 \tan^2\phi} \left[\left(\frac{\partial E_y}{\partial \phi} \right)^2 - 2\cos^2\phi \frac{dE_y}{d\phi} \frac{\partial E_y}{\partial \phi} + \cos^2\phi \left(\frac{dE_y}{d\phi} \right)^2 \right] \tag{4.19}$$

where $\vec{H}_\rho^{\,*}$ and $\vec{H}_\phi^{\,*}$ denote complex conjugate vectors. Upon substituting (4.18) and (4.19) into (4.6) the angle of incidence of the equivalent plane wave expressed in terms of differential parameters of an incident cylindrical wave at the dielectric discontinuity surface is found to be

$$\sin\theta_1 = \frac{\sin\phi\cos\phi \dfrac{dE_y}{d\phi}}{\sqrt{\left(\dfrac{\partial E_y}{\partial \phi} \right)^2 - 2\cos^2\phi \dfrac{dE_y}{d\phi} \dfrac{\partial E_y}{\partial \phi} + \cos^2\phi \left(\dfrac{dE_y}{d\phi} \right)^2}} \tag{4.20}$$

All derivatives in the above equation are with respect to the incident wave given by (4.4) . Let us express E_y as $E_y = T_m(\phi) H_{m\nu}^{(2)}(k\rho)$. Hence we can express the derivatives of (4.20), i. e.

$$\frac{dE_y}{d\phi} = \frac{dT_m(\phi)}{d\phi} H_{m\nu}^{(2)}\left(\frac{kh_2}{\cos\phi} \right) + T_m(\phi) \frac{d}{d\phi} \left[H_{m\nu}^{(2)}\left(\frac{kh_2}{\cos\phi} \right) \right] \tag{4.21}$$

$$\frac{\partial E_y}{\partial \phi} = \frac{\partial}{\partial \phi} [T_m(\phi) H_{m\nu}^{(2)}(k\rho)] = \frac{dT_m(\phi)}{d\phi} H_{m\nu}^{(2)}\left(\frac{kh_2}{\cos\phi} \right) \tag{4.22}$$

Introducing the notation $\alpha = \dfrac{1}{T_m(\phi)} \dfrac{dT_m(\phi)}{d\phi}$ and $\beta = \dfrac{1}{H_{m\nu}^{(2)}(\phi)} \dfrac{dH_{m\nu}^{(2)}(\phi)}{d\phi}$ after using (4.21) and (4.22), (4.20) is transformed into the form

$$\sin\theta_1 = \sqrt{\frac{\sin^2\phi(\alpha+\beta)^2}{\alpha^2\tan^2\phi + \beta^2}} \tag{4.23}$$

Let us express components of (4.13) and (4.14) in terms of the incident, reflected and transmitted wave at an arbitrary point, say A, of the dielectric discontinuity, i.e.

$$E_{my1}=T_{m1}H_{m\nu}^{(2)}\left(\frac{kh_2}{\cos\phi}\right) \tag{4.24}$$

$$E_{ym2}=T_{m1}(\phi)\Gamma_m(\phi)H_{m\nu}^{(1)}\left(\frac{kh_2}{\cos\phi}\right) \tag{4.25}$$

$$E_{ym3}=T_{m2}(\phi)H_{m\nu}^{(2)}\left(\frac{kh_2}{\cos\phi}\right) \tag{4.26}$$

where T_{m1} is an *a priori* known function. After substituting (4.23) - (4.26) into (4.13) and (4.14), the following system of equations is obtained

$$T_{m1}(\phi)H_{m\nu}^{(2)}\left(\frac{kh_2}{\cos\phi}\right)+T_{m1}(\phi)\Gamma_m(\phi)H_{m\nu}^{(1)}\left(\frac{kh_2}{\cos\phi}\right)=T_{m2}(\phi)H_{m\nu}^{(2)}\left(\frac{kh_2}{\cos\phi}\right) \tag{4.27}$$

$$T_{m1}(\phi)H_{m\nu}^{(2)}\left(\frac{kh_2}{\cos\phi}\right)-T_{m1}(\phi)\Gamma_m(\phi)H_{m\nu}^{(1)}\left(\frac{kh_2}{\cos\phi}\right)=$$

$$=T_{m2}(\phi)H_{m\nu}^{(2)}\left(\frac{kh_2}{\cos\phi}\right)\sqrt{\frac{\eta^2(\alpha^2\tan^2\phi+\beta^2)+\sin^2(\alpha+\beta)^2}{\alpha^2\tan^2\phi+\beta^2+\sin^2\phi(\alpha+\beta)^2}} \tag{4.28}$$

By solving the above system of equations we obtain the following expression for the unknown reflection and transmission coefficients,

$$\Gamma_m(\phi)=\frac{H_{m\nu}^{(2)}\left(\frac{kh_2}{\cos\phi}\right)}{H_{m\nu}^{(1)}\left(\frac{kh_2}{\cos\phi}\right)}\frac{\left[1-\sqrt{\frac{\eta^2(\alpha^2\tan^2\phi+\beta^2)+\sin^2(\alpha+\beta)^2}{\alpha^2\tan^2\phi+\beta^2+\sin^2\phi(\alpha+\beta)^2}}\right]}{\left[1+\sqrt{\frac{\eta^2(\alpha^2\tan^2\phi+\beta^2)+\sin^2(\alpha+\beta)^2}{\alpha^2\tan^2\phi+\beta^2+\sin^2\phi(\alpha+\beta)^2}}\right]} \tag{4.29}$$

$$T_{m2}(\phi)=\frac{2T_{m1}(\phi)}{\left[1+\sqrt{\frac{\eta^2(\alpha^2\tan^2\phi+\beta^2)+\sin^2(\alpha+\beta)^2}{\alpha^2\tan^2\phi+\beta^2+\sin^2\phi(\alpha+\beta)^2}}\right]} \tag{4.30}$$

In the above analysis it was assumed that the phase centre remains unchanged for the reflected and transmitted waves. In order to prove this, some additional investigation of the problem is necessary, which is beyond the scope of this thesis.

Equation (4.29) shows that exact analytical solution for reflection coefficient of a cylindrical wave is possible with respect to a certain class of discontinuities. The function $T_{m1}(\phi)$ depends on the condition of elctromagnetic cylindrical wave generation and must be known in advance.

It is necessary to point out that this approach to the problem is different from that presented by Fock in [28]. Fock based his analysis on the assumption that the amplitude of an arbitrary wave is slowly varing function of space coordinates, i.e. all spatial derivatives of the amplitude function approach zero. This assumption is prohibited in the above analysis and leads to very strong contradiction with physical essence of the problem, namely the magnetic field given by (4.3) would be equal to zero and the electromagnetic wave would no longer propagate as a cylindrical wave in the sectoral waveguide fed by the parallel plate waveguide. This would lead to an assumption that a line source is placed at the apex of the sectoral portion of the structure.

4.3 Formulation of the method of solution

Let us consider an arbitrarily chosen rectangle **EFGH** within the meniscus region R_2, fig.4.1 . The region R_2 coincides with the overlapping boundaries of the parallel plate and sectoral waveguides, (2.19.1) - (2.19.2).

Let the rectangle **EFGH** be always coherent with the cylindrical coordinate system. Applying Stokes' theorem to the above rectangle we may write

$$\int_{EFGH} \vec{E}_y \, d\vec{s} = \int_{\Delta S} (\nabla \times \vec{E}_y) d\vec{S} \tag{4.31}$$

using Maxwell's first equation

$$\nabla \times \vec{E}_y = -j\omega\mu_0 \vec{H} \tag{4.32}$$

and substituting (4.32) into (4.31) we obtain

$$\int_{EFGH} \vec{E}_y \cdot d\vec{s} = -j\omega\mu_0 \int_{\Delta S} \vec{H}_i \cdot d\vec{S} \tag{4.33}$$

From (4.2) and (4.3) it results that

$$\vec{H}_i = \vec{H}_\rho + \vec{H}_\phi = -\frac{1}{j\omega\mu_0}\left(\frac{1}{\rho}\frac{\partial E_y}{\partial \phi}\vec{a}_\rho - \frac{\partial E_y}{\partial \rho}\vec{a}_\phi\right) \tag{4.34}$$

According to fig. 4.3 we may write

$$d\vec{S} = \vec{n}\, dS = \vec{a}_\phi \cdot dS = \vec{a}_\phi d\rho dy \tag{4.35.1}$$

$$d\vec{s} = \vec{a}_y dy \quad on\ \text{EF} \tag{4.35.2}$$

$$d\vec{s} = -\vec{a}_y dy \quad on\ \text{GH} \tag{4.35.3}$$

$$d\vec{s} = \vec{a}_\rho dy \quad on\ \text{FG} \tag{4.35.4}$$

$$d\vec{s} = -\vec{a}_\rho dy \quad on\ \text{HE} \tag{4.35.5}$$

Substituting (4.34) and (4.35.1 - 4.35.5) into (4.33) the following equation is obtained

$$E_y\left(\frac{h_1}{\cos\phi}, \phi\right)\int_E^F \vec{a}_y \cdot \vec{a}_y dy + E_y(\rho, \phi)\int_F^G \vec{a}_\rho \cdot \vec{a}_y d\rho - E_y(\rho_0, \phi)\int_G^H \vec{a}_y \cdot \vec{a}_y dy - E_y(\rho, \phi)\int_H^E \vec{a}_\rho \cdot \vec{a}_y d\rho =$$

$$= \int_{\frac{h_1}{\cos\phi}}^{\rho_0}\int_E^F \left(\frac{1}{\rho}\frac{\partial E_y}{\partial \phi}\vec{a}_\rho - \frac{\partial E_y}{\partial \rho}\vec{a}_\phi\right)\vec{a}_\phi d\rho dy \tag{4.36}$$

where

$$\frac{h_1}{\cos\phi} \leq \rho \leq \rho_0$$

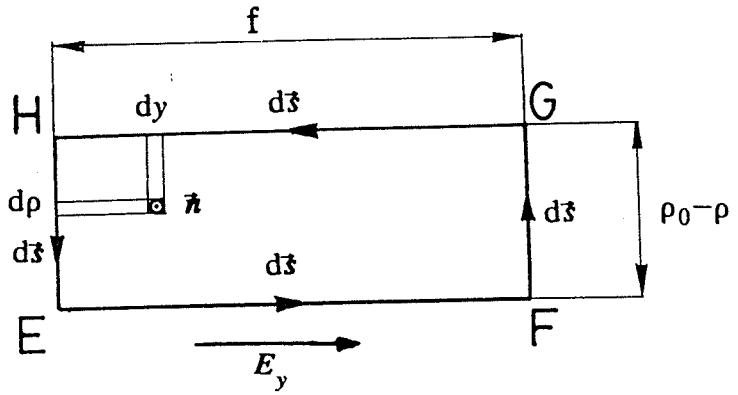

Fig. 4.3 Electric vector circulation about the rectangle EFGH in meniscus region R_2.

Since

$$\vec{a}_y \cdot \vec{a}_y = 1 \tag{4.37.1}$$

$$\vec{a}_\rho \cdot \vec{a}_y = 0 \tag{4.37.2}$$

$$\vec{a}_\rho \cdot \vec{a}_\phi = 0 \tag{4.37.3}$$

$$\vec{a}_\phi \cdot \vec{a}_\phi = 1 \tag{4.37.4}$$

(4.36) becomes a scalar equation of the form

$$E_y\left(\frac{h_1}{\cos\phi},\phi\right)\int_E^F dy - E_y(\rho_0,\phi)\int_G^H dy = -\int_{\frac{h}{\cos\phi}}^{\rho_0}\int_E^F \frac{\partial E_y(\rho,\phi)}{\partial\rho}\,d\rho\,dy \tag{4.38}$$

Applying to the RHS of (4.38) the formula

$$\frac{dE_y(\rho,\phi)}{d\rho}=\frac{dE_y(\rho,\phi)}{d\rho}-\frac{\partial E_y}{\partial\phi}\frac{d\phi}{d\rho} \tag{4.39}$$

we obtain

$$2E_y(\rho_0,\phi)=\frac{\partial E_y}{\partial\phi}\frac{d\phi}{d\rho}(\rho_0-\rho) \tag{4.40}$$

Next we recall Neumann's concept [19] that the field in the meniscus region R_2 is expressed as a sum of wave equation solutions in each region creating the considered structure, i.e. (3.9) and (3.18). Expressing both equations in the cylindrical coordinate system and denoting the first solution by E_{y1} and the second solution by E_{y2} we obtain

$$E_y(\rho,\phi)=E_{y1}(\rho,\phi)+E_{y2}(\rho,\phi) \tag{4.41}$$

By letting ρ_0 tend to $\rho=\frac{h_1}{\cos\phi}$ i.e. $z=h_1$ in (4.40) and using (4.41) the following equation (which is only valid on the "boundary" associated with the parallel plate waveguide) we find that

$$E_{y1}(\frac{h_1}{\cos\phi},\phi)+E_{y2}(\frac{h_1}{\cos\phi},\phi)=0 \tag{4.42}$$

Repeating the same procedure when ρ tends to ρ_0 we obtain

$$E_{y1}(\rho_0,\phi)+E_{y2}(\rho_0,\phi)=0 \tag{4.43}$$

Both equations hold for any arbitrary angle $-\frac{\alpha}{2}<\phi<\frac{\alpha}{2}$.

In recognition to the suggestion given by Lewin [11] the problem can be solved in any coordinate system, but an appropriate system is the cylindrical one

as shown in the next section. Equations (4.42) and (4.43) can be used as a basis for the field matching solution of the considered junction. It should also be pointed out that Rud' [29] solved the problem of wave diffraction at a T-junction of rectangular waveguides in the H −plane using a technique similar to the above and based on Green's second equation.

4.4 Behavior of the electromagnetic field in the transition region

Considering that the parallel plate waveguide feeds the horn-like waveguide and that continuity of electric field across "boundaries" is given by (4.42) and (4.43), the unknown total reflection coefficient Γ_m of (3.9) may be found by substituting (3.9) into the wave equation, (3.14) of the sectoral waveguide. First let us assume the following form of (3.9)

$$E_y = \left\{ e^{-j\gamma_p \rho \cos\phi} + \Gamma(\rho,\phi) \right\} \sin\left[p\pi \left(\frac{\rho \sin\phi}{a} + \frac{1}{2} \right) \right] \tag{4.44}$$

where the index p denotes an arbitrary single wave number. In order to substitute (4.44) into (3.14) the partial derivatives of (4.44) must be found, i.e.

$$\frac{\partial E_y}{\partial \rho} = \left(-j\gamma_p \cos\phi e^{-j\gamma_p \cos\phi} + \frac{\partial \Gamma}{\partial \rho} \right) \sin\left[p\pi \left(\frac{\rho \sin\phi}{a} + \frac{1}{2} \right) \right] +$$

$$+ \sin\phi \frac{p\pi}{a} \cos\left[p\pi \left(\frac{\rho \sin\phi}{a} + \frac{1}{2} \right) \right] \left\{ e^{-j\gamma_p \rho \cos\phi} + \Gamma \right\} \tag{4.45}$$

$$\frac{\partial^2 E_y}{\partial \rho^2} = \sin\left[p\pi \left(\frac{\rho \sin\phi}{a} + \frac{1}{2} \right) \right] \frac{\partial^2 \Gamma}{\partial \rho^2}$$

$$+ \frac{2p\pi \sin\phi}{a} \cos\left[p\pi \left(\frac{\rho \sin\phi}{a} + \frac{1}{2} \right) \right] \frac{\partial \Gamma}{\partial \rho}$$

$$-\frac{p^2\pi^2}{a}\sin^2\phi\sin\left[p\pi\left(\frac{\rho\sin\phi}{a}+\frac{1}{2}\right)\right]-j\frac{\gamma_p p\pi}{a}\sin 2\phi\cos\left[p\pi\left(\frac{\rho\sin\phi}{a}+\frac{1}{2}\right)\right]e^{-j\gamma_p\rho\cos\phi}$$

$$-\left(k^2\cos^2\phi-\frac{p^2\pi^2}{a_2}\cos 2\phi\right)\sin\left[p\pi\left(\frac{\rho\sin\phi}{a}+\frac{1}{2}\right)\right]\frac{\partial^2\Gamma}{\partial\rho^2} \qquad (4.46)$$

$$\frac{\partial^2 E_y}{\partial\phi^2}=-\left(k^2\sin^2\phi+\frac{p^2\pi^2}{a^2}\cos 2\phi+j\gamma_p\rho\cos\phi\right)\sin\left[p\pi\left(\frac{\rho\sin\phi}{a}+\frac{1}{2}\right)\right]e^{-j\gamma_p\rho\cos\phi}$$

$$+\frac{\partial^2\Gamma}{\partial\phi^2}\sin\left[p\pi\left(\frac{\rho\sin\phi}{a}+\frac{1}{2}\right)\right]-\frac{p\pi\rho}{a}\sin\phi\cos\left[p\pi\left(\frac{\rho\sin\phi}{a}+\frac{1}{2}\right)\right]e^{-j\gamma_p\rho\cos\phi}$$

$$-\left\{\frac{p\pi\rho}{a}\sin\phi\cos\left[p\pi\left(\frac{\rho\sin\phi}{a}+\frac{1}{2}\right)\right]+\frac{p^2\pi^2\rho^2}{a^2}\cos^2\phi\sin\left[p\pi\left(\frac{\rho\sin\phi}{a}+\frac{1}{2}\right)\right]\right\}\Gamma$$

$$+2\frac{p\pi\rho}{a}\cos\phi\cos\left[p\pi\left(\frac{\rho\sin\phi}{a}+\frac{1}{2}\right)\right]\frac{\partial\Gamma}{\partial\phi}$$

$$+j2\frac{\sin\phi\cos\phi p\pi\rho^2\gamma^p}{a}\cos\left[p\pi\left(\frac{\rho\sin\phi}{a}+\frac{1}{2}\right)\right]e^{-j\gamma_p\rho\cos\phi} \qquad (4.47)$$

Upon substituting (4.45) - (4.47) in to (3.14) we obtain in effect the following partial differential equation for the unknown reflection coefficient Γ

$$\frac{\partial^2\Gamma}{\partial\rho^2}+\left(\frac{2p\pi\sin\phi}{a\tan\Psi}+\frac{1}{\rho}\right)\frac{\partial\Gamma}{\partial\rho}+\left(k^2-\frac{p^2\pi^2}{a^2}\right)\Gamma+\frac{1}{\rho^2}\frac{\partial^2\Gamma}{\partial\phi^2}+\frac{2p\pi}{a\rho\tan\Psi}\cos\phi\frac{\partial\Gamma}{\partial\phi}=0 \qquad (4.48)$$

where

$$\Psi=p\pi\left(\frac{\rho\sin\phi}{a}+\frac{1}{2}\right) \qquad (4.48.1)$$

which is valid for $\rho \geq \frac{h_1}{\cos\phi}$ and $-\frac{\alpha}{2} < \phi < \frac{\alpha}{2}$. It is clear that this equation is nonlinear and not amenable to analytical solution by standard methods.

Let us assume that the electric field component is expressed in the form of the series (3.9),i.e. the m −th component in polar coordinate system equals

$$E_{ym} = \sin\left[p\pi\left(\frac{\rho\sin\phi}{a}+\frac{1}{2}\right)\right]e^{-j\gamma_p\rho\cos\phi} + \Gamma_m e^{j\gamma_m(\rho\cos\phi - h_1)}\sin\left[m\pi\left(\frac{\rho\sin\phi}{a}+\frac{1}{2}\right)\right]$$

(4.49)

Repeating the same procedure we get, after routine but lengthy calculations,

$$\frac{\partial^2\Gamma_m}{\partial\rho^2} + 2\left(\frac{m\pi\sin\phi}{a\tan\Psi} + j\gamma_m\cos\phi + \frac{1}{\rho}\right)\frac{\partial\Gamma_m}{\partial\phi} + \frac{1}{\rho^2}\frac{\partial^2\Gamma_m}{\partial\phi^2} + 2\left(\frac{m\pi}{a\rho\tan\Psi}\cos\phi - j\frac{\gamma_m\sin\phi}{\rho}\right)\frac{\partial\Gamma_m}{\partial\rho}$$

$$+2\left(\frac{m\pi\sin\phi}{a\rho\tan\Psi} - \gamma_m\cos^2\phi\right)\Gamma_m = \left[2\gamma_p^2 - j\frac{p\pi\gamma_p}{a}\sin 2\phi\left(1-\frac{1}{\tan\Psi}\right)\right]e^{-j\rho\cos\phi(\gamma_p+\gamma_m)+j\gamma_m h_1}$$

(4.50)

for $\rho \geq \frac{h_1}{\cos\phi}$ and $-\frac{\alpha}{2} < \phi < \frac{\alpha}{2}$, where Ψ is given by (4.48.1).

By comparing (4.48) and (4.50) we see the nonlinearity of the latter is with respect to both ρ and ϕ. The coefficients depend on the wave number m. Morever (4.50) is inhomogeneous.

Derivations of this section prove the nonlinear character of the reflection coefficient Γ_m and, related to it, the transmission coefficient T_m. In the scope of the above results the following can be stated:

- the reflection process in the junction is a nonlinear process and originates somewhere in the internal space of the junction due to interaction between incident and outgoing waves in the transitional region,

- for surfaces defined by a constant value of radius ρ or by a known function of ϕ the process reduces to a nonlinear ordinary differential equation with respect to the angle ϕ,

- Lewin's postulate [11] on the limits of orthogonal field expansion validity along certain boundaries has been proven by (4.50), although it is based on different reasoning than that of Lewin,

- in order to overcome all difficulties related to the problem it is necessary to treat this in one more dimension, i.e. solve the nonlinear partial differential equation (4.50) for each mode m,

- in the region of sectoral waveguide, there is no unique plane or surface on which reflection occurs.

4.5 Zero order reflection and transmission coefficients of the parallel plate-sectoral waveguide junction.

In the preceding section it is proven that the process of the electromagnetic field passage has nonlinear properties. Let us consider solution of (4.50) along surface $\rho=f(\phi)$. Along such a surface the reflection coefficient is a function of the angle ϕ for summation index m =constant. Instead of solving (4.48) or (4.50) it is suggested here to use a method of field matching at planes defined by $\phi=$ constant, such that the required coefficients will be found in terms of the variable angle ϕ.

In order to match the fields of the two considered waveguides a certain equation, to be shown in this section, must be fulfilled along boundaries, where the electric vector is continous [11].

Zero order reflection and transmision coefficients are defined as those of the junction between parallel plate and infinite sectoral waveguides.

From the continuity equations (4.42) and (4.43) we are allowed to match electric fields expressed by the solution of the wave equation associated with regions of interest. Using (3.7) to express the electric field in the parallel plate waveguide and (3.18) in the sectoral waveguide, and transforming the first into the polar coordinate system (since the problem is reduced to two dimensions) and substituting into (4.42) and (4.43), we find a system of equations for the unknown reflection and transmission coefficients.

Instead of an orthogonal series expansion in the "Zwischenmedium" region [17] containing meniscus region R_2, let as assume that the solutions are represented by their first harmonics and nonlinear reflection and transmission coefficients, $\Gamma(\phi)$ and $T(\phi)$, respectively. $\Gamma(\phi)$ and $T(\phi)$ are continuous functions having continuous derivatives in the interval $[-\frac{\alpha}{2},\frac{\alpha}{2}]$. Both assumptions mathematically mean that the series corresponding to $\Gamma(\phi)$ and $T(\phi)$ are their

appropriate series representations. According to the above, equation (3.7) is expressed in the meniscus region R_2 by

$$E_y^0=[e^{-j\gamma_p z}+\Gamma^0(\phi)e^{j\gamma_p z}]\sin\left[p\,\Pi\left(\frac{\tan\phi}{\tan\frac{\alpha}{2}}+\frac{1}{2}\right)\right] \tag{4.51}$$

and equation (3.18) by

$$E_y^0=T^0(\phi)\sin\left[p\,\Pi\left(\frac{\phi}{\alpha}+\frac{1}{2}\right)\right]H_{p\nu}^{(2)}(k\rho) \tag{4.52}$$

where p denotes the number of forward propagating single modes supported by the parallel plate waveguide. In further analysis it is assumed that $p=1$ according to (3.9).

Since the preceding section shows that in the meniscus region R_2 there is no unique plane on which reflection occurs, let us arbitrarily assume that it is located at $z=h_1$. In order to have a solution suitable for experimental verification at this stage, a location of reference plane at the parallel plate region R_1 must be assumed. Let us denote this plane by $z=h_0$ such that $h_0<h_1$, (fig. 4.1).

Applying the above assumptions, the considered system of equation has the form:

$$\sin\left[\frac{\pi}{2}\left(\frac{\tan\phi}{\tan\frac{\alpha}{2}}+1\right)\right]e^{j\gamma_1 2(h_0-h_1)}\Gamma_1^0(\phi)+$$

$$+\sin\left[\pi\left(\frac{\phi}{\alpha}+\frac{1}{2}\right)\right]H_\nu^{(2)}\left(\frac{kh_1}{\cos\phi}\right)T^0(\phi)=$$

$$=-e^{-j\gamma_1(h_1-h_0)}\sin\left[\frac{\pi}{2}\left(\frac{\tan\phi}{\tan\frac{\alpha}{2}}+1\right)\right] \tag{4.53}$$

which is valid along $z = h_1$ or $\rho = \frac{h_1}{\cos\phi}$ by virtue of (4.42), and

$$-\sin\left[\frac{\pi}{2}\left(\frac{\tan\phi}{\tan\frac{\alpha}{2}}+1\right)\right]e^{j\gamma_1 2(h_0-h_1)}\Gamma_1^0(\phi)$$

$$+\sin\left[\pi\left(\frac{\phi}{\alpha}+\frac{1}{2}\right)\right]H_\nu^{(2)}(k\rho_0)T^0(\phi)=$$

$$=-e^{-j\gamma_1(\rho_0\cos\phi-h_0)}\sin\left[\frac{\pi}{2}\left(\frac{\sin\phi}{\sin\frac{\alpha}{2}}+1\right)\right] \tag{4.54}$$

valid along $z = \rho_0\cos\phi$ or $\rho = \rho_0$ by (4.43), where $\Gamma_1^0(\phi)$ denotes the zero order transmission coefficient of the junction under consideration, $T^0(\phi)$ denotes the zero order transmission coefficient from parallel plate to sectoral waveguide and $h_1 \geq h_0 \geq 0$.

Solving the above system of equations which have parametric coefficients with respect to the angle ϕ, the coefficients of interest are obtained:

$$\Gamma_1^0(\phi)=-\frac{e^{-j\gamma_1(\rho_0\cos\phi-h_1)}f_1(\phi)f_2(\phi)-1}{f_1(\phi)+1}e^{j\gamma_1(h_1-h_0)} \tag{4.55}$$

and

$$T^0(\phi)=-\frac{e^{-j\gamma_1(\rho_0\cos\phi-h_1)}f_2(\phi)+1}{H_\nu^{(2)}(k\rho_0)[1+f_1(\phi)]}\frac{\sin\left[\frac{\pi}{2}\left(\frac{\tan\phi}{\tan\frac{\alpha}{2}}+1\right)\right]}{\sin\left[\frac{\pi}{2}\left(\frac{\phi}{\alpha}+\frac{1}{2}\right)\right]}e^{j\gamma_1(h_1-h_0)} \tag{4.56}$$

where

$$f_1(\phi)=\frac{H_\nu^{(2)}\left(\frac{kh_1}{\cos\phi}\right)}{H_\nu^{(2)}(k\rho_0)} \quad , \tag{4.57}$$

$$f_2(\phi)=\frac{\sin\left[\frac{\pi}{2}\left(\frac{\sin\phi}{\sin\frac{\alpha}{2}}+1\right)\right]}{\sin\left[\frac{\pi}{2}\left(\frac{\tan\phi}{\tan\frac{\alpha}{2}}+1\right)\right]} \tag{4.58}$$

and

$$\nu=\frac{\pi}{\alpha} \tag{4.59}$$

Substituting (4.55) and (4.56) into (4.51) and (4.52) respectively, we obtain two equivalent field representations in meniscus region R_2, which match the fields: given by (3.9) at $z=h_1=h_0$ and by (3.18) at $\rho=\rho_0$. The first of them is that of parallel plate region R_1 and is given by

$$E_y^0=\sin\left[\pi\left(\frac{x}{a}+\frac{1}{2}\right)\right]\left(1+\Gamma^0(x)\right) \quad , \tag{4.60}$$

where

$$\Gamma^0(x)=-\frac{e^{-j\gamma_1\left(\frac{\rho_0^2\cos\frac{\alpha}{2}}{\sqrt{x^2+\rho_0^2\cos^2\frac{\alpha}{2}}}-h_1\right)}f_1(x)f_2(x)-1}{f_1(x)+1} \quad , \tag{4.61}$$

is the uncorrected reflection coefficient at point x .

Functions $f_1(x)$ and $f_2(x)$ may be obtained from (4.57) and (4.58) by replacing functions of ϕ by

$$\sin(\phi)=\frac{x}{\sqrt{x^2+\rho_0^2\cos^2\frac{\alpha}{2}}} \tag{4.62}$$

$$\cos(\phi)=\frac{\rho_0\cos\frac{\alpha}{2}}{\sqrt{x^2+\rho_0^2\cos^2\frac{\alpha}{2}}} \tag{4.63}$$

$$\tan(\phi)=\frac{x}{\rho_0\cos\frac{\alpha}{2}} \tag{4.64}$$

The second field representation is that of the sectoral region R_3 and is given by

$$E(\phi)=T^0(\phi)\sin\left[\frac{\pi}{2}\left(\frac{\tan\phi}{\tan\frac{\alpha}{2}}+1\right)\right]H_\nu^{(2)}(k\rho_0) \tag{4.65}$$

where $T^0(\phi)$ is given by

$$T^0(\phi)=-\frac{e^{-j\gamma_1(\rho_0\cos\phi-h_1)}f_2(\phi)+1}{H_\nu^{(2)}(k\rho_0)[1+f_1(\phi)]} \tag{4.66}$$

Equations (4.60) and (4.61) clearly show that the amplitude of the reflected wave is nonuniform with respect to the transverse coordinate of the parallel plate waveguide x. A distortion of the amplitude of reflected wave depends on the parameters of sectoral waveguide (or junction) i.e. the flare angle α and, strictly connected with it, location of the apex of the sectoral part, h_1 and ρ_0.

The transmitted wave has modified amplitude factor in (4.65) which depends on the character of the sectoral feed region.

If the reference plane does not coincide with $z=h_1$ the phase correction coefficients are necessary, i.e. $e^{j\gamma_1(h_1-h_0)}$ for reflection coefficient (4.55) and $e^{-j\gamma_1(h_1-h_0)}$ for transmission coefficient (4.56).

There are two possibilities:

- to convert the obtained expressions for the electric field, (4.61) in region R_1 and (4.66) in region R_3, into classical form of Fourier series expansion, or in general orthogonal expansion, and find total zero order reflection and transmission coefficients in the form of series, or
- to use the form of solution given by (4.51) and (4.52) (i.e. nonlinear coefficient and first term of expansion) to find total reflection and transmission coefficients by integration over the required interval.

Both methods are alternative. However for further consideration the second method is chosen due to the ease of finding the zero order reflection coefficient $\Gamma_2^0(\phi)$ on the dielectric boundary and first order coefficients due to multiple scattering in presence of dielectrics.

4.6 Inverse scattering at the dielectric boundary

The zero order reflection coefficient $\Gamma_2^0(\phi)$ is to be determined using the method of section 4.2 . Equation (4.39) expresses the reflection coefficient in terms of parameters α and β of the incident wave. By substituting (4.66) into (4.65) the electric field of an empty infinite sectoral waveguide is obtained as

$$E^o(\phi)=-\frac{e^{-j\gamma_1(\rho_0\cos\phi-h_1)}f_1(\phi)f_2(\phi)-1}{H_\nu^{(2)}(k\rho_0)[f_1(\phi)+1]}\sin\left[\frac{\pi}{2}\left(\frac{\tan\phi}{\tan\frac{\alpha}{2}}+1\right)\right]H_\nu^{(2)}(k\rho) \qquad (4.67)$$

for $z = h_1 = h_0$,

where

$$f_1(\phi) = \frac{H_\nu^{(2)}\left(\frac{kh_1}{\cos\phi}\right)}{H_\nu^{(2)}(k\rho_0)} \quad . \tag{4.68}$$

Knowing that the phase factor of such a wave at the dielectric interface is equal to $H_\nu^{(2)}\left(\frac{kh_2}{\cos\phi}\right)$ the unknown differential coefficients, α and β, may be found. The coefficient α is equal to

$$\alpha(\phi) = \frac{e^{-j\gamma_1(\rho_0\cos\phi - h_1)} j\gamma_1\rho_0 \sin\phi \sin[\Psi_1(\phi)] + \frac{\pi}{2\sin\frac{\alpha}{2}} \cos\phi\cos[\Psi_1(\phi)]]}{e^{-j\gamma_1(\rho_0\cos\phi - h_1)}\sin[\Psi_1(\phi)] + \sin[\Psi_2(\phi)]}$$

$$+ \frac{\frac{\pi}{2\tan\frac{\alpha}{2}\cos^2\phi}\cos[\Psi_2(\phi)]}{e^{-j\gamma_1(\rho_0\cos\phi - h_1)}\sin[\Psi_1(\phi)] + \sin[\Psi_2(\phi)]} - \frac{\frac{d}{d\phi}\left[H_\nu^{(2)}\left(\frac{kh_1}{\cos\phi}\right)\right]}{H_\nu^{(2)}(k\rho_0) + H_\nu^{(2)}\left(\frac{kh_1}{\cos\phi}\right)} \quad , \tag{4.69}$$

where

$$\Psi_1(\phi) = \frac{\pi}{2}\left(\frac{\sin\phi}{\sin\frac{\alpha}{2}} + 1\right) \tag{4.70.1}$$

and

$$\Psi_2(\phi) = \frac{\pi}{2}\left(\frac{\tan\phi}{\tan\frac{\alpha}{2}} + 1\right) \quad . \tag{4.70.2}$$

The functions $f_1(\phi)$ and $f_2(\phi)$ are given by (4.57) and (4.58), respectively. Using a reccurence formula given by [31] the derivative of (4.70) is equal to:

$$\frac{d}{d\phi}\left[H_\nu^{(2)}\left(\frac{kh_1}{\cos\phi}\right)\right]=\tan\phi\left[\frac{kh_1}{\cos\phi}H_{\nu-1}^{(2)}\left(\frac{kh_1}{\cos\phi}\right)-\frac{\pi}{\alpha}H_\nu^{(2)}\left(\frac{kh_1}{\cos\phi}\right)\right] \qquad (4.71)$$

The coefficient β equals

$$\beta(\phi)=\tan\phi\left[\frac{kh_2}{\cos\phi}\frac{H_{\nu-1}^{(2)}\left(\frac{kh_2}{\cos\phi}\right)}{H_\nu^{(2)}\left(\frac{kh_2}{\cos\phi}\right)}-\frac{\pi}{\alpha}\right], \qquad (4.72)$$

where

$$-\frac{1}{2}\pi<-\frac{\alpha}{2}<\phi<\frac{\alpha}{2}<\frac{1}{2}\pi \ .$$

Having found the coefficients α and β, the zero order reflection coefficient due to the dielectric discontinuity $\Gamma_2^0(\phi)$, is given by

$$\Gamma_2^0(\phi)=\frac{H_\nu^{(2)}\left(\frac{kh_2}{\cos\phi}\right)}{H_\nu^{(1)}\left(\frac{kh_2}{\cos\phi}\right)}\frac{\left[1-\sqrt{\frac{\eta^2+f_3(\phi)}{1+f_3(\phi)}}\right]}{\left[1+\sqrt{\frac{\eta^2+f_3(\phi)}{1+f_3(\phi)}}\right]}, \qquad (4.73)$$

where

$$f_3(\phi)=\frac{(\alpha+\beta)^2}{\left(\frac{\alpha}{\cos\phi}\right)^2+\left(\frac{\beta}{\sin\phi}\right)^2}, \qquad (4.73.1)$$

with α and β given by (4.70) and (4.72), respectively.

From (4.73) it follows that the reflection coefficient at a point on the dielectric interface depends on three complex functions:

- index of refraction, η, which in general is function of frequency, ω,
- ratio of two Hankel functions being function of the distance h_2 at which the interface is located,
- function $f_3(\phi)$ being dependent on the angle of incidence ϕ of the cylindrical wave.

In further analysis we will consider the problem of finding an appropriate model of dielectric properties of the medium. Let us consider first a dipolar model. The well known Debye's formula [32] for such dielectrics has the form

$$\tan\delta=\tan\delta_m \frac{2\frac{\omega}{\omega_m}}{1+\left(\frac{\omega}{\omega_m}\right)^2}, \tag{4.74}$$

where ω_m is the angular frequency at which maximum loss angle $\tan\delta_m$ occurs. The high frequency dielectric constant $\epsilon_r=\epsilon_\infty$ in many practical cases is constant [32, p. 101]. After substituting (4.74) into (4.11) we obtain the following equation for the complex index of refraction.

$$\eta=\left\{\epsilon_r\left[1-\frac{\tan\delta_m}{\epsilon_r}\frac{2\frac{\omega}{\omega_m}}{1+\left(\frac{\omega}{\omega_m}\right)}\right]\right\}^{\frac{1}{2}}. \tag{4.75}$$

In order to obtain the general solution for the reflection coefficient, given by (4.55), the problem of inverse scattering at the dielectric discontinuity, $z=h_2$, must be solved first. Therefore the appropriate common order of equations used for computation of the total reflection and transmission coefficients is as follows: (4.59), (4.62), (4.63), (4.64), (4.70.1), (4.70.2), (4.70), (4.72), (4.75), and (4.73) keeping in mind that equation (4.55) is issued for the reflection coefficient and (4.56) for the transmission coefficient.

The total reflection coefficient of the parallel plate waveguide is given in the next section.

4.7 The total reflection and transmission coefficients in the presence of transverse dielectric loading in the near field.

The near field is understood to be the sectoral region where $k\rho<8$. The total electric field in the sectoral region is given

$$E_y=T_t(\phi)\sin\Psi_2 H_2^{(2)}(k\rho)+\Gamma_2^0(\phi)\sin\Psi_2 H_\nu^{(1)}(k\rho)\ , \tag{4.76}$$

where Ψ_2 is given by (4.75).

The total transmission coefficient at the junction is equal to

$$T_t(\phi)=T^0(\phi)+T^1(\phi)+\sum_{n=2}^{\infty}T^n(\phi)\ , \tag{4.77}$$

where

T^0 is transmission coefficient of an infinite sectoral waveguide,

T^1 is the first order inverse transmission coefficient at the junction for backward travelling wave in sectoral region, R_3.

Similarily, the total electric field in the parallel plate region R_1 is given by

$$E_y = \sin\left[\frac{\pi}{2}\left(\frac{x}{a}+\frac{1}{2}\right)\right]\left[e^{-j\gamma_{1z}z}+\Gamma_{1t}e^{j\gamma_{1z}z}\right], \tag{4.78}$$

where

$$\Gamma_{1t}(\phi)=\Gamma_1^0(\phi)+\Gamma_1^1(\phi)+\sum_{m=2}^{\infty}\Gamma_1^n(\phi)\ . \tag{4.79}$$

Both (4.77) and (4.79) are a result of multiple scattering occuring in the closed region R_3. It is well known fact that, for a number of practical purposes, the resultant reflection coefficient is just that obtained by taking only first order reflection into account [3,pp.224-233] since all higher order terms of (4.79) are dependent on the inverse transmission coefficient $T^1(\phi)$, which is small. Therefore we are allowed to neglect second and higher order components in (4.77) and (4.79).

In order to find the first order reflection and transmission coefficients we are allowed to apply once again Neumann's concept to region R_2 with overlapping boundaries. This time the first order inverse transmission coefficient $T^1(\phi)$ and first order reflection coefficient $\Gamma_1^1(\phi)$ of the junction are caused by reflection of the round interface $\rho=\rho_0$ associated with the polar coordinate system and transmission through the meniscus region of the back travelling wave. Therefore we may write the folowing system of equations for both sides of meniscus region R_2:

$$\Gamma_1^1(\phi)\sin\Psi_1 e^{-j\gamma_1(\rho_0\cos\phi-h_1)}+T^1(\phi)\sin\Psi_2 H_\nu^{(2)}(k\rho_0)=$$

$$=-\Gamma_2^0(\phi)\sin\Psi_2 H_\nu^{(1)}(k\rho_0)\ , \tag{4.80}$$

at $\rho=\rho_0$ and

$$\Gamma_1^1(\phi)\sin\Psi_2 - T^1(\phi)\sin\Psi_2 H_\nu^{(2)}(k\rho_0) =$$

$$= -\Gamma_2^0(\phi)\sin\Psi_2 H_\nu^{(1)}\left(\frac{kh_1}{\cos\phi}\right), \tag{4.81}$$

at $\rho = \dfrac{h_1}{\cos\phi}$.

From the above, the reflection coefficient $\Gamma_1^1(\phi)$ is found, i.e.

$$\Gamma_1^1(\phi) = -\Gamma_2^0(\phi)\frac{H_\nu^{(1)}\left(\dfrac{kh_1}{\cos\phi}\right) + H_\nu^{(1)}(k\rho_0)}{e^{-j\gamma_1(\rho_0\cos\phi - h_1)}f_2(\phi) + 1} \tag{4.82}$$

as well as the inverse transmission coefficient $T^1(\phi)$

$$T^1(\phi) = \Gamma_2^0(\phi)\left[\frac{H_\nu^{(1)}\left(\dfrac{kh_1}{\cos\phi}\right) - H_\nu^{(1)}(k\rho_0)}{H_\nu^{(2)}\left(\dfrac{kh_1}{\cos\phi}\right) + H_\nu^{(2)}(k\rho_0)} - \frac{e^{-j\gamma_1(\rho_0\cos\phi - h_1)}f_2(\phi) - 1}{e^{-j\gamma_1(\rho_0\cos\phi - h_1)}f_2(\phi) + 1}\right] \tag{4.83}$$

According to the preceding analysis the total reflection coefficient of the waveguide region R_1 is given by

$$\Gamma_{1t}(\phi) = \Gamma_1^0(\phi) + \Gamma_1^1(\phi) \tag{4.84}$$

and the total transmission coefficient is given by

$$T_t(\phi) = T^0(\phi) + T_1^1(\phi) \ , \tag{4.85}$$

where

$\Gamma_1^0(\phi)$ and $\Gamma_1^1(\phi)$ are given by (4.56) and (4.82) while $T^0(\phi)$ and $T_1(\phi)$ are given by (4.55) and (4.83), respectively.

The analysis of components involving Hankel functions is given in the next chapter in order to ascertain the most efficient form for computation.

CHAPTER 5

Analysis of the Solution

5.1 The total reflection coefficient

Further consideration will be confined to the reflection coefficients $\Gamma_1(x)$ and $\Gamma_2(x)$ to achieve the purpose of the thesis stated in introduction (chapter 1). The complex reflection coefficient $\Gamma(x)$ given by (4.61) at a point depends on other complex functions such as $f_1(\phi)$, $\Gamma_2(\phi)$ and $f_3(\phi)$ given by (4.57), (4.73) and (4.73.1), respectively.

Since the reflection coefficient is nonuniform with respect to the transverse coordinate x in waveguide region R_1, the equivalent uniform coefficient of interest must be found in order to compare with classical results and experiment.

The uniform reflection coefficient may be defined by

$$\Gamma_t = \frac{1}{a} \int_{-\frac{\alpha}{2}}^{\frac{\alpha}{2}} \Gamma(\phi) d\phi \tag{5.1}$$

in the region R_2 at $z = h_1$ or

$$\Gamma_t = \frac{1}{a} \int_{-\frac{a}{2}}^{\frac{a}{2}} \Gamma(x) dx \tag{5.2}$$

everywhere in the waveguide region R_1 at $z < h_1$.

Because of the complexity of the integrand functions in (5.1) and (5.2), integration may be carried out using an adequate numerical procedure. The integrand must be free of singularities, i.e. analytical in the interval of integration.

The integral given by (5.1) or (5.2) may be evaluated by using the well known inequality [36]

$$\left| \int_C \Gamma(\phi) d\phi \right| \leq \int_C |\Gamma(\phi)| d\phi \leq |\Gamma|_m \quad , \tag{5.3}$$

where $|\Gamma|_m$ is the upper bound of the modulus. After substituting (5.3) into (5.1) the uniform reflection coefficient is given by

$$\Gamma_t \leq \frac{1}{a} \int_{-\frac{\alpha}{2}}^{\frac{\alpha}{2}} |\Gamma(\phi)| d\phi \leq \frac{1}{a} |\Gamma|_m \tag{5.4}$$

The dependence of the total reflection coefficient on the transverse coordinate is given by (4.81) and shows that the result may be considered as a correction factor to the traditional cosine multiplier.

5.2 Analysis of components involving Hankel functions

Before applying numerical treatment of the results, some additional investigation is necessary in order to determine both convergence and the most suitable form of the solution for numerical treatment. Since the Hankel functions are defined by series, involving them components determine convergence of solution.

Let us consider all components of the solution involving Hankel functions. Function $f_1(\phi)$ given by (4.57) is a function of ratio of Hankel functions. The component of $\alpha(\phi)$, (4.70), containing Hankel functions, may be denoted by $\alpha_{13}(\phi)$, and may be expressed in a form dependent on the ratio of Hankel functions,i.e.

$$\alpha_{13}(\phi)=\tan\phi\,\frac{\left[\dfrac{kh_1}{\cos\phi}\,\dfrac{H_{\nu-1}^{(2)}\left(\dfrac{kh_1}{\cos\phi}\right)}{H_{\nu}^{(2)}\left(\dfrac{kh_1}{\cos\phi}\right)}-\dfrac{\pi}{\alpha}\right]}{\left[1+\dfrac{H_{\nu}^{(2)}(k\rho_0)}{H_{\nu}^{(2)}\left(\dfrac{kh_1}{\cos\phi}\right)}\right]}\quad . \tag{5.5}$$

From (4.72), (4.73), and (5.5) it is clearly seen that all equations depend on the ratio of two Hankel functions. Hence properties of these ratios must be examined.

By applying Cauchy's residue theorem to Sommerfeld integral representation of Hankel functions, Debye [24] obtained the following series representations

$$H_{\nu}^{(1)}(k\rho)=\frac{1}{\pi}e^{jk\rho(\sin\tau_0-\tau_0\cos\tau_0)}\times\sum_{n=0}^{n=N}A_n(\tau_0)\frac{e^{-j(2n+1)\frac{\pi}{4}}\Gamma(n+\frac{1}{2})}{\left(\frac{k\rho}{2}\sin\tau_0\right)^{(n+\frac{1}{2})}} \tag{5.6}$$

and

$$H_{\nu}^{(2)}(k\rho)=\frac{1}{\pi}e^{-jk\rho(\sin\tau_0-\tau_0\cos\tau_0)}\times\sum_{n=0}^{n=N}A_n(\tau_0)\frac{e^{j(2n+1)\frac{\pi}{4}}\Gamma(n+\frac{1}{2})}{\left(\frac{k\rho}{2}\sin\tau_0\right)^{(n+\frac{1}{2})}}\quad , \tag{5.7}$$

where

$$A_0(\tau_0)=1\quad , \tag{5.8.1}$$

$$A_1(\tau_0)=\frac{1}{8}+\frac{5}{24}\frac{1}{\tan^2\tau_0} \quad , \tag{5.8.2}$$

$$A_2(\tau_0)=\frac{3}{128}+\frac{7}{576}\frac{1}{\tan^2\tau_0}+\frac{385}{3456}\frac{1}{\tan^4\tau_0} \quad , \tag{5.8.3}$$

. . .

for

$$\cos\tau_0=\frac{\nu}{k\rho}=\frac{\pi}{\alpha k\rho}<1 \tag{5.9}$$

Using equations (5.6), (5.7), (5.8.1) and (5.8.2) the ratios of Hankel functions of interest are to be replaced by

$$\frac{H_\nu^{(2)}\left(\frac{kh_1}{\cos\phi}\right)}{H_\nu^{(2)}(k\rho_0)}=e^{j\left[\frac{kh_1}{\cos\phi}(\sin\tau_1-\tau_1\cos\tau_1)-k\rho_0(\sin\tau_2-\tau_2\cos\tau_2)\right]}\times\frac{f^{(2)}(\tau_1)}{f^{(2)}(\tau_2)} \quad , \tag{5.10}$$

in (4.57),

$$\frac{H_\nu^{(1)}\left(\frac{kh_1}{\cos\phi}\right)}{H_\nu^{(1)}(k\rho_0)}=e^{j[\frac{kh_1}{\cos\phi}(\sin\tau_1-\tau_1\cos\tau_1)-k\rho_0(\sin\tau_2-\tau_2\cos\tau_2)]}\times\frac{f^{(1)}(\tau_1)}{f^{(1)}(\tau_2)} \tag{5.11}$$

and by

$$\frac{H_\nu^{(1)}(k\rho_0)}{H_\nu^{(2)}(k\rho_0)}=e^{j2k\rho_0(\sin\tau_2-\tau_2\cos_2)}\times\frac{f^{(1)}(\tau_2)}{f^{(2)}(\tau_2)} \quad , \tag{5.12}$$

in (4.82), where

$$\cos\tau_1=\frac{\pi\cos\phi}{\alpha kh_1} \quad , \tag{5.13}$$

$$\cos\tau_2=\frac{\pi}{\alpha k\rho_0} \quad , \tag{5.14}$$

and

$$f^{(1,2)}(\tau_1)=\frac{e^{(-,+)j\frac{\pi}{4}}\Gamma(\frac{1}{2})}{\left(\frac{kh_1}{2\cos\phi}\sin\tau_1\right)^{\frac{1}{2}}}+\left(\frac{1}{8}+\frac{5}{24}\frac{1}{\tan^2\tau_1}\right)\frac{e^{(-,+)j\frac{3\pi}{4}}\Gamma\left(\frac{3}{2}\right)}{\left(\frac{kh_1}{2\cos\phi}\sin\tau_1\right)^{\frac{3}{2}}}+$$

$$+\left(\frac{3}{128}+\frac{7}{576}\frac{1}{\tan^2\tau_1}+\frac{385}{3456}\frac{1}{\tan^4\tau_1}\right)\frac{e^{(-,+)j\frac{5\pi}{4}}\Gamma\left(\frac{5}{2}\right)}{\left(\frac{kh_1\sin\tau_1}{2\cos\phi}\right)^{\frac{5}{2}}}+\ldots \qquad (5.15)$$

$$f^{(1,2)}(\tau_2)=\frac{e^{(-,+)j\frac{\pi}{4}}\Gamma(\frac{1}{2})}{\left(\frac{k\rho_0\sin\tau_2}{2}\right)^{\frac{1}{2}}}+\left(\frac{1}{8}+\frac{5}{24}\frac{1}{\tan^2\tau_2}\right)\frac{e^{(-,+)j\frac{3\pi}{4}}\Gamma\left(\frac{3}{2}\right)}{\left(\frac{k\rho_0\sin\tau_2}{2}\right)^{\frac{3}{2}}}+$$

$$+\left(\frac{3}{128}+\frac{7}{576}\frac{1}{\tan^2\tau_2}+\frac{385}{3456}\frac{1}{\tan^4\tau_2}\right)\frac{e^{(-,+)j\frac{5\pi}{4}}\Gamma\left(\frac{5}{2}\right)}{\left(\frac{k\rho_0\sin\tau_2}{2}\right)^{\frac{2}{5}}}+\ldots, \qquad (5.16)$$

where Γ denotes the gamma function and the adequate ratios of Hankel functions in (5.5) are equal to

$$\frac{H_{\nu-1}^{(2)}\left(\frac{kh_1}{\cos\phi}\right)}{H_{\nu}^{(2)}\left(\frac{kh_1}{\cos\phi}\right)}=e^{-j\frac{kh_1}{\cos\phi}\left[(\sin\tau_3-\tau_3\cos\tau_3)-(\sin\tau_1-\tau_1\cos\tau_1)\right]}\times\frac{f^{(2)}(\tau_3)}{f^{(2)}(\tau_1)}, \qquad (5.17)$$

where

$$\cos\tau_3=\frac{(\pi-\alpha)\cos\phi}{\alpha kh_1} \qquad (5.18)$$

and $f^{(2)}(\tau_3)$ is obtained by replacing in (5.16) τ_1 by τ_2,i.e.

$$\frac{H_\nu^{(2)}(k\rho_0)}{H_\nu^{(2)}\left(\frac{kh_1}{\cos\phi}\right)} = e^{j\frac{kh_1}{\cos\phi}\left[(\sin\tau_1-\tau_1\cos\tau_1)-k\rho_0(\sin\tau_2-\tau_2\cos\tau_2)\right]} \times \frac{f^{(2)}(\tau_2)}{f^{(2)}(\tau_1)} \quad . \quad (5.19)$$

The appropriate ratio of Hankel functions of (4.73) has the form

$$\frac{H_\nu^{(2)}\left(\frac{kh_2}{\cos\phi}\right)}{H_\nu^{(1)}\left(\frac{kh_2}{\cos\phi}\right)} = e^{-j\frac{kh_2}{\cos\phi}(\sin\tau_4-\tau_4\cos\tau_4)} \times \frac{f^{(2)}(\tau_4)}{f^{(1)}(\tau_4)} \quad (5.20)$$

where

$$\cos\tau_4 = \frac{\pi\cos\phi}{\alpha kh_2} \quad , \quad (5.21)$$

while the function $f^{(2)}(\tau_4)$ is given by

$$f^{(2)}(\tau_4) = \frac{e^{j\frac{\pi}{4}}\Gamma(\frac{1}{2})}{\left(\frac{kh_2}{2\cos\phi}\sin\tau_4\right)^{\frac{1}{2}}} + \left(\frac{1}{8}+\frac{5}{24}\frac{1}{\tan^2\tau_4}\right)\frac{e^{j\frac{3\pi}{4}}\Gamma\left(\frac{3}{2}\right)}{\left(\frac{kh_2}{2\cos\phi}\sin\tau_4\right)^{\frac{3}{2}}} +$$

$$+\left(\frac{3}{128}+\frac{7}{576}\frac{1}{\tan^2\tau_4}+\frac{385}{3456}\frac{1}{\tan^4\tau_4}\right)\frac{e^{j\frac{5\pi}{4}}\Gamma\left(\frac{5}{2}\right)}{\left(\frac{kh_2\sin\tau_4}{2\cos\phi}\right)^{\frac{5}{2}}} + \ldots \quad (5.22)$$

and the function $f^{(1)}(\tau_4)$ is given by

$$f^{(1)}(\tau_4) = \frac{e^{-j\frac{\pi}{4}}\Gamma(\frac{1}{2})}{\left(\frac{kh_2}{2\cos\phi}\sin\tau_4\right)^{\frac{1}{2}}} + \left(\frac{1}{8}+\frac{5}{24}\frac{1}{\tan^2\tau_4}\right)\frac{e^{-j\frac{3\pi}{4}}\Gamma\left(\frac{3}{2}\right)}{\left(\frac{kh_2}{2\cos\phi}\sin\tau_4\right)^{\frac{3}{2}}} +$$

$$+\left(\frac{3}{128}+\frac{7}{576}\frac{1}{\tan^2\tau_4}+\frac{385}{3456}\frac{1}{\tan^4\tau_4}\right)\frac{e^{-j\frac{5\pi}{4}}\Gamma\left(\frac{5}{2}\right)}{\left(\frac{kh_2\sin\tau_4}{2\cos\phi}\right)^{\frac{5}{2}}}+\ldots. \qquad (5.23)$$

All series given by (5.15), (5.16), (5.22) and (5.23) were proven by Debye [24] to be nondivergent (or semiconvergent). In a similar manner Isao [35] investigated properties of Hankel functions ratios. Debye's representation of the above form is valid for $\tau_0 < 1$ and $0 < \cos^{-1}\tau_0 < \frac{\pi}{2}$.

The limit of validity of the above representation of Hankel functions results from (5.21)

$$\left[\frac{\pi\cos\phi}{\alpha kh_1}\right]_{\max} < 1 , \qquad (5.24)$$

which leads to the inequalities:

$$\tan\frac{\alpha}{2}-\frac{a}{\lambda_0}\alpha < 0 , \qquad (5.25)$$

or

$$\tan\frac{\alpha}{2}-\frac{\lambda_c}{2\lambda_o}\alpha < 0 , \qquad (5.26)$$

or

$$\tan\frac{\alpha}{2}-\frac{f_o}{2f_c}\alpha < 0 , \qquad (5.27)$$

where

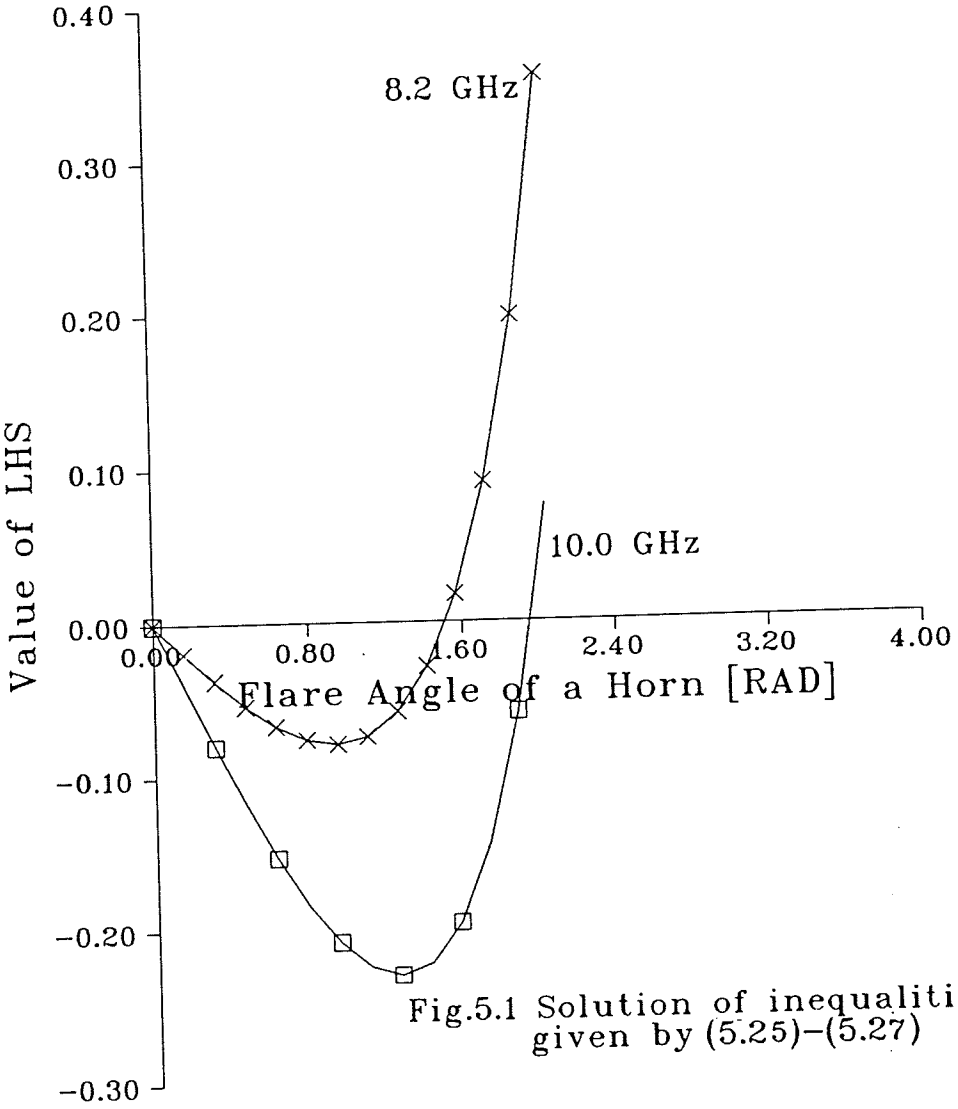

Fig.5.1 Solution of inequalities given by (5.25)–(5.27)

- a denotes distance between plates of parallel plate waveguide,

- λ_o and λ_c denote free space and cutoff wavelengths, respectively,

- f and f_c - frequency and critical frequency, respectively.

The above inequalities have an easy graphical solution shown on fig. 5.1 . From fig.5.1 it is seen that for frequencies approaching the cutoff frequency f_c of the waveguide the applicability of the representation of Hankel functions as considered in this section is limited to lower values of flare angle. For the frequency of 8.2 GHz this value it is less than 100°. and for 10.0 GHz - less than 110°.

Above these values of flare angles a different representation of Hankel functions is required, i.e. for $\tau_0 \approx 1$ and $\tau_0 > 0$. Such representations may be found in the Debye's paper [24] as for $\tau_0 < 0$ but, due to the little practical importance of sectoral waveguides and horns of large flare angles, these are not considered in this thesis.

5.3 Problem of an appropriate model of dielectric properties

The simplest type of dielectric loss described by Debye's model, i.e. (4.74), is based on the assumption that, in the constant field, the polarization of a medium approaches its equilibrium value exponentially with time.

The restriction of the validity of Debye's model to frequences below a certain limit ω_L underlies all possible models. Therefore the initially considered model is valid in a certain interval of frequency where no resonance occurs.

Frölich [35] in the appendix of his book derives Kramers-Kröning relations valid for a great number of dielectrics:

$$\epsilon_r'(\omega) - \epsilon_{r\infty} = \frac{2}{\pi} \int_0^\infty \epsilon_r''(\omega) \frac{\omega' d\omega'}{\omega'^2 - \omega^2} \tag{5.28}$$

and

$$\epsilon_r''(\omega)=-\frac{2}{\pi}\int_0^{\infty}[\epsilon_r'-\epsilon_{r\infty}]\frac{\omega d\omega'}{\omega'^2-\omega^2} \tag{5.29}$$

Both these relations follow from from fundamental physical property of causal connection between the polarization and the dielectric field, i.e.

$$\vec{D}(\vec{x},t)=\vec{E}(\vec{x},t)+\int_0^{\infty}G(\tau)e^{j\omega\tau}d\tau \tag{5.30}$$

where the kernel $G(\tau)$ is the Fourier transform of $\chi=\epsilon(\omega)-1$ and may be used to express the dielectric constant

$$\epsilon(\omega)=1+\int_0^{\infty}G(\tau)e^{j\omega\tau}d\tau \tag{5.31}$$

The simplest model including a single resonance for square of the index of refraction $\eta^2(\omega)=\epsilon(\omega)$ and which satisfies Kramers-Kröning relations [38] has the form:

$$\eta^2(\omega)=1+\frac{\omega_p^2}{\omega_0^2-\omega^2-j\omega\beta} \tag{5.32}$$

where

ω_0 is the resonant frequency, β is damping constant and ω_p is the plasma frequency of the medium.

The singularity structure of $\eta(\omega)$ may be determined by the location of the poles and zeros of $\eta^2(\omega)$ in the complex ω plane. The zeros of $\eta^2(\omega)$ are given by

$$\omega_a=\omega_1-j\frac{\beta}{2} \tag{5.33.1}$$

and

$$\omega_b = -\omega_1 - j\frac{\beta}{2}, \tag{5.33.2}$$

where

$$\omega_1^2 = \omega_0^2 + \omega_p^2 - \frac{\beta^2}{2}, \tag{5.33.3}$$

and the poles of $\eta^2(\omega)$ are located at

$$\omega_c = \omega_2 - j\frac{\beta}{2} \tag{5.34.1}$$

and

$$\omega_d = -\omega_2 - j\frac{\beta}{2}, \tag{5.34.2}$$

where

$$\omega_2^2 = \omega_0^2 - \frac{\beta^2}{4}. \tag{5.34.3}$$

In effect by using the above equations the complex index of refraction may be written as

$$\eta(\omega) = \sqrt{\frac{(\omega-\omega_a)(\omega-\omega_b)}{(\omega-\omega_c)(\omega-\omega_d)}} \tag{5.35}$$

In general the complex parameters of (5.35) are unknown for any dielectric material commercially available for microwave use. Therefore they must be determined experimentally.

The considered structure may allow such an identification. Having found the total complex reflection coefficient Γ_{1t}, the first order reflection coefficient Γ_2^0 may be computed from (4.83) and (4.81). From (4.73) and (5.35) a simultaneous system of equations may be obtained for each measured frequency in the range of

interest. In order to obtain an accurate solution the minimal norm should be searched for, i.e. method of least squares must be applied.

This way we arrive at the problem of synthesis of an appropriate model of dielectric properties of an insertion. By finding the model in certain constant conditions the behavior of the dielectrics in different conditions may be predicted. Equation (4.74) shows that both the field properties, depending on the waveguide parameters, and the dielectric properties determine the value of reflection coefficient. At certain values of these parameters the structural transparency for the electric field may appear, thus the line becomes perfectly matched. This does not mean the medium is transparent for the electromagnetic field due to the fact that this process is expected to happen close to the resonance region where the parameters of a dielectric change very rapidly, i.e. the real part of the dielectric constant decreases and the imaginary part, called also the loss factor, increases causing much higher dissipation of energy than in the equilibrium state.

The identification problem lies beyond the scope of the thesis.

5.4 Numerical solution

The analytical solution given in the chapter 4 was programmed for the University of Manitoba Amdahl 5850 main computer. Depending on the desired input and output data, a number of interconnected programs were written (see sample program in Appendix). There is assumed that the dielectric properties are described by Debye's model in the equilibrium range, i.e. $\tan\delta$ given by (4.74) and high frequency dielectric constant $\epsilon_r = \epsilon_\infty$.

From the great number of data obtained, only those which allow us to give a brief clear picture of the investigated process were selected. Complex values were converted into measureable modulus and amplitude of reflection coefficient and

electric field, respectively.

The frequency dependence of the reflection coefficient of the junction under consideration is shown in fig.5.2 for infinite sectoral waveguides having different flare angles. The results were obtained using (4.55).

The reflection coefficients of a sectoral waveguide having fixed flare angle of 24^o are plotted against frequency in fig.5.3. for different dielectric materials.

Figure 5.4 shows the frequency response of the reflection coefficient for sectoral waveguides characterized by different flare angles loaded with the same dielectric substance at the same distance from the apex.

Figures 5.5 and 5.6 show the angular distribution of the reflection coefficient and the electric field amplitude,respectively,at dielectric interface h_2= 128.5 mm for three different values of flare angle of the sectoral part of the considered structure.

The distribution of the reflected electric field between plates in the parallel plate region shown in figures 5.5 and 5.6 is presented in fig.5.7.

The dependence of the total axial reflection coefficient value on the location of dielectric dicontinuity measured from the apex is shown in fig.5.8 for the same flare angle and three different frequencies. These results are discussed together with experimental results in chapter 7.

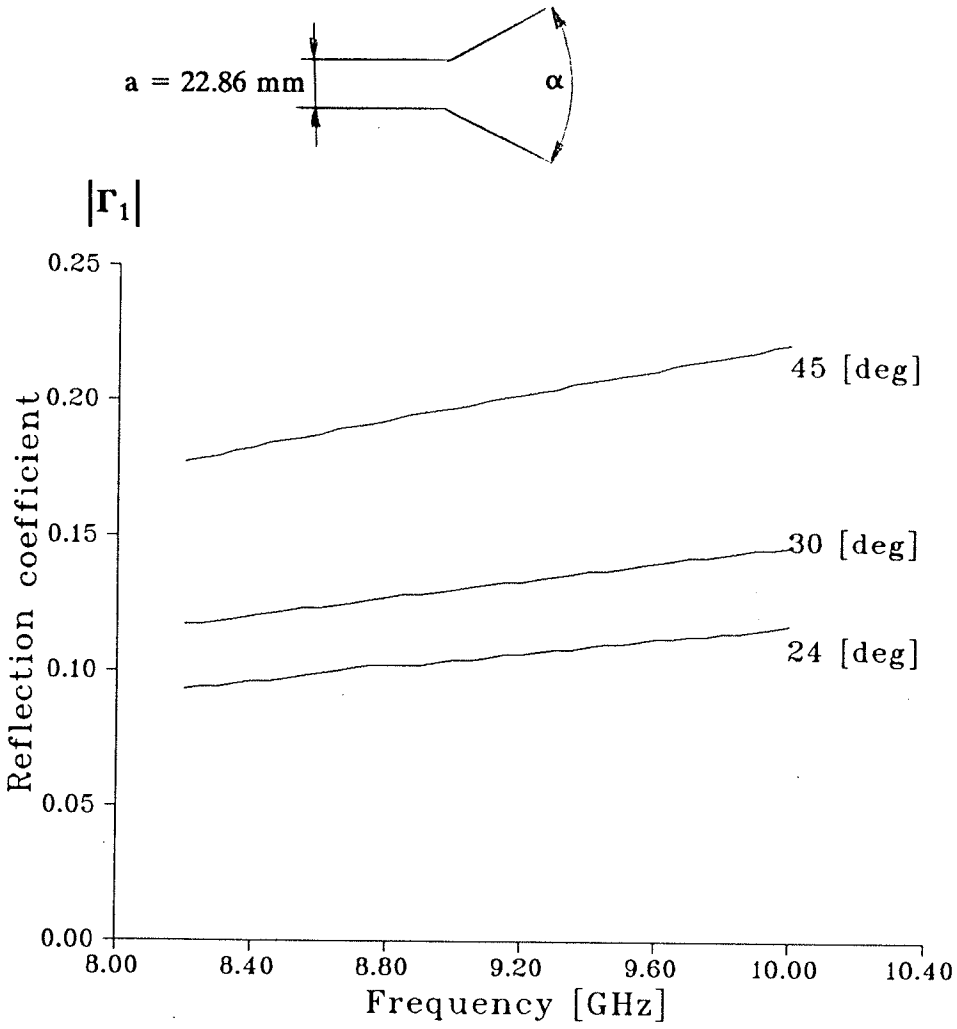

Fig.5.2 Axial value of reflection coefficient for various flare angles of sectoral waveguide against frequency, an infinite sectoral waveguide.

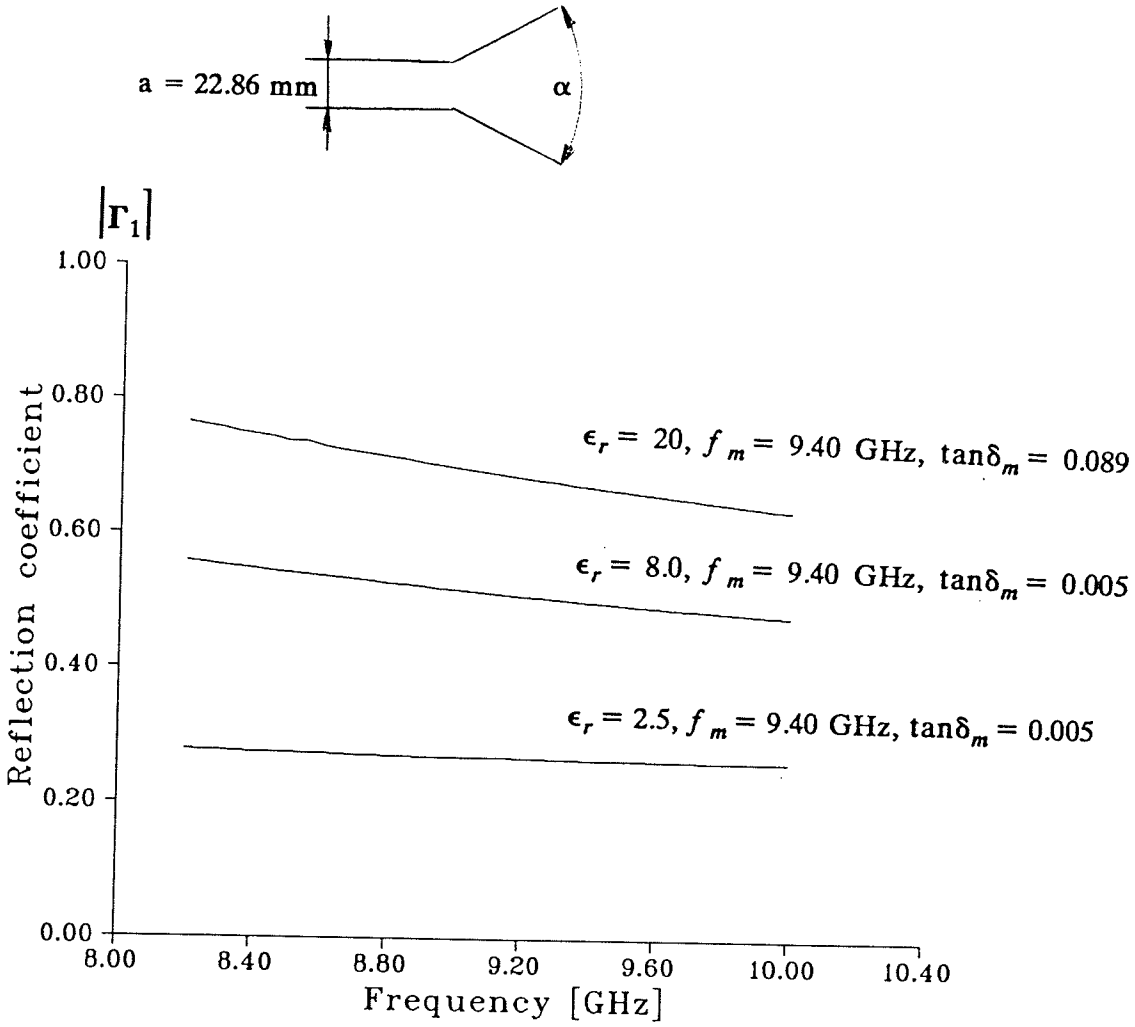

Fig.5.3 Axial value of reflection coefficient for sectoral waveguide of flare angle of 24 [deg] against frequency for different dielectrics located at h_2=128.5 mm, represented by Debye model

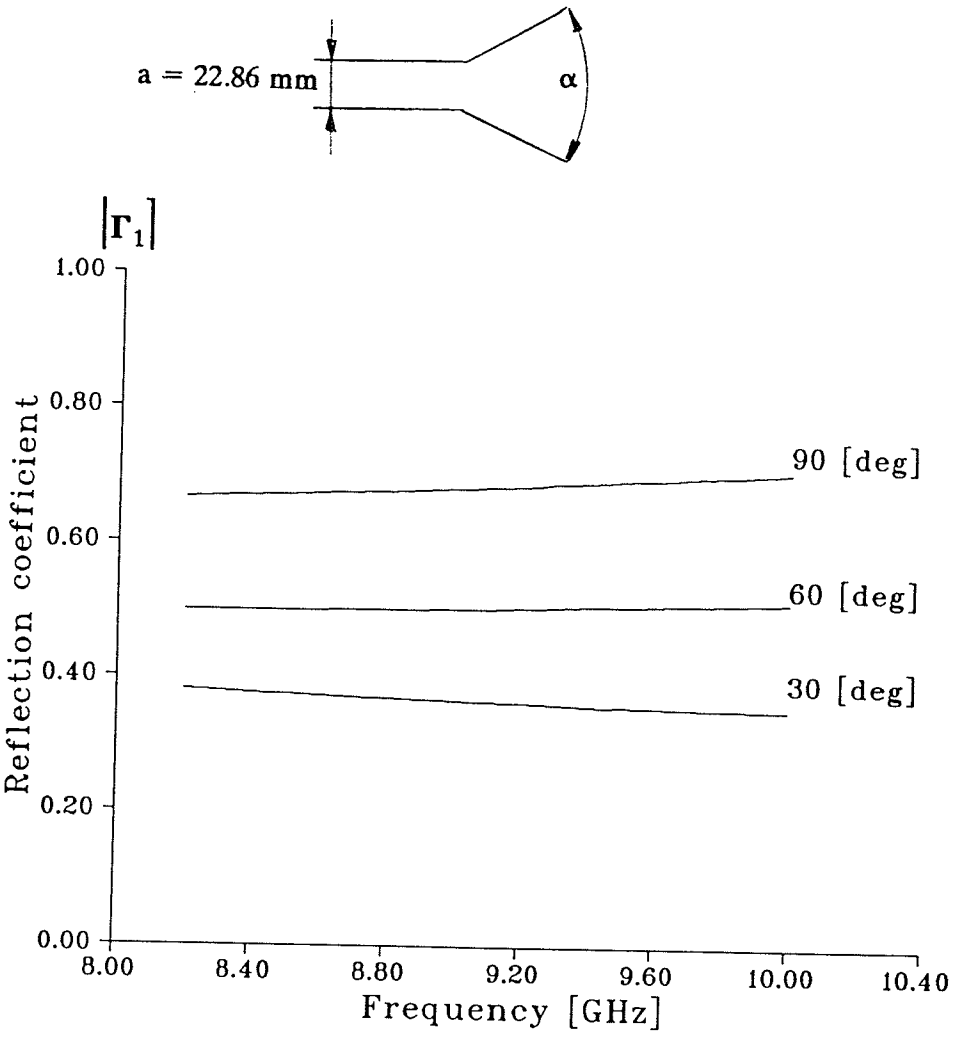

Fig.5.4 Axial value of reflection coefficient for various flare angles of sectoral waveguide against frequency, Debye model:
h_2=65 mm, ϵ_r=4.0, tanδ_m= 0.089, f_m=10 [GHz]

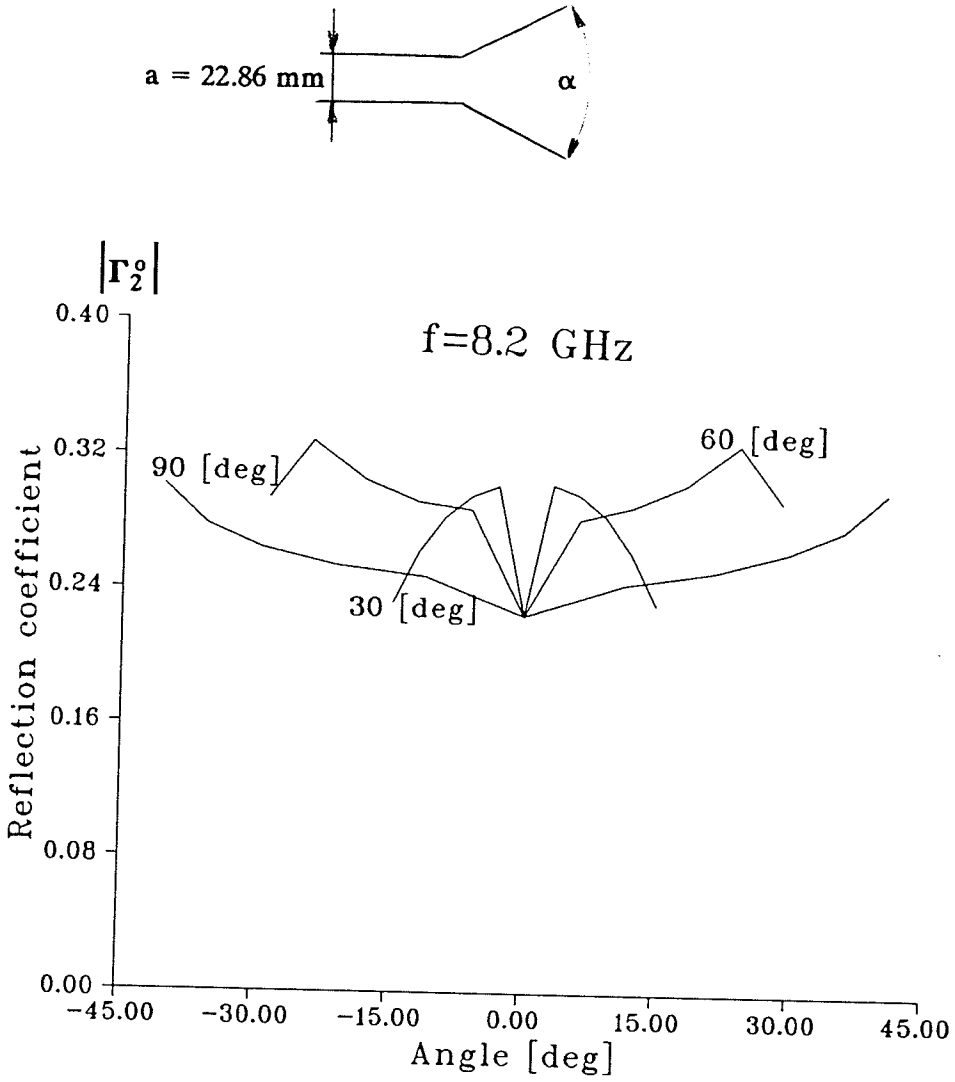

Fig.5.5 Angular distribution of reflection coefficient for sectoral waveguides of different flare angle at dielectric interface located at h_2=128.5 mm. Dielectrics is represented by Debye model ϵ_r=4.0, f_m=10.0, $\tan\delta_m$=0.089

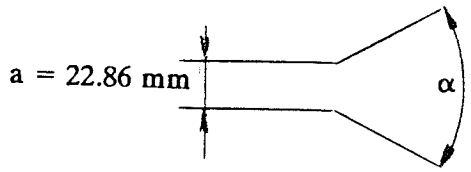

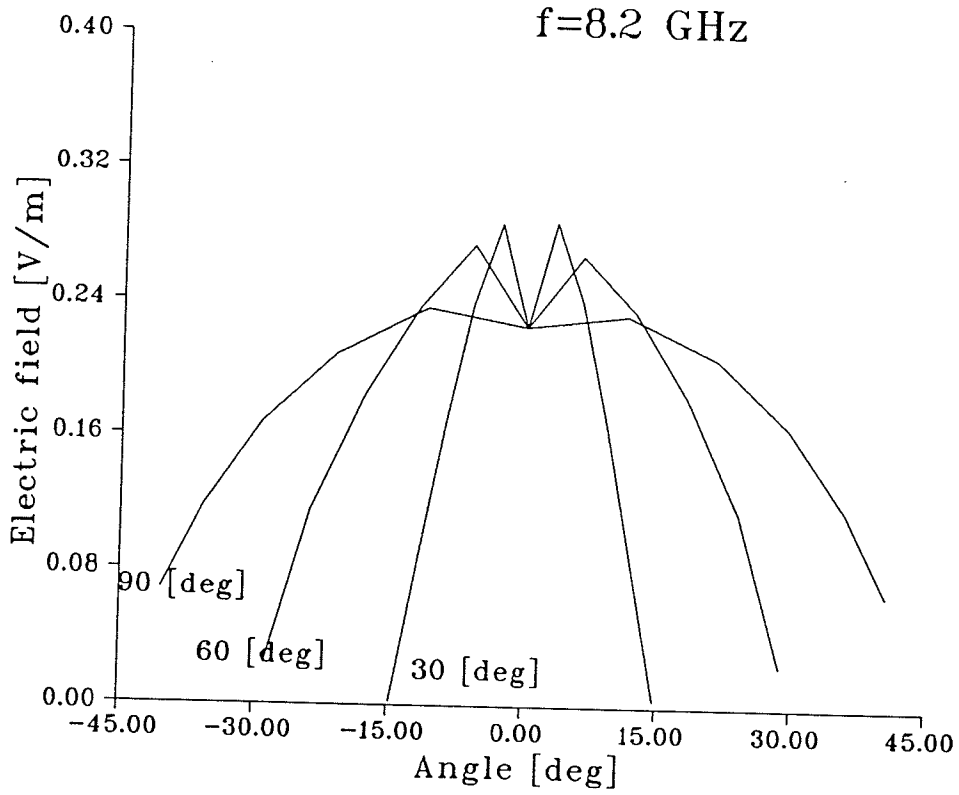

Fig.5.6 Angular distribution of reflected electric field for sectoral waveguides of different flare angle at dielectric interface located at h_2=128.5 mm. Dielectrics is represented by Debye model ϵ_r=4.0, f_m=10.0, $\tan\delta_m$=0.089

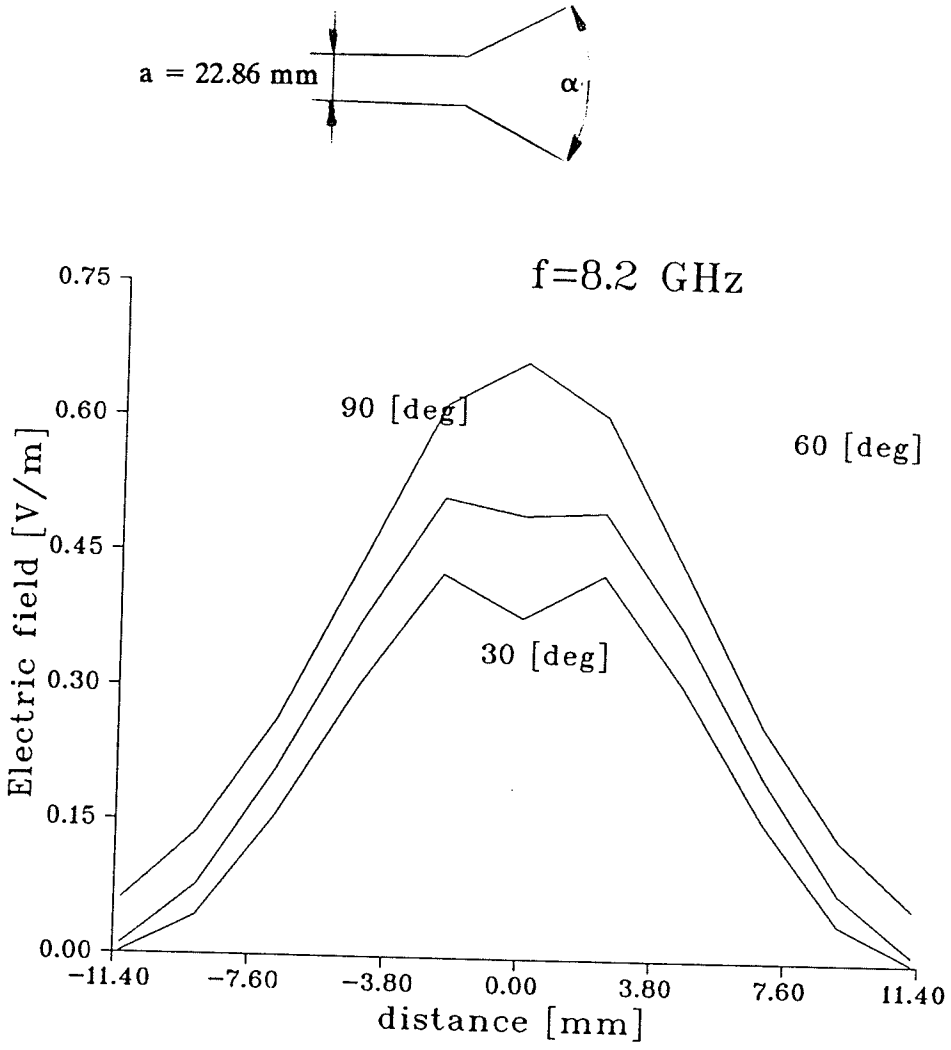

Fig.5.7 Distribution of reflected electric field between plates of parallel plate waveguide terminated with sectoral waveguides of different flare angle for the case from fig.(5.6)

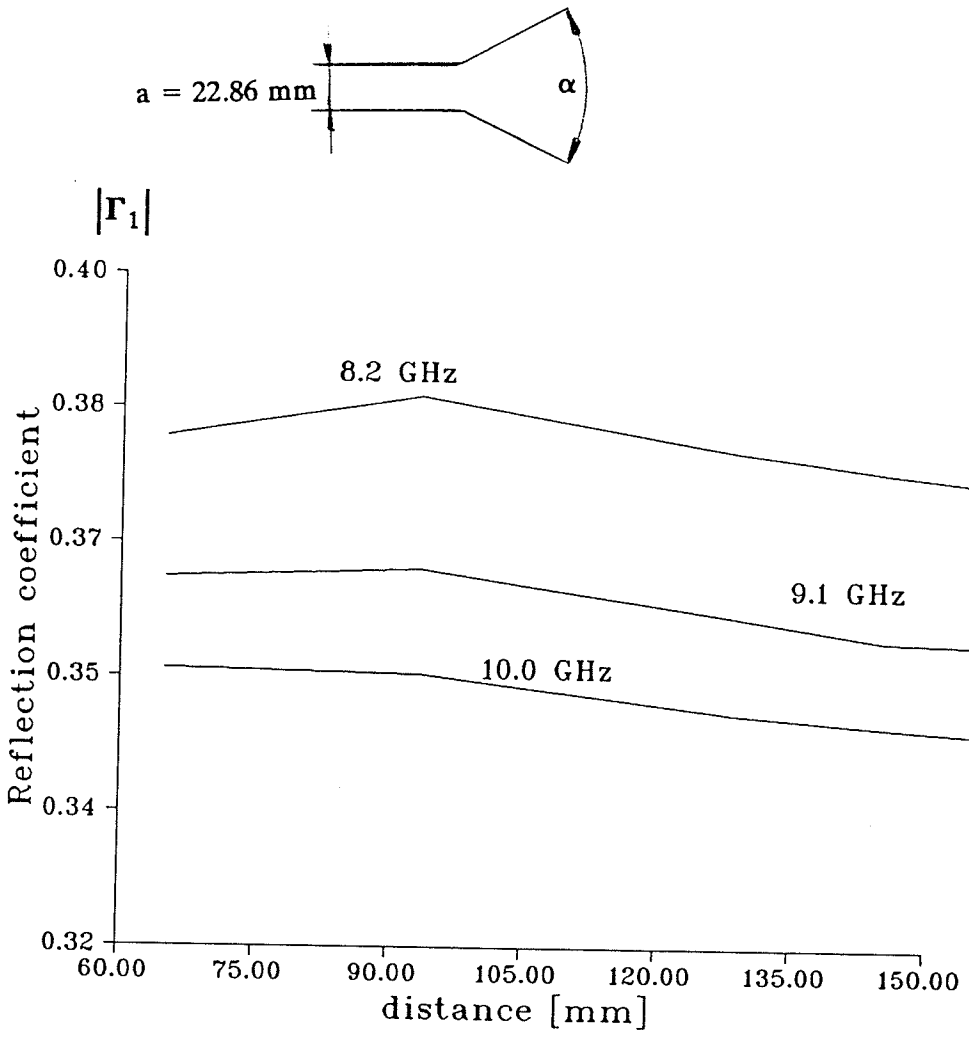

Fig.5.8 Dependence of axial reflection coefficient value of parallel plate waveguide on location of dielectric interface from the apex of sectoral waveguide for flare angle 30 [deg] Dielectrics is charactarized by Debye model ϵ_r=4.0, f_m=10.0, $\tan\delta_m$=0.089

CHAPTER 6
Experimental Procedure and Results

6.1 Description of the experimental setup

As a model of the parellel plate waveguide was used an x-band rectangular waveguide operating in the TE_{m0} field was employed since the behavior in this case does not depend on the narrow dimension of the waveguide.

In order to verify the effect of dielectric loading of the sectoral waveguide, a long sectoral horn antenna, having a flare angle of 24°, was connected to the rectangular waveguide, of the standard dimensions 22.86 × 10.10 mm (see fig. 6.4). The horn had one of two walls screwed on to allow insertion of the dielectric which was superpolyamide and which was described by standard parameters. During the experiment the horn was imbedded into a container filled with absorbing substance "Eccosorb LS26" (fig. 6.50).

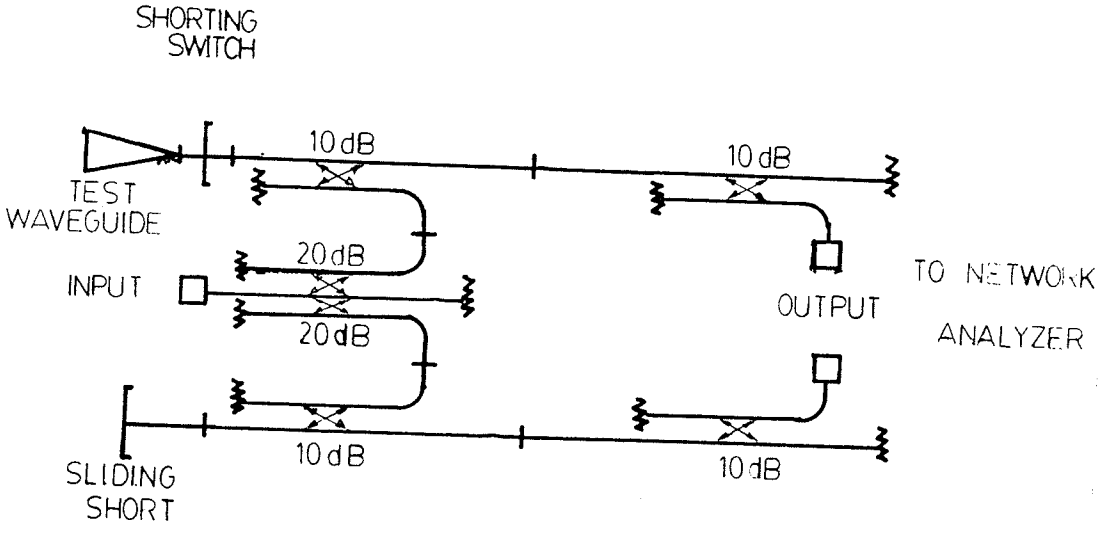

Fig. 6.1 Schematic diagram of the power splitter

The reflection coefficient measurements were performed using a substitution method based on an individually built power splitter of directional couplers, connected to a network analyzer and schematically shown in fig.6.1. The power splitter furnished isolation between the reference and test channels and fed them with two equal signals. The reference channel was terminated in a sliding short while the reference was terminated in a shorting switch connected to the dielectric loaded sectoral waveguide.

During the calibration procedure, the shorting switch in the test channel was on and the electrical length of the reference channel was adjusted by a sliding short so as to equalize the electric lengths of both channels, i.e. the reflection coefficient was equal to unity in both channels with constant phase response against frequency in the range of interest.

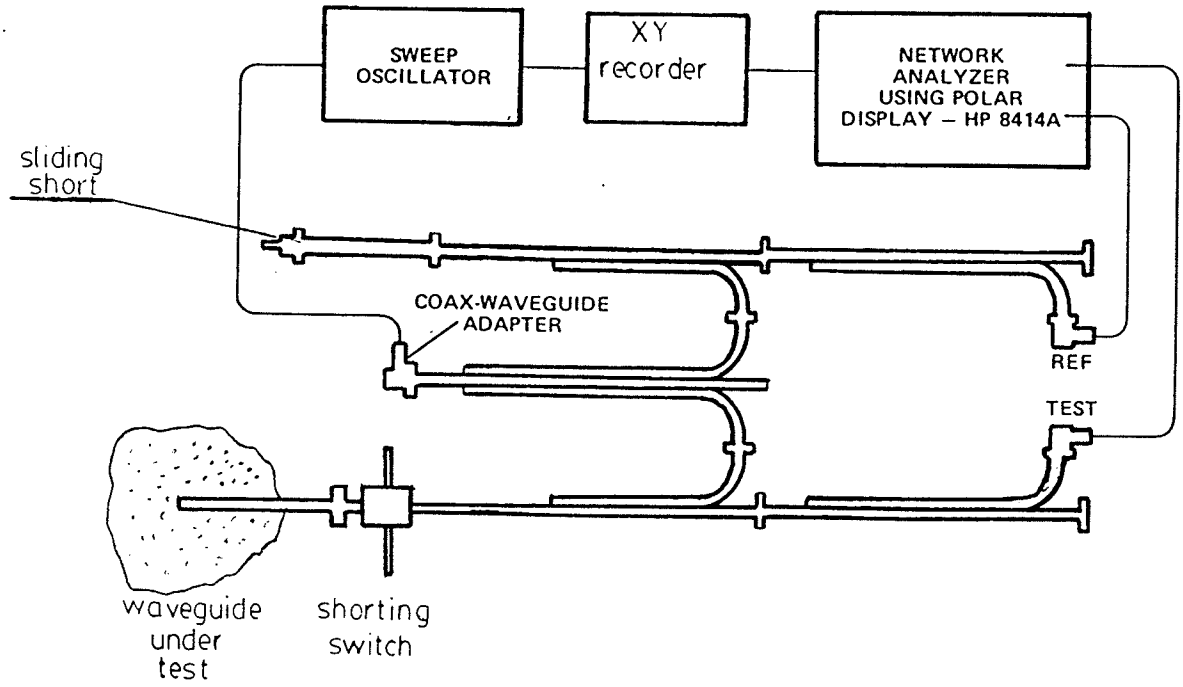

Fig 6.2 The experimental setup for reflection coefficient measurements

NOTICE/AVIS

PAGE(S) 76+77 IS/ARE EST/SONT colour photos

PLEASE WRITE TO THE AUTHOR FOR INFORMATION, OR CONSULT THE ARCHIVAL COPY HELD IN THE DEPARTMENT OF ARCHIVES AND SPECIAL COLLECTIONS, ELIZABETH DAFOE LIBRARY, UNIVERSITY OF MANITOBA, WINNIPEG, MANITOBA, CANADA, R3T 2N2.

VEUILLEZ ECRIRE A L'AUTEUR POUR LES RENSEIGNEMENTS OU VEUILLEZ CONSULTER L'EXEMPLAIRE DONT POSSEDE LE DEPARTEMENT DES ARCHIVES ET DES COLLECTIONS SPECIALES, BIBLIOTHEQUE ELIZABETH DAFOE, UNIVERSITE DU MANITOBA, WINNIPEG, MANITOBA, CANADA, R3T 2N2.

During the measurement the shorting switch in the test channel was off and the reflection coefficient was recorded by an HP 7035 X-Y analog recorder and read on a display unit. The plane at which the shorting switch was placed, $z = h_0$, did not coincide with the plane $z = h_1$ (fig. 4.1) thus the corrected formula (4.55) for reflection coefficient had to be employed. The schematic diagram of the experimental setup is shown in fig. 6.2.

The complete setup was composed of the following equipment:

- Reflection-Transmission unit, individually built, as shown in fig. 6.1,
- Harmonic Frequency Converter HP 8411A,
- Sweep Oscilator HP 8690A/RT, 8.2 - 12.2 GHz,
- Phase-Magnitude Display HP 8412A,
- Polar Display HP 8414A,
- Digital Counter - M37 I - Source Locking Microwave Counter,
- X-Y Recorder HP-2035B.

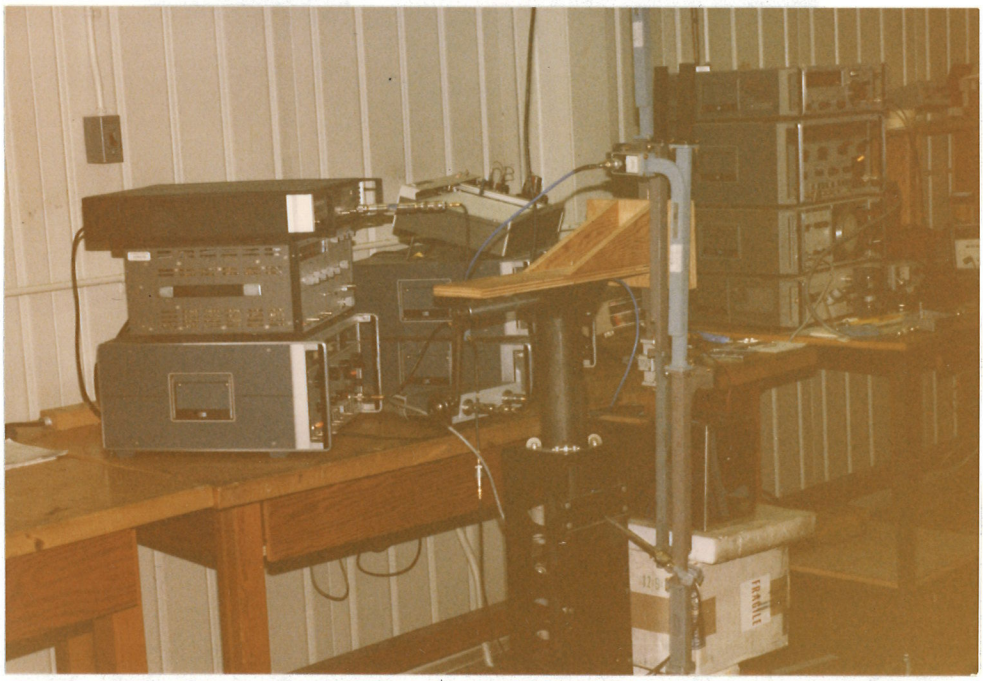

Fig.6.3 General layout of the experimental setup

Fig.6.4 (*above*) Sectoral horn and shorting switch used for experiments in the test channel

Fig.6.5 (*below*) The absorbing container of the setup

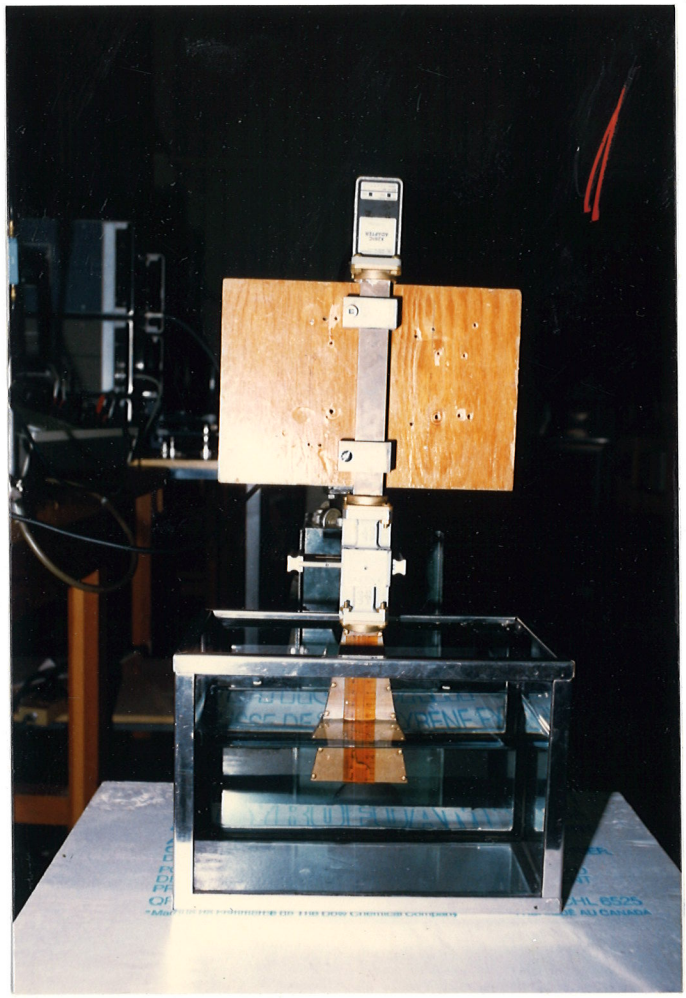

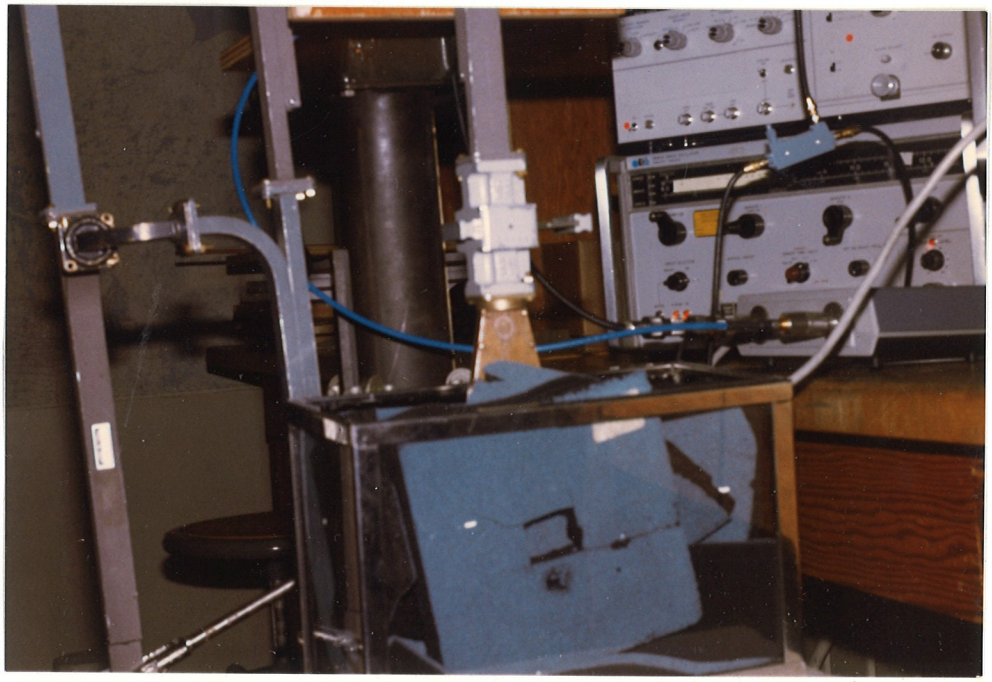

6.2 Experimental results

Experimental results were needed both to verify the proposed method (due to lack of relavant data in the literature) and to exhibit further complexity of the investigated problem. Since the considered model of dielectric properties is confined to the equilibrium state of a dielectric, an agreement between theory and experiment can only be expected for that state. The superpolyamide used for the experiment was characterized by standard parameters i.e. $\epsilon_r = 4.00$, $\tan\delta = 0.089$ at f=10.00 MHz. It was arbitrarily assumed that this data represents the constant parameters of Debye's model for dipolar solids. The reflection coefficient was measured in the frequency range of 8.2 - 10.0 GHz using the method described in section 6.1. The frequency range had to be upper bounded due to limited available power of the sweep oscilator to drive the frequency converter of the network analyzer.

Figures 6.6, 6.8, 6.10 and 6.11 present the amplitude of the measured reflection coefficient expressed in dB for different loading of parallel plate waveguide, i.e. h_2=93.3 mm, 128.5 mm, 145.5 mm and 161.2 mm, respectively. Such a representation of reflection coefficient is called return loss of the waveguide and is defined by the relation

$$r_m = 20\log|\Gamma| \tag{6.1}$$

Figures 6.7 and 6.9 show Smith charts for h_2=93.3mm, and 128.5 mm. Each of these simultaneously allows one to read both amplitude and phase, thus giving the complete set of data to carry out the identification process mentioned in section 5.3.

Data for the case of the unloaded sectoral waveguide are compared with those given in [37] in figure 6.12.

Figure 6.13 exhibits experimental data for the sectoral waveguide being short circuited at the plane h_2= 184.3 mm.

The agreement between theory and experiment is satisfactory within the entire frequency range where the dielectric is in the equilibrium state.

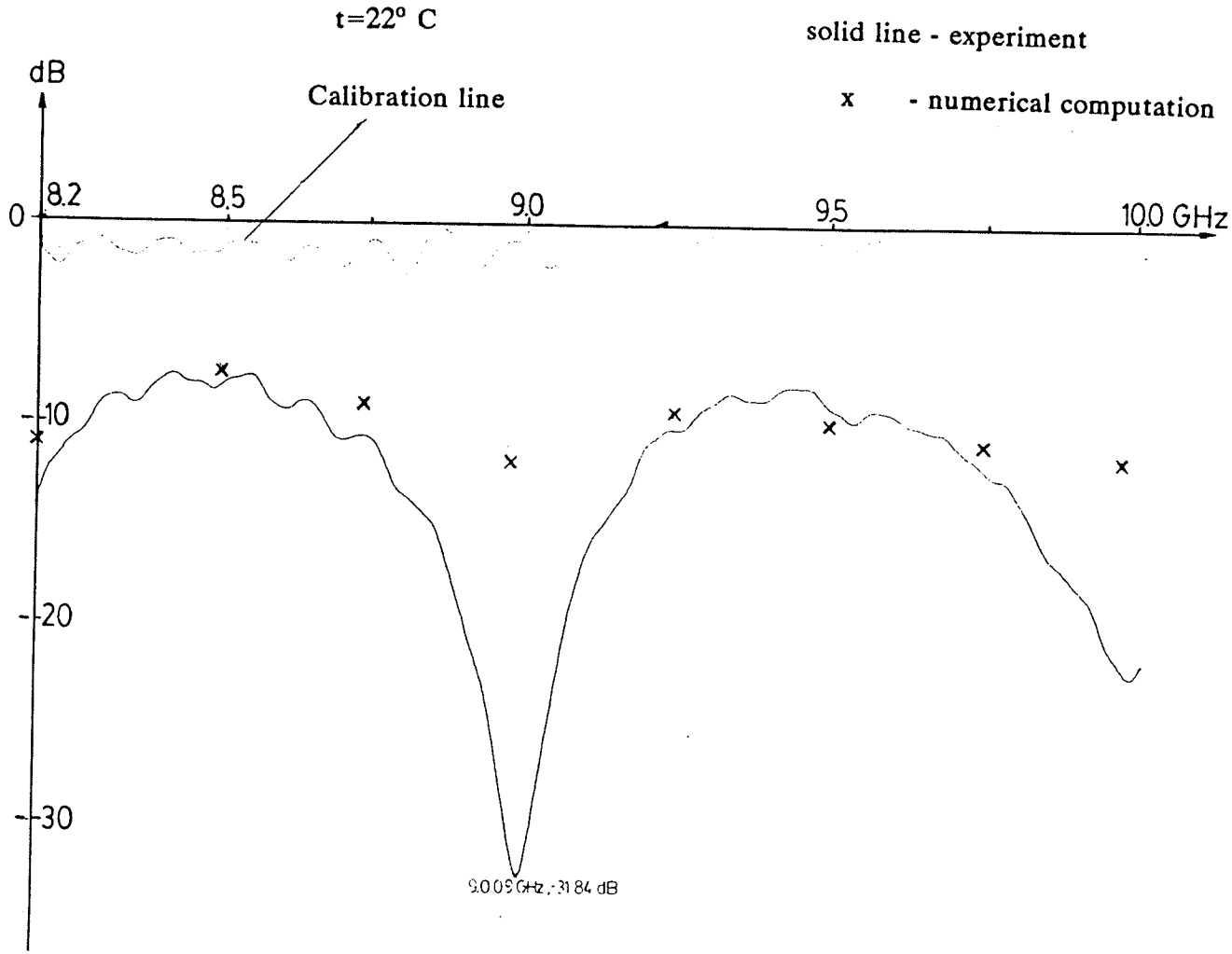

Fig. 6.6 Reflection coefficient for the loaded sectoral waveguide h_2= 93.3 mm

Calibration line

t=22° C

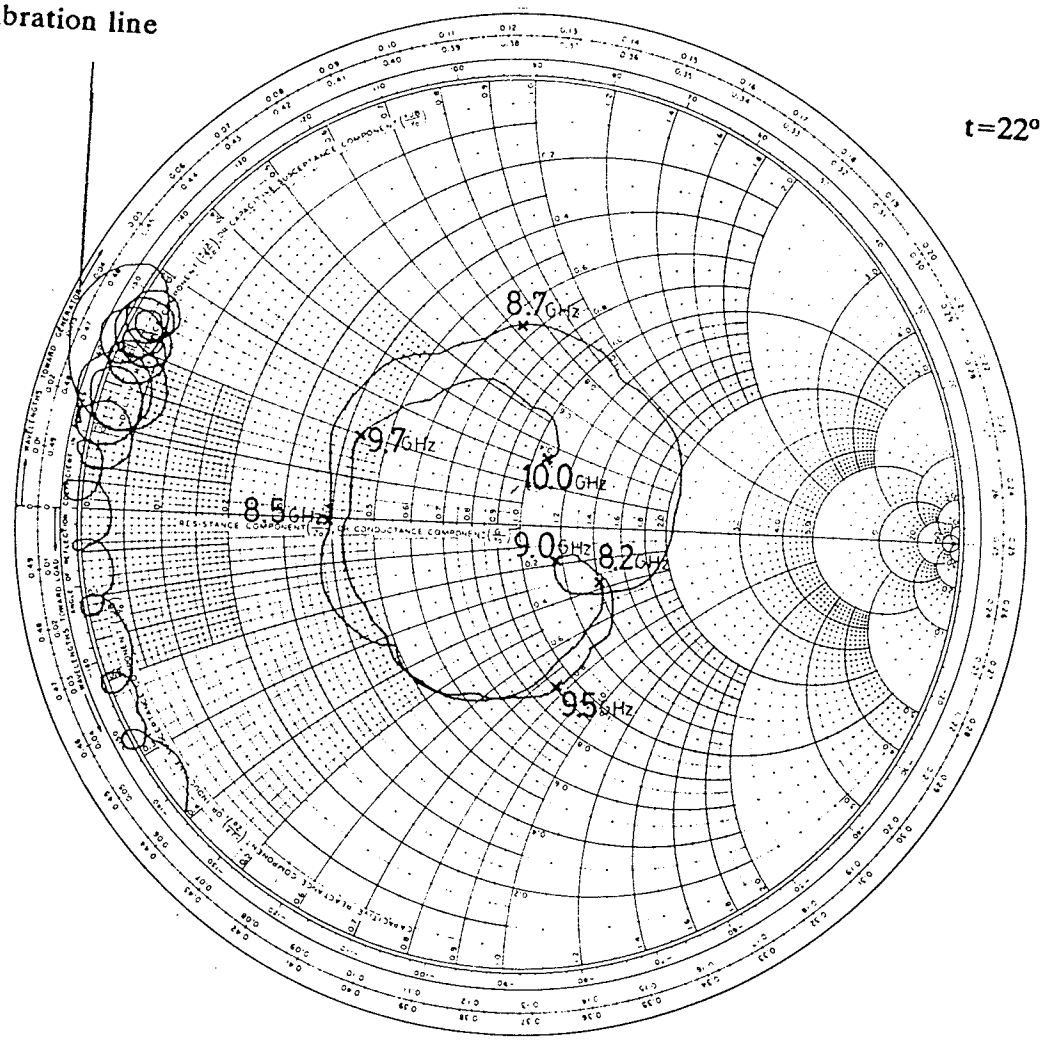

Fig 6.7 Smith Chart of reflection coefficient

for the case from fig. 6.6

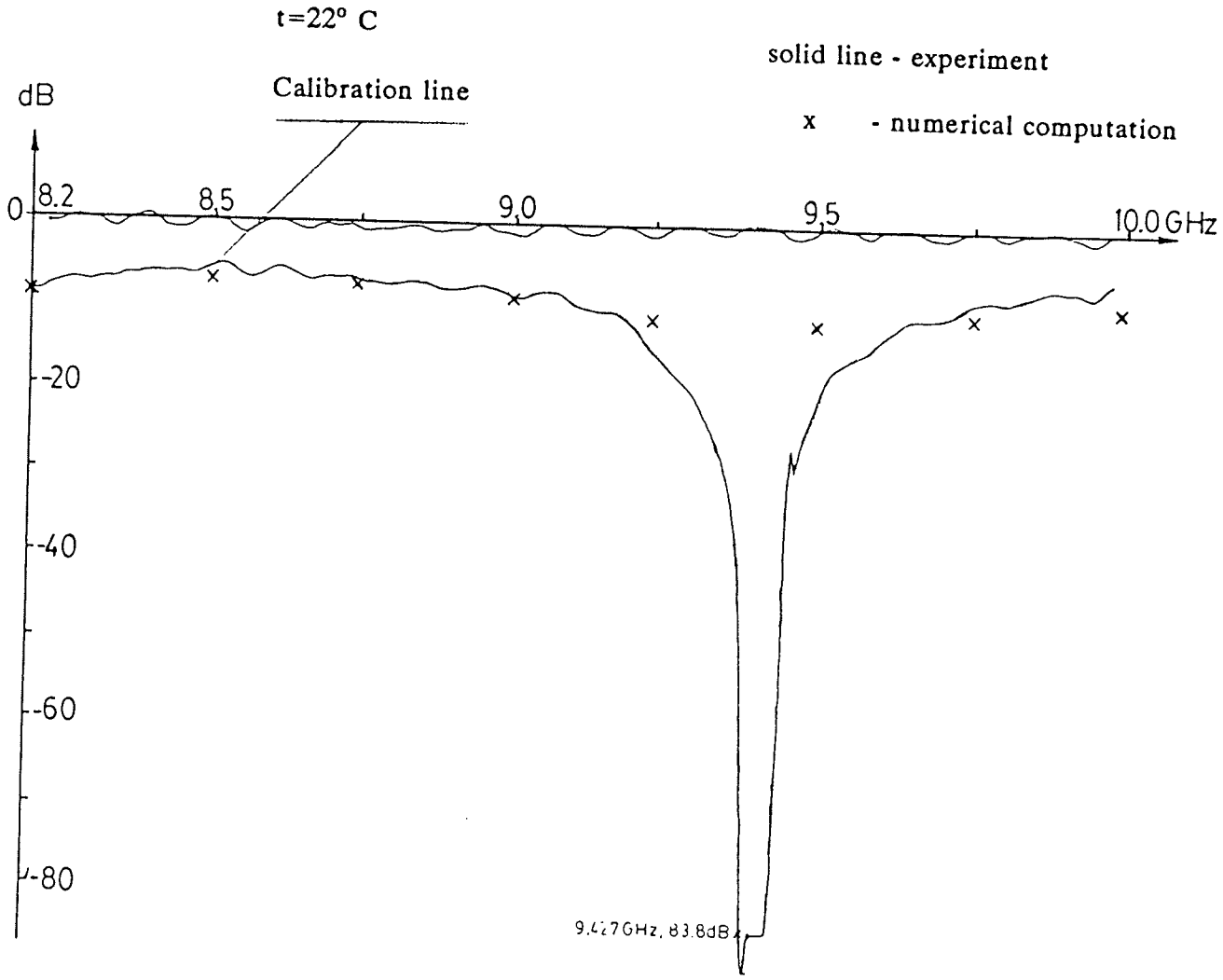

Fig. 6.8 Reflection coefficient for the loaded sectoral waveguide h_2= 128.5 mm

t=22° C

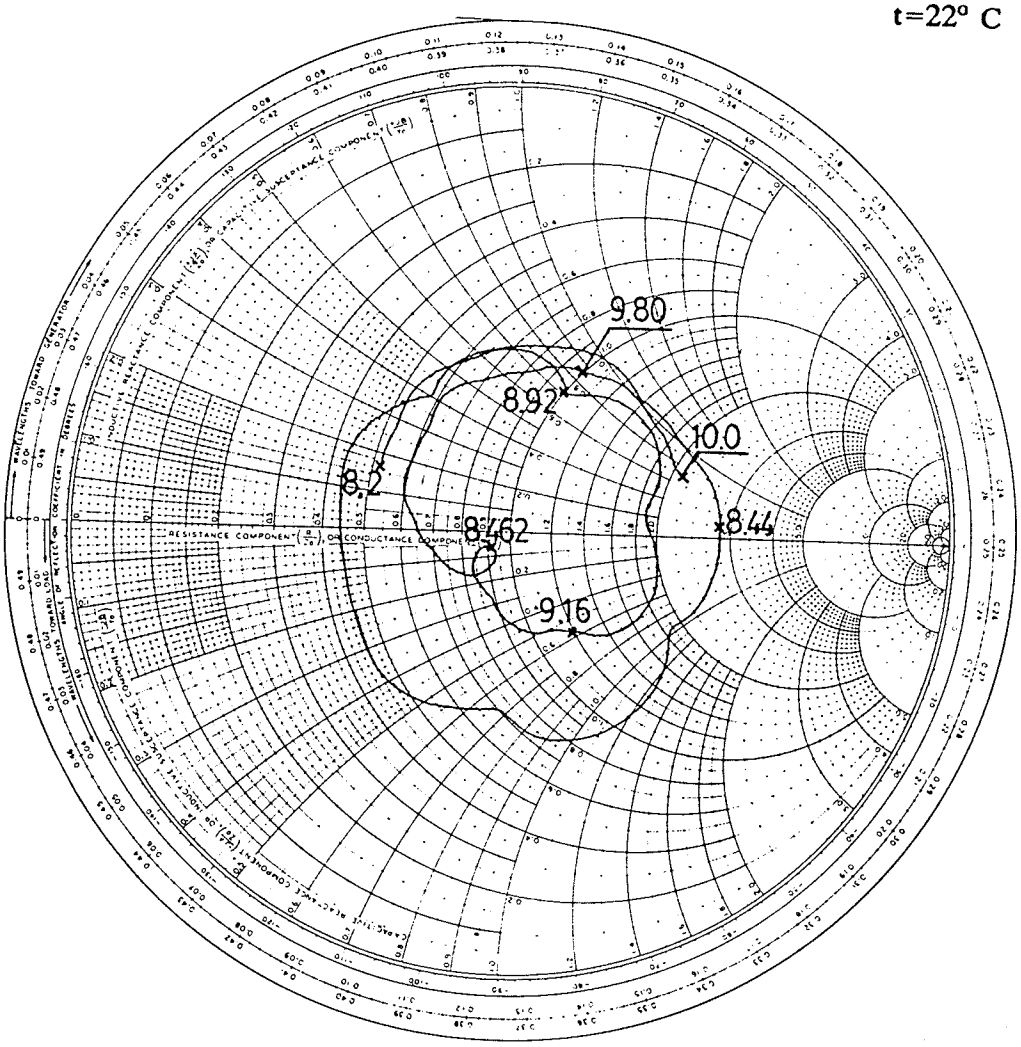

Fig 6.9 Smith Chart of reflection coefficient

for the case from fig. 6.8

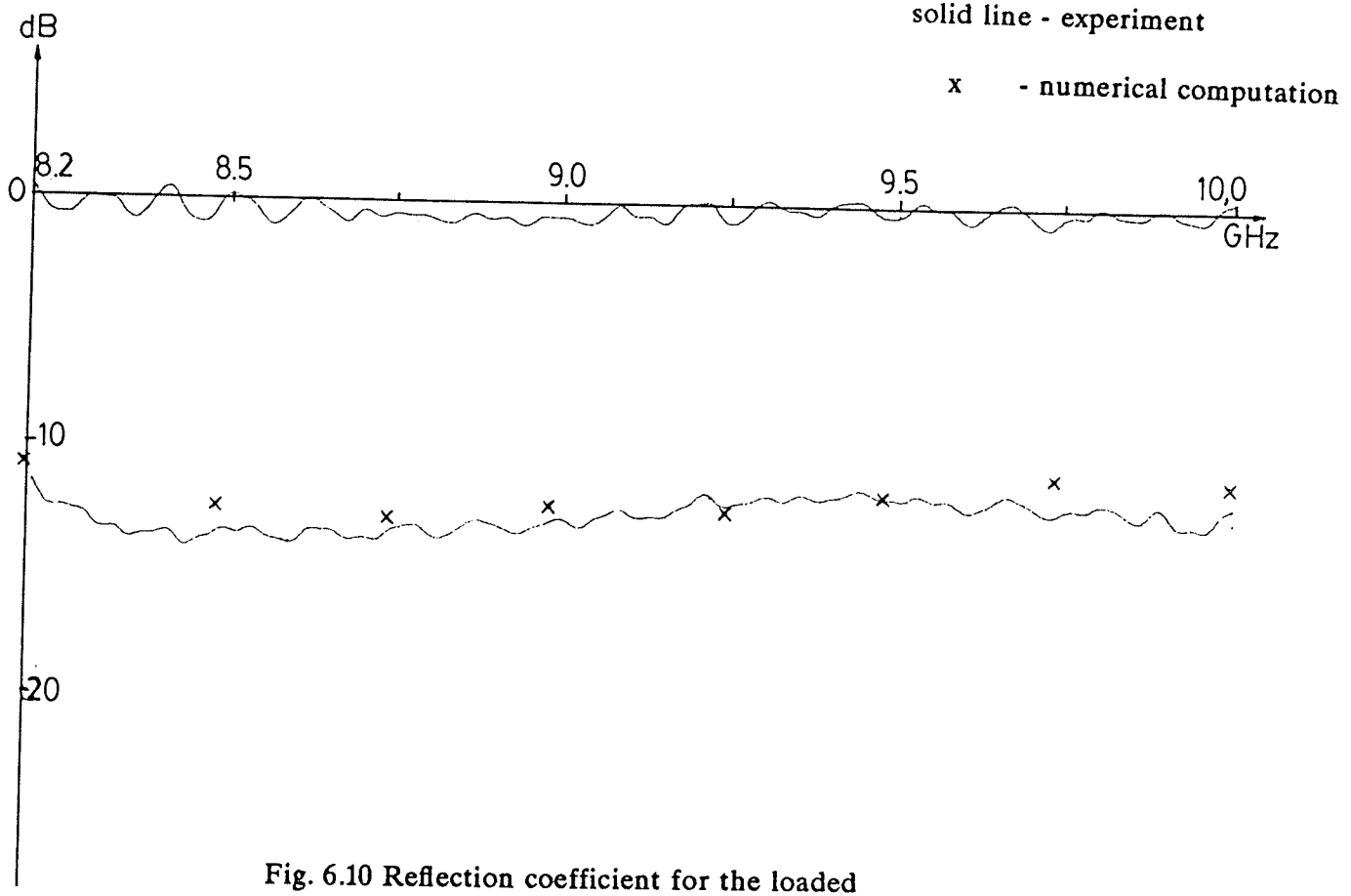

Fig. 6.10 Reflection coefficient for the loaded sectoral waveguide h_2= 145.5 mm

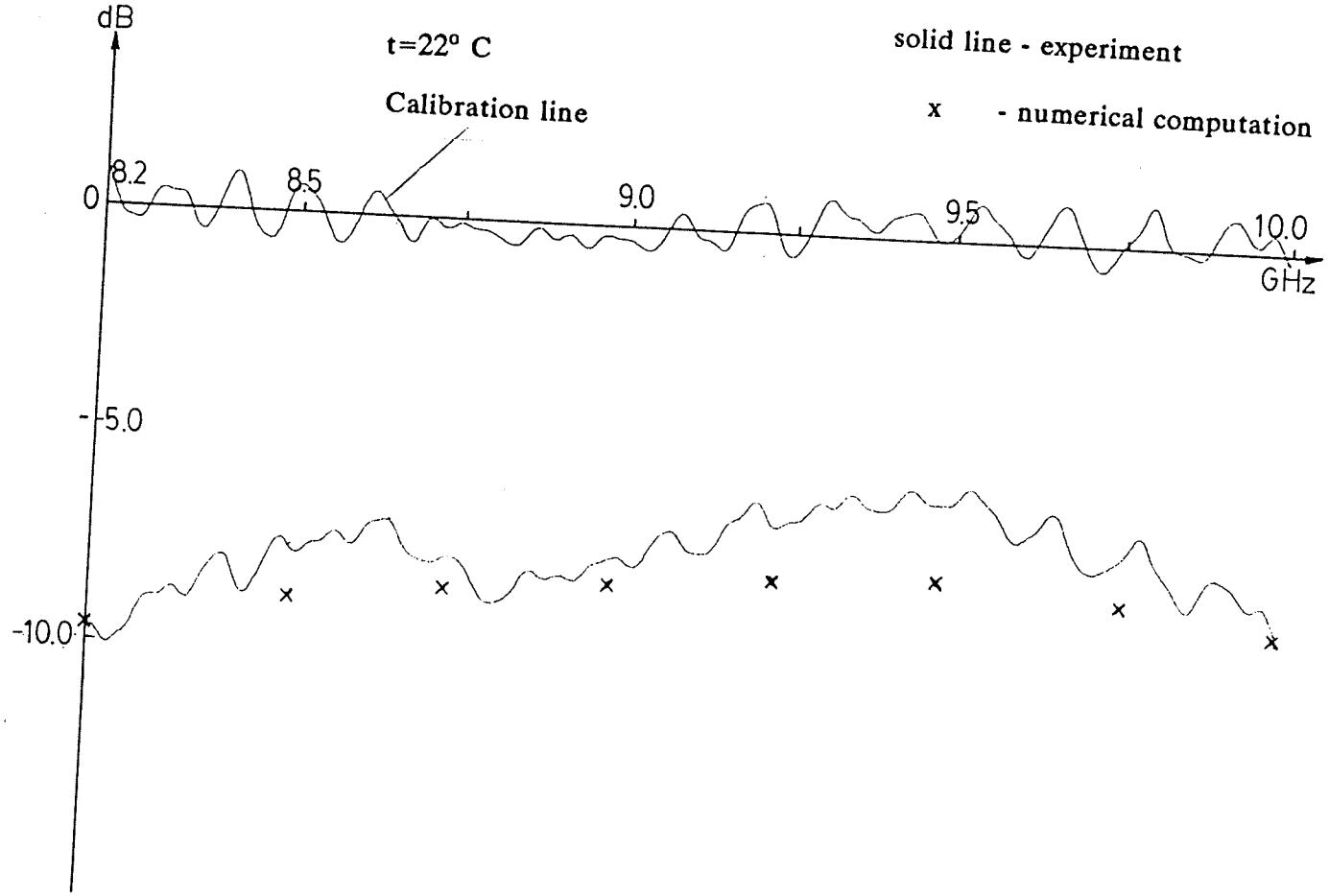

Fig. 6.11 Reflection coefficient for the loaded sectoral waveguide h_2= 161.2 mm

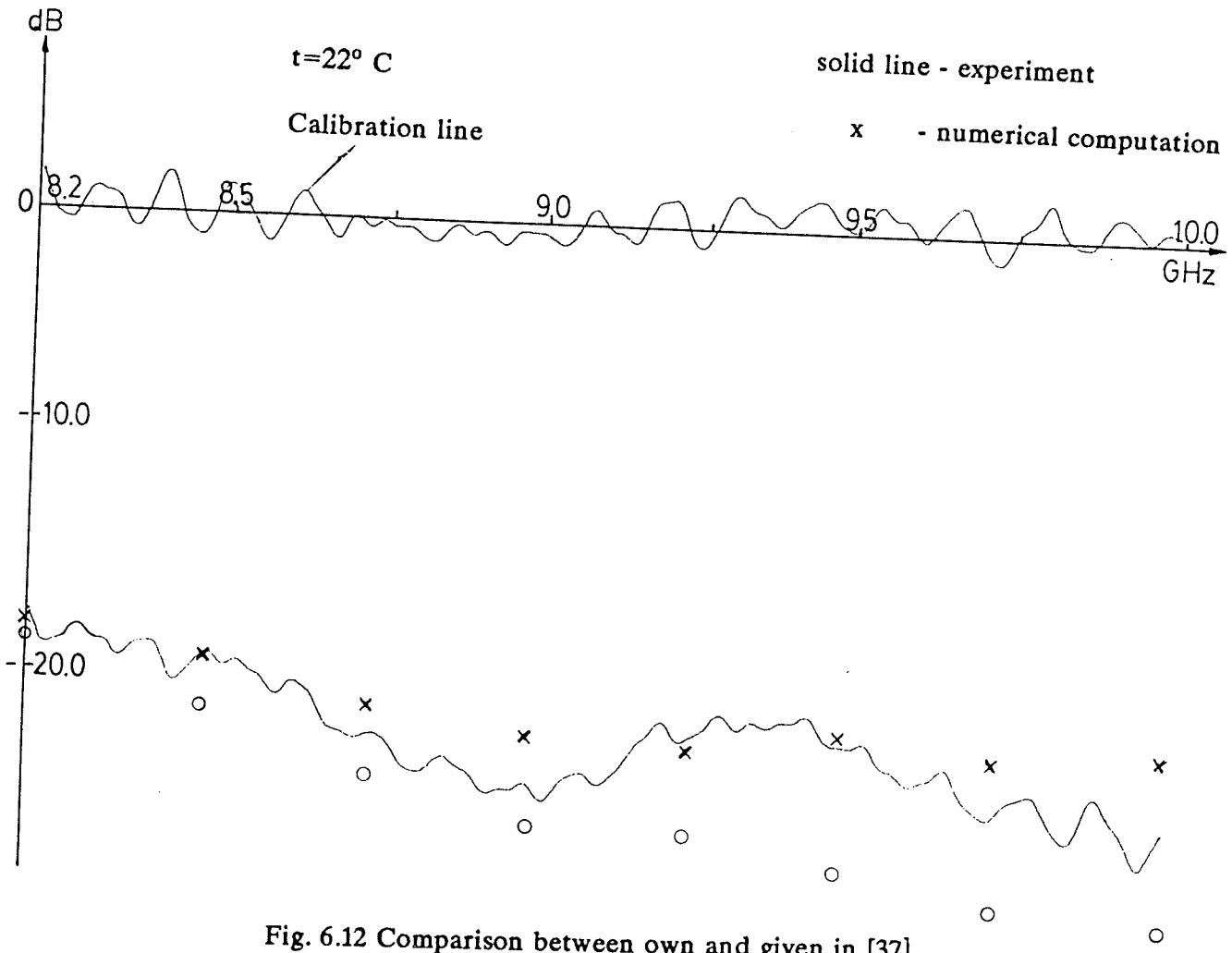

Fig. 6.12 Comparison between own and given in [37]

theoretical data for reflection coefficient of an unloaded horn

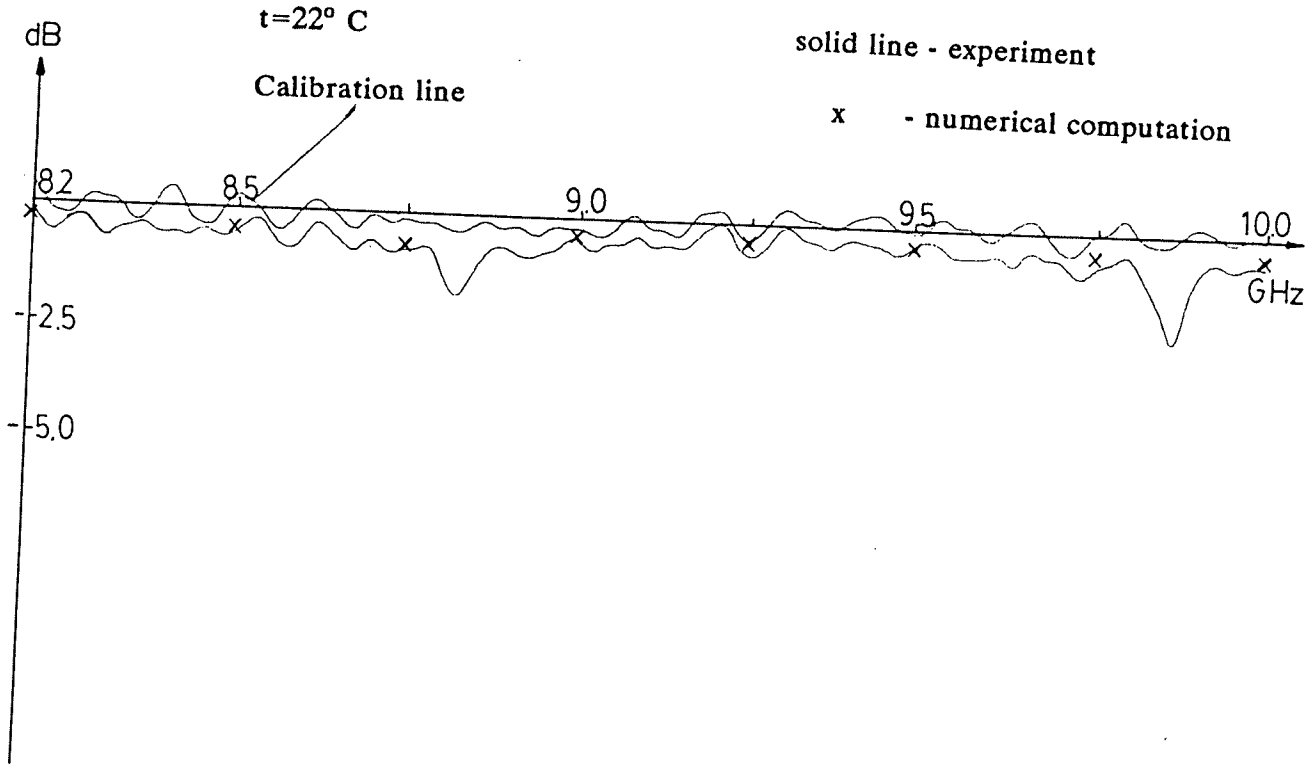

Fig. 6.13 Experimental data for sectoral waveguide being short at the plane $z = h_2 = 184.3$mm

6.3 Discussion and analysis of accuracy

The discrepancy between theoretical and experimental results is primarily caused by inadequacy of the structure employed in the experiment and the theoretically considered model. The main reasons are:

- the length of dielectric insertion (along z-coordinate, fig.4.1) is finite, thus the total reflection coefficient is the sum of reflection occuring at the considered discontinuity at $z = h_2$ and the neglected dicontinuity at $z = h_3 > h_2$,
- the length of the sectoral waveguide is finite, hence scattering on its edges contributes additionally to the reflection coefficient if the medium has low loss tangent,
- the dipolar model of dielectric properties of the load only approximately describes its behavior.

The power splitter converts the network analyzer to essentially a ratiometer by measuring the power ratio between the reference and test channels. Both reference and test channels are initially and during calibration process at the same power level, i.e.

$$r_c = \frac{P_t}{P_r} = 1 \quad , \tag{6.2}$$

where

P_r denotes reflected power in the reference channel,

P_t denotes reflected power in the test channel.

While the measuring procedure is carried out, the reflected power P_r remains constant in the reference channel and that of the test channel is equal to

$$P_{tm} = |\Gamma|^2 P_r \tag{6.3}$$

In effect the return loss of signal measured by the network analyzer is given by

$$r_m[dB]=10\log|\Gamma|^2=20\log|\Gamma| \quad . \tag{6.4}$$

If the power ratio of feed signals in both channels remains constant within the measuring frequency range, it may be shown that the relative error of return loss measurement is dependent both on the absolute error of the reflection coefficient and on the reflection coefficient itself according to the following relation:

$$\delta r_m[\%]=\frac{\Delta r_m}{r_m}\times 100=\frac{43.43\Delta|\Gamma|}{\log|\Gamma|\,|\Gamma|} \tag{6.5}$$

Since the absolute error of return loss, Δr_{mdB}, for the measuring equipment used is $\pm$ 0.10 [dB] the relative error of return loss measurement is found to be

$$\delta r_m[\%]=\pm\frac{1}{2\log|\Gamma|} \tag{6.6}$$

The dependence of relative error of return loss coefficient on the reflection coefficient is shown in fig.6.6. Accuracy of the measured reflection coefficient below 0.8 or return loss coefficient below -0.2 [dB] is within the range of $\pm$ 5 %. The dynamic error of the x-y recorder additionally contributes to the total error, but its detailed analysis is beyond the scope of the thesis. The accuracy of the reflection coefficient measurement using the network analyzer cannot be higher than $\pm$ 0.17 % due to the high values of the signal-noise ratio for reflection coefficients less than 0.001 or return loss coefficients less than -60 dB.

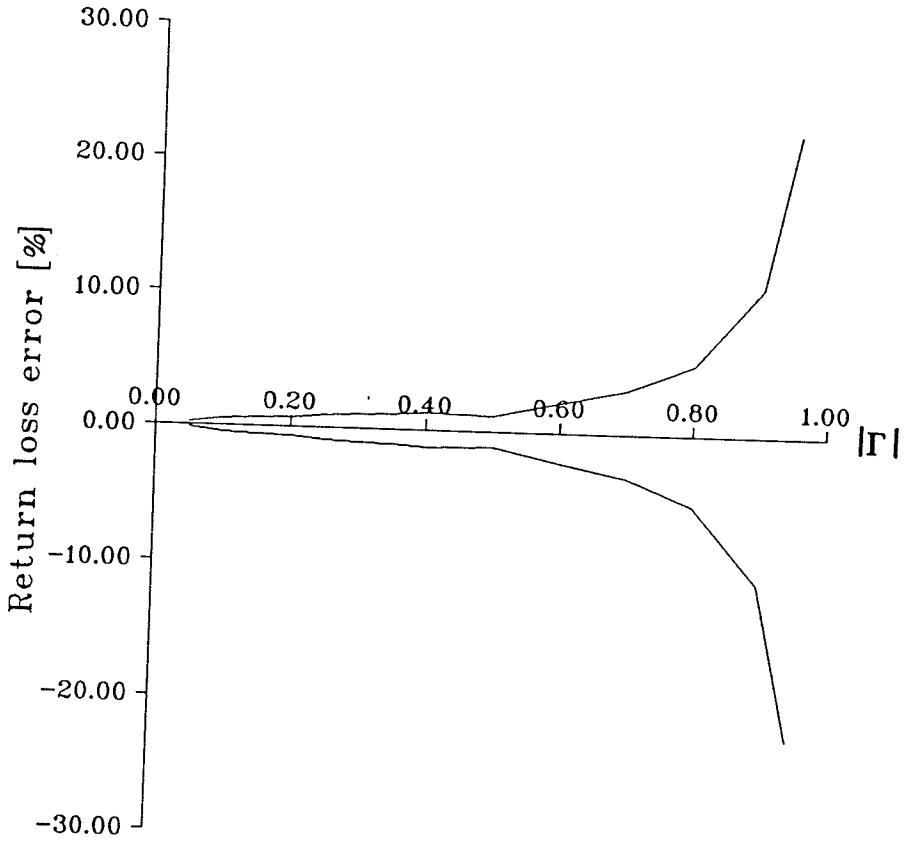

Fig.6.6 Dependence of relative return loss error on the reflection coefficient

CHAPTER 7
Conclusions and Suggestion for Future Research

A significant step has been taken towards determination of the complete performance of dielectrically filled sectoral waveguide or horn. The background for future research has been established. By applying the proposed methods of solution, both for the parallel plate - sectoral waveguide junction and for inverse scattering at the transverse dielectric discontinuity in sectoral waveguide, the determination of dielectric properties of a dielectric insert may be accurately solved for using a large class of dielectric constant models.

Numerical results allow us to predict both the reflected wave amplitude and its phase at an arbitrary point in terms of location of the dielectric discontinuity and properties of dielectrics for an infinite sample in the sectoral part with the restriction that the dielectric is homogeneous, isotropic and linear.

The experimental results proved to be in satisfactory agreement with the presented theory for the frequency range where Debye's model of the dielectric constant and all the restrictions related to the structure under investigation are valid. The accuracy for that region is within the range $\pm 5\%$ with respect to the measured quantity.

The axial value of the reflection coefficient depends only on properties of the dielectric insert (figs.5.5 and 5.6.). The reflected electric field amplitude has its maximum shifted with respect to the axis. Both the amplitude and shift of the maximum depend on the flare angle of the sectoral waveguide for the same dielectric inserts (fig.5.6).

Practical application of the method is limited to dielectric media which may be considered to have an infinite length with respect to the wavelength. Since a great number of industrial products have such properties, this condition is easily

satisfied.

Any model of dielectric properties, including the resonance region, can be determined with accuracy limited by the equipment used and the assumptions made.

The interdependence between the structural properties of the junction, dielectric and electric field is established in a unique manner. The answer to the question of recovering the information about dielectric properties is positive. However the ease with which the sectoral waveguide or horn may be used as a sensor is at the expense of additional computational effort. Such a computer program was created and favorably tested, and can be implemented using any standard computer.

Since the research in this area is far from complete due to interaction between microscopic and macroscopic behavior of electromagnetic field, there still remain the following problems to be solved:

- the multiple scattering in the cavity created between junction and dielectric for highly reflective materials, i.e. $|\Gamma| > 0.5$,
- power transmission across the junction and dielectric,
- reflection and transmission of the electromagnetic field by a sample of finite length,
- optimization of a multilayer transverse dielectric insert depending on the application and function desired.
- determination of the total impedance represented by the insert considered.

Appendix

A.1 Program description

The main program calls four soubroutines. It declares many of the variables used throughout the program. The parameters of the dielectric and its location in the sectoral waveguide are read and then the total reflection coefficient of the structure is evaluated. Output data is stored in a three-dimensional matrix and, depending on need, printed or transferred for plotting. The standard Calcomp subroutines are used for plotting. The program listing is enclosed followed by an example of the printed output.

```
                                                                                40.
      $JOB
1           DIMENSION   MOD(37,11,5),F(37),X(11),EPSR(5),TANDEM(5),FREQAM(5)    50.
2           DIMENSION   MOD2(37,11),MTR1(37,11),MOD1(37,11),H2(5),PHI(11)       60.
3           DIMENSION   PHI1(11)                                                70.
                                                                                80.
      C                                                                         90.
4           REAL   X,FMIN,FMAX,PHAMIN,MOD2,MOD,EPSR,TANDEM,FREQAM               100.
5           REAL   PHAMAX,AMIN,AMAX,A,RHOO,MOD1                                 110.
6           REAL   HO,H1,H2,PHI,PSI1,PSI2,SGAM1,TAU1,TAU2                       120.
7           REAL   TAU3,TAU4,TAU5,TAU6,FLARE                                    130.
8           REAL   K,OMEGA,R1,R2,EWY,ARG,OMR                                    140.
9           REAL   N1,M1,KH,ND,X1,EF2                                           150.
10          REAL P,S,MTR1                                                       160.
                                                                                170.
      C                                                                         180.
11          INTEGER A1/'GAM='/                                                  190.
12          INTEGER A2/'LOG='/                                                  200.
13          INTEGER A3/'GA2='/                                                  210.
14          INTEGER G1/'GAMM'/,G2/'A'/,G3/'LOG '/,G4/'INV.'/,G5/' GA2'/         220.
      C                                                                         230.
15          COMPLEX ETA,BETA,ALFA12,ALFA13,ALFA                                 240.
16          COMPLEX EF1,EF3,EWY1,GAMMA,R  ,E2                                   250.
17          COMPLEX EP3,EP4,GAMMA1,GAMMA2                                       260.
18          COMPLEX EP1,EP2,PHA12,PHA13,PHA,RHAN1,RHAN2                         270.
19          COMPLEX FHAN1,FHAN2,TR1,GAMO,GAM1                                   280.
20          DO 30 L=1,5                                                         290.
21          READ,EPSR(L),FREQAM(L),TANDEM(L),H2(L)                              300.
      C-------------------------------------------------------------------------310.
      C*****SET ANGULAR FREQUENCY OMEGA                                         320.
      C                                                                         330.
22          DO 20 I=1,37                                                        340.
23          PI=3.1415926535897                                                  350.
24          FMIN=8.2                                                            360.
25          FMAX=10.0                                                           370.
26          F(I)=FMIN + (I-1) * (FMAX - FMIN)/36                                380.
27          OMEGA=2*PI*F(I)*1.E 9                                               390.
      C-------------------------------------------------------------------------400.
      C*****SET PARAMETERS OF WAVEGUIDES, A AND ALPHA                           410.
      C                                                                         420.
28          DO 10 J=1,11                                                        430.
29          FLARE=30                                                            440.
30          ALFA=FLARE*PI/180                                                   450.
31          PHAMIN=-ALFA/2                                                      460.
32          PHAMAX=ALFA/2                                                       470.
33          A=0.02284                                                           480.
34          H1 = A / (2*TAN(PHAMAX))                                            490.
35          X(J) =- A/2+(J-1)*A/10                                              500.
36          RHOO=A/2/SIN(PHAMAX)                                                510.
37          PHI(J)=ARSIN(X(J))/SQRT ( X(J)**2 + (RHOO*COS(PHAMAX))**2)          520.
38          CALL TRYFUN (PHI(J),PHAMAX,PSI1,PSI2)                               530.
39          EF2=(SIN(PSI1)) / (SIN(PSI2))                                       540.
      C-------------------------------------------------------------------------550.
      C*****CALCULATE GUIDE PROPAGATION CONSTANT                                560.
      C                                                                         570.
40          C=2.9979E8                                                          580.
41          K=OMEGA/C                                                           590.
42          SGAM1 =SQRT (K**2 - (PI/A)**2)                                      600.
      C-------------------------------------------------------------------------610.
      C*****CALCULATE ALPHA12,EQU.(4.70) - FIRST TWO COMPONENTS                  620.
      C                                                                         630.
43          EWY=-SGAM1*(RHOO*COS(PHI(J)) - H1)                                  640.
44          A=0                                                                 650.
45          EWY1=CMPLX(A,EWY)                                                   660.
46          EWY1=CEXP(EWY1)                                                     670.
47          R1=PI*COS(PHI(J))*COS(PSI1)/2/SIN(PHAMAX)                           680.
48          R2=SGAM1*RHOO*SIN(PHI(L))*SIN(PSI1)                                 690.
49          R1=R1+PI*COS(PSI2)/2/TAN(PHAMAX)/(COS(PHI(J)))**2
50          R=CMPLX(R1,R2)


                                                                                700.
51          PHA12=R/(EWY1*SIN(PSI1) +SIN(PSI2))                                 710.
      C                                                                         720.
      C*****CALCULATE ALPHA13, EQUS. (5.6),(5.18),(5.20)                        730.
      C                                                                         740.
52          TAU3=((PI-ALFA)*COS(PHI(J)))/(ALFA* K * H1)                         750.
53          TAU1=PI*COS(PHI(J))/(ALFA * K * H1)                                 760.
54          ARG= K*H1/COS(PHI(J))                                               770.
55          CALL HAN2(P,S,TAU3,ARG)                                             780.
56          EP2=CMPLX(P,S)                                                      790.
57          EP3=EP2                                                             800.
58          CALL HAN2(P,S,TAU1,ARG)                                             810.
59          EP2=CMPLX(P,S)                                                      820.
60          EP3=EP3/EP2                                                         830.
      C                                                                         840.
      C*****CALCULATE EQN.(5.18)                                                850
      C                                                                         860.
61          Z=-ARG*((SIN(TAU3)-TAU3*COS(TAU3))-(SIN(TAU1)-TAU1*COS(TAU1)))      870.
62          A=0                                                                 880.
63          E2=CMPLX(A,Z)                                                       890.
64          EP4=CEXP(E2)*EP3                                                    900.
65          TAU2=PI/(RHOO*K*ALFA)                                               910.
66          ARG=K*RHOO                                                          920.
67          EP3=EP2
```

```
      C
      C***** CALCULATE EQU.(5.20)
      C
      C                                                                    930.
       68           CALL HAN2 (P,S,TAU2,ARG)                               940.
       69           EP2=CMPLX(P,S)                                         950.
       70           EP3=EP2/EP3                                            960.
       71           Z=K*H1/COS(PHI(J))*(SIN(TAU1)-TAU1*COS(TAU1))          970.
       72           Z=Z-ARG*(SIN(TAU2)-TAU2*COS(TAU2))                     980.
       73           E2=CMPLX(A,Z)                                          990.
       74           EP3=CEXP(E2)*EP3                                       1000.
      C                                                                    1010.
      C***** CALCULATE ALPHA13, EQN.(5.6)                                  1020.
      C                                                                    1030.
       75          PHA13=TAN(PHI(J))*(K*H1*EP4/COS(PHI(J))-PI/ALFA)/(1+EP3)  1040.
      C                                                                    1050.
      C***** CALCULATE ALPHA,EQU.(4.70)                                    1060.
      C                                                                    1070.
       76          PHA=PHA12+PHA13                                         1080.
      C                                                                    1090.
      C-------------------------------------------------------------------1100.
      C*****CALCULATE BETA(PHI), EQN. (4.72)                               1110.
      C                                                                   -1120.
       77          TAU3=((PI-ALFA)*COS(PHI(J)))/(ALFA * K * H2(L))        1130.
       78          TAU1=PI*COS(PHI(J))/(ALFA * K * H2(L));                1140.
       79          ARG= K*H2(L)/COS(PHI(J))                               1150.
       80          CALL HAN2(P,S,TAU3,ARG)                                1160.
       81          EP2=CMPLX(P,S)                                         1170.
       82          EP3=EP2                                                1180.
       83          CALL HAN2(P,S,TAU1,ARG)                                1190.
       84          EP2=CMPLX(P,S)                                         1200.
       85          EP3=EP3/EP2                                            1210.
       86          Z=-ARG*((SIN(TAU3)-TAU3*COS(TAU3))-(SIN(TAU1)-TAU1*COS(TAU1)))  1220.
       87          E2=CMPLX(A,Z)                                          1230.
       88          EP4=CEXP(E2)*EP3                                       1240.
       89          BETA=TAN(PHI(J))*(K*H2(L)*EP4/COS(PHI(J))-PI/ALFA)     1250.
      C-------------------------------------------------------------------1260.
      C*****CALCULATE F3(PHI), EQN.(4.75.1)                                1270.
      C                                                                   -1280.
       90          EF3=(PHA+BETA)**2/((PHA/COS(PHI(J)))**2+(BETA/COS(PHI(J)))**2)  1290.
      C-------------------------------------------------------------------1300.
      C*****CALCULATE ETA, EQN.(4.75)                                      1310.
      C                                                                   -1320.
       91          OMR=F(I)*1.E8/FREQAM(L)                                1330.
                                                                          1340.
                                                                          1350.
       92          S=-(TANDEM(L)*OMR*2)/(1+OMR**2)
       93          P=EPSR(L)
       94          E2=CMPLX(P,S)                                          1360.
       95          ETA=CSQRT(E2)                                          1370.
      C-------------------------------------------------------------------1380.
      C*****CALCULATE GAMMA2, EQN.(4.73)                                   1390.
      C                                                                   -1400.
       96          TAU4=PI*COS(PHI(J))/(ALFA*K*H2(L))                     1410.
       97          ARG=K*H2(L)/COS(PHI(J))                                1420.
       98          CALL HAN2(P,S,TAU4,ARG)                                1430.
       99          EP2=CMPLX(P,S)                                         1440.
      100          CALL HAN1(P,S,TAU4,ARG)                                1450.
      101          EP1=CMPLX(P,S)                                         1460.
      102          Z=-2*K*H2(L)*(SIN(TAU4)-TAU4*COS(TAU4))/COS(PHI(J))    1470.
      103          E2=CMPLX(A,Z)                                          1480.
      104          EP3=CEXP(E2)                                           1490.
      105          EP3=EP3*EP2/EP1                                        1500.
      106          E2=CSQRT((ETA**2+EF3)/(1+EF3))                         1510.
      107          GAMMA2=EP3*(1-E2)/(1+E2)                               1520.
      C-------------------------------------------------------------------1530.
      C*****CALCULATE EF1, EQN(5.3)                                        1540.
      C                                                                   -1550.
      C*****CALCULATE EQN.(5.9)                                            1560.
      C                                                                    1570.
      108          TAU1=PI*COS(PHI(J))/(ALFA*K*H1)                        1580.
      109          TAU2=PI/(ALFA*K*RHOO)                                  1590.
      110          ARG=K*H1/COS(PHI(J))                                   1600.
      111          CALL HAN2(P,S,TAU1,ARG)                                1610.
      112          EP2=CMPLX(P,S)                                         1620.
      113          EP1=EP2                                                1630.
      114          ARG=K*RHOO                                             1640.
      115          CALL HAN2(P,S,TAU2,ARG)                                1650.
      116          EP2=CMPLX(P,S)                                         1660.
      117          EP3=EP1/EP2                                            1670.
      118          Z=-K*H1/COS(PHI(J))*(SIN(TAU1)-TAU1*COS(TAU1))         1680.
      119          Z=Z+K*RHOO*(SIN(TAU2)-TAU2*COS(TAU2))                  1690.
      120          E2=CMPLX(A,Z)                                          1700.
      121          EF1=CEXP(E2)*EP3                                       1710.
                                                                          1720.
                                                                          1730.
```

```
      C-------------------------------------------------------------------------
      C*****CALCULATE GAMMA1 OF A LONG HORN, EQN(4.61)                          1740.
      C                                                                         1750.
  122       GAMMA1=-(EWY1*EF1*EF2-1)/(EF1+1)                                    1760.
      C-------------------------------------------------------------------------1770.
      C*****CALCULATE GAMMA1(GAM1) OF THE FIRST ORDER EQU.(4.81)                 1780.
      C                                                                         1790.
  123       ARG=K*H1/COS(PHI(J))                                                1800.
  124       CALL HAN1(P,S,TAU1,ARG)                                             1810.
  125       EP1=CMPLX(P,S)                                                      1820.
  126       Z=K*H1/COS(PHI(J))*(SIN(TAU1)-TAU1*COS(TAU1))                       1830.
  127       E2=CMPLX(A,Z)                                                       1840.
  128       FHAN1=E2*EP1                                                        1850.
  129       ARG=K*RH00                                                          1860.
  130       CALL HAN1(P,S,TAU2,ARG)                                             1870.
  131       EP1=CMPLX(P,S)                                                      1880.
  132       Z=K*RH00*(SIN(TAU2)-TAU2*COS(TAU2))                                 1890.
  133       E2=CMPLX(A,Z)                                                       1900.
  134       RHAN1=CEXP(E2)*EP1                                                  1910.
  135       GAM1=-GAMMA2*(FHAN1+RHAN1)/(EWY1*EF2+1)                             1920.
      C-------------------------------------------------------------------------1930.
      C*****CALCULATE TOTAL REFLECTION COEFFICIENT GAMMA1, EQU.(4.83)            1940.
      C                                                                         1950.
  136       GAMMA=GAMMA1+GAM1                                                   1960.
      C-------------------------------------------------------------------------1970.
      C                                                                         1980.
      C*****CALCULATE THE FIRST ORDER INVERSE TRANS. COEF. TR1, EQN.(4.82)       1990.
      C                                                                         2000.
  137                                                                           2010.
  138       ARG=K*RH00
  139       CALL HAN2(P,S,TAU2,ARG)
  140       EP2=CMPLX(P,S)                                                      2020.
  141       Z=-K*RH00*(SIN(TAU2)-TAU2*COS(TAU2))                                2030.
  142       E2=CMPLX(A,Z)                                                       2040.
  143       RHAN2=EP2*CEXP(E2)                                                  2050.
  144       ARG=K*H1/COS(PHI(J))                                                2060.
  145       CALL HAN2(P,S,TAU1,ARG)                                             2070.
  146       EP2=CMPLX(P,S)                                                      2080.
  147       Z=-K*RH00*(SIN(TAU2)-TAU2*COS(TAU2))                                2090.
  148       E2=CMPLX(A,Z)                                                       2100.
  149       FHAN2=CEXP(E2)*EP2                                                  2110.
            TR1=GAMMA2*((FHAN1-RHAN1)/(FHAN2+RHAN2)-(EWY1*EF2-1)/(EWY1*EF2+1))2120.
      C-------------------------------------------------------------------------2130.
      C*****CALCULATE MODULUS                                                   2140.
      C                                                                         2150.
  150                                                                           2160
  151       ARG=REAL(GAMMA)                                                     2170.
  152       MOD1(I,J)=CABS(GAMMA)                                               2180.
  153       MTR1(I,J)=CABS(GAMMA2)                                              2190.
  154       MOD(I,J,L)=20*ALOG10(MOD1(I,J))                                     2200.
  155       MOD2(I,J)=20*ALOG10(MOD1(I,J))                                      2210.
  156       PHI1(J)=PHI(J)*180/PI                                               2220.
  157    10 CONTINUE                                                            2230.
  158    20 CONTINUE                                                            2240.
  159       FREQAM(L)=FREQAM(L)/1.E9                                            2250.
  160       PRINT 25,G1,G22                                                     2260.
  161       PRINT  5,FLARE                                                      2270.
  162     5 FORMAT (10X,F4.1)                                                   2280.
  163    25 FORMAT (36X,A4,A4)                                                  2290.
  164       PRINT 25                                                            2300.
  165       PRINT,H2(L)                                                         2310.
  166       PRINT 15 ,EPSR(L),FREQAM(L),TANDEM(L)                               2320.
  167    15 FORMAT (6X,2F5.2,F7.4)                                              2330.
  168       CALL PRTS (X,F,MOD1,37,11,A1,37)                                    2340.
  169       PRINT 25                                                            2350.
  170       PRINT 25 ,G1,G2,G3                                                  2360.
  171       PRINT  5,FLARE                                                      2370.
  172       PRINT 35                                                            2380.
  173    35 FORMAT (34X,3A4)                                                    2390.
  174       PRINT 15 ,EPSR(L),FREQAM(L),TANDEM(L)                               2400.
  175       PRINT,H2(L)                                                         2410.
  176       CALL PRTS (X,F,MOD2,37,11,A2,37)                                    2420.
  177       PRINT 25                                                            2430.
  178       PRINT 25 ,G4,G5                                                     2440.
  179       PRINT  5,FLARE                                                      2450.
  180       PRINT 25                                                            2460.
  181       PRINT 15 ,EPSR(L),FREQAM(L),TANDEM(L)                               2470.
  182       PRINT,H2(L)                                                         2480.
  183       CALL PRTS (PHI1,F,MTR1,37,11,A3,37)                                 2490.
  184    30 CONTINUE                                                            2500.
  185       STOP                                                                2510.
            END                                                                 2520.
                                                                                2530.
```

```
      C-------------------------------------------------------------------------
      C*****SUBROUTINE TRYFUN, EQUS.(4.62),(4.64),(4.70.1),(4.70.2)            -2540.
      C                                                                         2550.
                                                                                2560.
186           SUBROUTINE TRYFUN (PHI,PHAMAX,PSI1,PSI2 )
187           PI=3.1415926535897
188           PSI1=PI*(SIN(PHI)/SIN(PHAMAX) + 1)/2                              2570
189           PSI2=PI*(TAN(PHI)/TAN(PHAMAX)+1)/2                                2580.
190           RETURN                                                            2590.
191           END                                                               2600.
      C-------------------------------------------------------------------------2610.
      C*****COMPUTE SERIES OF HANKEL FUNCTION OF THE FIRST KIND                 2620.
192           SUBROUTINE HAN1(P,S,TAU5,ARG)                                     2630.
                                                                                2640.
                                                                                2650.
      C
193           COMPLEX E2,SUM,EP1
194           PI=3.1415926535897                                                2660.
195           A=0                                                               2670.
196           Z=-PI/4                                                           2680.
197           E2=CMPLX(A,Z)                                                     2690.
198           EP1=(1.77245*CEXP(E2))/SQRT(ARG*SIN(TAU5)/2)                      2700.
199           Z=-3*PI/4                                                         2710.
200           E2=CMPLX(A,Z)                                                     2720.
201           SUM=0.88623*CEXP(E2)*(3/8+5/24/(TAN(TAU5))**2)                    2730.
202           SUM=SUM/SQRT(ARG*SIN(TAU5)/2)/(ARG*SIN(TAU5)/2)                   2740.
203           EP1=EP1+SUM                                                       2750.
204           Z=-5*PI/4                                                         2760.
205           E2=CMPLX(A,Z)                                                     2770.
206           SUM=1.3293*CEXP(E2)*(3/128+385/3456/(TAN(TAU5))**4)               2780.
207           SUM=SUM/SQRT(ARG*SIN(TAU5)/2)/(ARG*SIN(TAU5)/2)**2                2790.
208           EP1=EP1+SUM                                                       2800.
209           P=REAL(EP1)                                                       2810.
210           S=AIMAG(EP1)                                                      2820.
211           RETURN                                                            2830.
212           END                                                               2840.
      C-------------------------------------------------------------------------2850.
      C*****COMPUTE SERIES OF HANKEL FUNCTION OF SECOND KIND                    2860.
213           SUBROUTINE HAN2(P,S,TAU6,ARG)                                     2870.
      C                                                                         2880.
214           COMPLEX E2,SUM,EP2                                                2890.
215           PI=3.1415926535897                                                2900.
216           Z=PI/4                                                            2910.
217           A=0                                                               2920.
218           E2=CMPLX(A,Z)                                                     2930.
219           EP2=(1.77245*CEXP(E2))/SQRT(ARG*SIN(TAU6)/2)                      2940.
220           Z=3*PI/4                                                          2950.
221           E2=CMPLX(A,Z)                                                     2960.
222           SUM=0.88623*CEXP(E2)*(3/8+5/24/(TAN(TAU6))**2)                    2970.
223           SUM=SUM/SQRT(ARG*SIN(TAU6)/2)/(ARG*SIN(TAU6)/2)                   2980
224           EP2=EP2+SUM                                                       2990.
225           Z=5*PI/4                                                          3000.
226           E2=CMPLX(A,Z)                                                     3010.
227           SUM=1.3293*CEXP(E2)*(3/128+385/3456/(TAN(TAU6))**4)               3020.
228           SUM=SUM/SQRT(ARG*SIN(TAU6)/2)/(ARG*SIN(TAU6)/2)**2                3030.
229           EP2=EP2+SUM                                                       3040.
230           P=REAL(EP2)                                                       3050.
231           S=AIMAG(EP2)                                                      3060.
232           RETURN                                                            3070.
233           END                                                               3080.
      C-------------------------------------------------------------------------3090.
      C*****                                                                    3100.
                                                                                3110.
                                                                                3120.
```

```
234           SUBROUTINE PRTS (X,F,Y,N,M,KH,ND)
              C
              C PRINT A MATRIX IN 11-COLUMN PARTITIONS                                  3130.
              C Y=ARRAY TO BE OUTPUT                                                    3140.
              C N=NUMBER OF ROWS OF Y TO BE PRINTED                                     3150.
              C M=NUMBER OF COLUMNS OF Y TO BE PRINTED                                  3160.
              C KH=NAME OF ARRAY FOR OUTPUT HEADING                                     3170.
              C 1,2 OR 3 CONSTANTS IN THE CALL STATEMENT FOR HEADING                    3180.
              C ND=NUMBER OF ROWS (OR ELEMENTS) DIMENSIONED FOR Y IN THE CALLING        3190.
              C PROGRAM                                                                 3200.
235                DIMENSION Y(ND,M),F(ND),X(M)                                         3210.
236                GOTO 20                                                              3220.
237             5  FORMAT (/A7,6X,11I10)                                               3230.
238            15  FORMAT (16X,11F10.4)                                                3240.
239            20  DO 25 K=1,M,11                                                      3250.
240                PRINT 15                                                            3260.
241                L=MINO(K+10,M)                                                      3270.
                                                                                       3280.
                                                                                       3290.
242                PRINT 5,KH,(J,J=K,L)
243                PRINT 15
244                PRINT 15, (X(J),J=K,L)                                              3300.
245                PRINT 15                                                            3310.
246                DO 25 I=1,N                                                         3320.
247            25  PRINT 30,I,F(I),(Y(I,J),J=K,L)                                      3330.
248            30  FORMAT (/I6,2X,F6.2,2X,11F10.4)                                     3340.
249                PRINT 15                                                            3350.
250                RETURN                                                              3360.
251                END                                                                 3370.
              C-------------------------------------------------------------------    3380.
              C                                                                        3390.
                                                                                       3400.
                                                                                       3410.
```

An example of the printed output

Reflection coefficient $\left|\Gamma_1\right|$ as a function of frequency (rows) and x coordinate of a parallel plate waveguide (columns) for: ϵ_r =2.54, f_m = 8.40 GHz, $\tan\delta_m$ = 0.005, flare angle of a sectoral waveguide, α=30°, and a distance from the apex, h_2=93.3 mm.

30.0

0.0933000

2.54 8.40 0.0050

GAM=

		1	2	3	4	5	6	7	8	9	10	11
		-0.0114	-0.0091	-0.0069	-0.0046	-0.0023	-0.0000	0.0023	0.0046	0.0069	0.0091	0.0114
1	8.20	0.1771	0.2296	0.2732	0.3050	0.3215	0.2854	0.3271	0.3073	0.2743	0.2300	0.1771
2	8.25	0.1757	0.2286	0.2724	0.3044	0.3210	0.2848	0.3265	0.3068	0.2735	0.2289	0.1757
3	8.30	0.1744	0.2276	0.2717	0.3038	0.3204	0.2843	0.3260	0.3062	0.2728	0.2279	0.1744
4	8.35	0.1732	0.2266	0.2709	0.3032	0.3199	0.2838	0.3255	0.3057	0.2720	0.2269	0.1731
5	8.40	0.1719	0.2256	0.2702	0.3027	0.3194	0.2833	0.3251	0.3051	0.2713	0.2259	0.1719
6	8.45	0.1707	0.2246	0.2695	0.3021	0.3189	0.2828	0.3246	0.3046	0.2706	0.2250	0.1706
7	8.50	0.1694	0.2237	0.2688	0.3016	0.3185	0.2823	0.3241	0.3041	0.2699	0.2240	0.1694
8	8.55	0.1682	0.2228	0.2681	0.3011	0.3180	0.2819	0.3237	0.3036	0.2692	0.2231	0.1682
9	8.60	0.1671	0.2218	0.2674	0.3006	0.3176	0.2814	0.3233	0.3031	0.2686	0.2222	0.1671
10	8.65	0.1659	0.2210	0.2668	0.3001	0.3171	0.2810	0.3228	0.3026	0.2679	0.2213	0.1659
11	8.70	0.1648	0.2201	0.2662	0.2997	0.3167	0.2806	0.3224	0.3022	0.2673	0.2204	0.1648
12	8.75	0.1637	0.2192	0.2656	0.2992	0.3163	0.2802	0.3220	0.3017	0.2667	0.2196	0.1637
13	8.80	0.1626	0.2184	0.2650	0.2988	0.3160	0.2798	0.3217	0.3013	0.2661	0.2187	0.1626
14	8.85	0.1615	0.2176	0.2644	0.2984	0.3156	0.2795	0.3213	0.3009	0.2656	0.2179	0.1615
15	8.90	0.1604	0.2168	0.2638	0.2980	0.3152	0.2791	0.3210	0.3005	0.2650	0.2171	0.1604
16	8.95	0.1594	0.2160	0.2633	0.2976	0.3149	0.2788	0.3206	0.3001	0.2645	0.2164	0.1594
17	9.00	0.1584	0.2152	0.2627	0.2973	0.3146	0.2785	0.3203	0.2998	0.2639	0.2156	0.1584
18	9.05	0.1574	0.2145	0.2622	0.2969	0.3143	0.2782	0.3200	0.2994	0.2634	0.2149	0.1574
19	9.10	0.1564	0.2138	0.2617	0.2966	0.3140	0.2779	0.3197	0.2991	0.2629	0.2141	0.1564
20	9.15	0.1555	0.2131	0.2613	0.2963	0.3137	0.2776	0.3194	0.2988	0.2624	0.2134	0.1555
21	9.20	0.1545	0.2124	0.2608	0.2959	0.3135	0.2774	0.3192	0.2984	0.2620	0.2127	0.1545
22	9.25	0.1536	0.2117	0.2603	0.2957	0.3132	0.2771	0.3189	0.2982	0.2615	0.2120	0.1536
23	9.30	0.1527	0.2110	0.2599	0.2954	0.3130	0.2769	0.3187	0.2979	0.2611	0.2114	0.1527
24	9.35	0.1518	0.2104	0.2595	0.2951	0.3128	0.2767	0.3185	0.2976	0.2607	0.2107	0.1518
25	9.40	0.1509	0.2097	0.2591	0.2949	0.3126	0.2765	0.3183	0.2974	0.2603	0.2101	0.1509
26	9.45	0.1501	0.2091	0.2587	0.2946	0.3124	0.2763	0.3181	0.2971	0.2599	0.2095	0.1501
27	9.50	0.1492	0.2085	0.2583	0.2944	0.3122	0.2762	0.3179	0.2969	0.2595	0.2089	0.1492
28	9.55	0.1484	0.2079	0.2580	0.2942	0.3121	0.2760	0.3177	0.2967	0.2592	0.2083	0.1484
29	9.60	0.1476	0.2074	0.2576	0.2940	0.3119	0.2759	0.3176	0.2965	0.2588	0.2077	0.1476
30	9.65	0.1468	0.2068	0.2573	0.2938	0.3118	0.2758	0.3174	0.2963	0.2585	0.2072	0.1468
31	9.70	0.1460	0.2063	0.2570	0.2937	0.3117	0.2757	0.3173	0.2961	0.2582	0.2066	0.1460
32	9.75	0.1452	0.2057	0.2567	0.2935	0.3116	0.2756	0.3172	0.2960	0.2579	0.2061	0.1452
33	9.80	0.1445	0.2052	0.2564	0.2934	0.3115	0.2755	0.3171	0.2958	0.2576	0.2056	0.1445
34	9.85	0.1438	0.2047	0.2561	0.2933	0.3114	0.2754	0.3170	0.2957	0.2573	0.2051	0.1437
35	9.90	0.1430	0.2042	0.2558	0.2932	0.3114	0.2754	0.3170	0.2956	0.2570	0.2046	0.1430
36	9.95	0.1423	0.2038	0.2556	0.2931	0.3113	0.2753	0.3169	0.2955	0.2568	0.2041	0.1423
37	10.00	0.1416	0.2033	0.2553	0.2930	0.3113	0.2753	0.3169	0.2954	0.2565	0.2037	0.1416

References

[1] Kraszewski, A., Kulinski, S., Stosio, Z., " Prelimnary Study on Microwave Monitoring of Moisture Content in Wheat ", Journ. of Microwave Power, no.12, 1977, pp. 241-252.

[2] Hamid, M. and Al-Sulaiman, A., New Types of Dielectric-loaded Horn Antennas ", Int'l J. of Electronics,vol.55,no5,1983, pp. 729-750.

[3] Collin, R., E., " Foundations for Microwave Engineering ", Mc-Graw Hill, New York, 1966, pp. 43-47.

[4] Fritz, J., " Plane Waves and Spherical Means ", Interscience Publishers, New York, 1955, pp. 7-13.

[5] Stevenson, A., F., " General Theory of Electromagnetic Horns ", J. of Appl. Physics, vol.22, December 1951, pp.1447-1454.

[6] Solymar, L., " Spurious Mode in Nonuniform Waveguide ", IRE Trans. MTT-7, July 1959, pp. 379-383.

[7] Fradin, A., " Microwave Antennas " (translated from Russian), Pergamon Press, 1961, pp.239-250.

[8] Piefke, G., " Reflection at Incidence of an E_{mn}-Wave at Junction of Circular Waveguide and Conical Horn ", in "Elelectromagnetic Theory and Antennas", vol.1, Jordan, E., -editor,Pergamon Press, 1963, pp. 209-234.

[9] Hamid, M., " Reflection Coefficient at a Horn- Waveguide Junction ", IEEE Trans., AP-15, July 1967, pp. 564-565.

[10] Bahar, E., " Wave Scattering in Nonuniform Waveguides with Large Flare Angles and Near Cutoff ", IEEE trans., MTT-16, no.8, August 1968, pp. 503-510.

[11] Lewin, L., " On the Inadequacy of Discrete Mode-Matching Techniques in Some Waveguide Discontinuity Problems ", IEEE Trans., MTT-18, July 1970, pp. 364-372.

[12] Lewin, L. and Nielsen D., " On the Restricted Validity of Point Matching Techniques " and following discussion , IEEE trans., MTT-18, December 1970, pp. 1041-1047.

[13] Iskander, M. and Hamid, M., " Scattering Coefficients at a Waveguide -Horn Junction ", Proc. IEE, vol.123, no.2, February 1976, pp. 123-127.

[14] Pace, J. and Mittra, R., " Generalized Scattering Matrix Analysis of Waveguide Discontinity Problems ", in " Quasi-Optics ", Pol. Inst. of Brooklyn Press, New York, 1964, pp. 177-197.

[15] Bates, R. and Ng, T., " Point Matching Computation of Transverse Resonances ", Interscience J. for Num. Meth. in Eng., vol.6, 1973, pp. 155-168.

[16] Bates, R., " The Theory of Point Matching Method for Perfectly Conducting Waveguides and Transmission Lines ", Trans. IEEE, MTT-17, 1969, pp. 294-301.

[17] Reisdorf, F. and Schminke, W., " Application of a "Zwischenmedium" to the Radiation from a Flanged Waveguide ", Proc. IEE, vol.120, 1973, pp. 739-740.

[18] Wexler, A., " Solutions of Waveguide Discontinuities by Modal Matching ", IEEE trans., MTT-15, September 1967, pp. 508-517.

[19] Kantorovich, L. and Krylov, V., " Approximate Methods of Higher Analysis " (translated from Russian), Interscience Publishers, P. Noordhoff Ltd., Groningen, the Netherlands, 1958, pp. 616-670.

[20] Moon, P., and Spencer, D., " Vectors ", Van Nostrand, Princeton, New Jersey, 1965, pp. 153,243.

[21] Kinber, V., " Diffraction at the Open End of a Sectoral Horn ", Radio Eng. and Elec. Phys. , vol.7-10, October 1962, pp. 1620-1632.

[22] Yee, H., Felsen, L., Keller, J., " Ray Theory of Reflection from the Open End of a Waveguide ", SIAM J. Appl. Math., vol. 16, no.3, 1968, pp. 268 - 300.

[23] Kinber, B., Popienchenko, V., " Radiation from a Sectoral Horn ", Radio Eng. and Elec. Phys. , no.17, 1972, pp. 1621 -1627.

[24] Debye, P., " Näherungsformeln für die Zylinderfunktionen für grosse Werte des Arguments und unbeschränkt veränderliche Werte des Index ", Matematische Annalen, band 67, 1909, pp. 535-558.

[25] Oden, J., "A general theory of finite elements", Int'l J. Num. Meth. in Engng., 1, 1969, pp. 205-221.

[26] Rice, S., "A Set of Second Order Differential Equations Associated with Reflections in Rectangular Waveguides - Applications to Guide Connected to Horn ", Bell Syst. Tech. Journ., no.28, 1949, pp. 136-156.

[27] Lewin, L., " Theory of Waveguides ", Newnes - Butterworths, London, 1975, pp. 25.

[28] Fock, V., " Generalization of the Reflection Formulae to the Case of Reflection of an Arbitrary Wave from a Surface of Arbitrary Form ", chapter 8 in " Electromagnetic Diffraction and Propagation Problems ", Pergamon Press, Oxford, 1965, pp. 147 - 170.

[29] Rud', L., " Wave Diffraction at a T-Junction of Rectangular Waveguides in the H -Plane", Radio Eng. and Elec. Phys., no.9, 1984, pp.1711 -1719.

[30] Poritsky, H. and Blewett, H., " A method of Solution of Field Problems by Means of Overlapping Regions ", Quart. J. of Appl. Math., no.3, 1946, pp. 336-347.

[31] Abramowitz, M., Stegun, J., " Handbook of Mathematical Functions ", National Bureau of Standard, USA, 1964, p.361.

[32] Frölich, H., "Theory of Dielectrics", Oxford at the Clarendon Press, 1958 .

[33] Killingbeck, J., Cole, G., "Mathematical Techniques and Physical Applications", Acadamic Press, New York & London, 1971, p.493 .

[34] Weinstein, L., "The Theory of Diffraction and Factorization Method", The Golem Press, Boulder, Colorado, 1969 .

[35] Isao, I., " Die Beugung Electromagnetischer Wellen an einem Kreiszylinder ", Zeitschrift für Physik, Bd.137, S. 31-48, 1954.

[36] Bajpai, A., Mustoe, L., Walker, D., "Advanced Engineering Mathematics", John Wiley and Sons, London, 1977, pp. 424-426.

[37] Leonard, D. and Yen, J., "Junction of Smooth Flared Waveguides", J. of Applied Physics, Vol. 28, No.12, Dec. 1957, pp. 1441-1448.

[38] Jackson, J., "Classical electrodynamics", John Wiley and Sons, New York, 1975, pp. 269-326.